

University of Massachusetts Boston

## ScholarWorks at UMass Boston

---

Graduate Doctoral Dissertations

Doctoral Dissertations and Masters Theses

---

12-31-2013

# Studying Soil Moisture and Land-to-Water Carbon Export in Urbanized Coastal Areas Using Remotely Sensed Data and a Regional Hydro-Ecological Model

Yun Yang

*University of Massachusetts Boston*

Follow this and additional works at: [https://scholarworks.umb.edu/doctoral\\_dissertations](https://scholarworks.umb.edu/doctoral_dissertations)



Part of the [Biogeochemistry Commons](#), [Hydrology Commons](#), and the [Remote Sensing Commons](#)

---

### Recommended Citation

Yang, Yun, "Studying Soil Moisture and Land-to-Water Carbon Export in Urbanized Coastal Areas Using Remotely Sensed Data and a Regional Hydro-Ecological Model" (2013). *Graduate Doctoral Dissertations*. 143.

[https://scholarworks.umb.edu/doctoral\\_dissertations/143](https://scholarworks.umb.edu/doctoral_dissertations/143)

This Open Access Dissertation is brought to you for free and open access by the Doctoral Dissertations and Masters Theses at ScholarWorks at UMass Boston. It has been accepted for inclusion in Graduate Doctoral Dissertations by an authorized administrator of ScholarWorks at UMass Boston. For more information, please contact [scholarworks@umb.edu](mailto:scholarworks@umb.edu).

STUDYING SOIL MOISTURE AND LAND-TO-WATER CARBON EXPORT IN  
URBANIZED COASTAL AREAS USING REMOTELY SENSED DATA AND A  
REGIONAL HYDRO-ECOLOGICAL MODEL

A Dissertation Presented

by

YUN YANG

Submitted to the Office of Graduate Studies,  
University of Massachusetts Boston,  
in partial fulfillment of the requirements for the degree of

DOCTOR OF PHILOSOPHY

December 2013

Environmental Science Program

© 2013 by Yun Yang  
All rights reserved

STUDYING SOIL MOISTURE AND LAND-TO-WATER CARBON EXPORT IN  
URBANIZED COASTAL AREAS USING REMOTELY SENSED DATA AND A  
REGIONAL HYDRO-ECOLOGICAL MODEL

A Dissertation Presented

by

YUN YANG

Approved as to style and content by:

---

Crystal B. Schaaf, Professor  
Chairperson of Committee

---

Robert F. Chen, Professor  
Member

---

Ellen M. Douglas, Associate Professor  
Member

---

Wei Ding, Assistant Professor  
Member

---

David E. Tenenbaum, Professor, Lund University  
Member

---

John A. Duff, Graduate Program Director  
School for the Environment

---

Robyn Hannigan, Chairperson  
School for the Environment

## ABSTRACT

# STUDYING SOIL MOISTURE AND LAND-TO-WATER CARBON EXPORT IN URBANIZED COASTAL AREAS USING REMOTELY SENSED DATA AND A REGIONAL HYDRO-ECOLOGICAL MODEL

December 2013

Yun Yang, B.A., Beijing Normal University, China  
M.S., University of Massachusetts Boston  
Ph.D., University of Massachusetts Boston

Directed by Professor Crystal B. Schaaf

The main objective of this research was to study the flux of dissolved organic carbon (DOC) from a terrestrial urbanized watershed to an estuarine system using a process-based regional hydro-ecological model and remotely sensed data.

While DOC is an important component of the global carbon cycle, the link of the variations in terrestrial carbon storage is still poorly understood. Soil moisture is a key factor that influences the amount of available water for vegetation growth and the

decomposition rate of organic matter in the soil and thus contributes to the amount of DOC in the soil at the land-water boundary. The Regional Hydro-Ecological Simulation System (RHESSys) was used to model the biogeochemical cycle in the Neponset Watershed, Boston, MA from 2006 to 2011. Remotely sensed indices and field measurements of soil moisture, locally measured watershed DOC values, and streamflow gauge amounts were used to evaluate the modeled results.

The fully parameterized high resolution RHESSys model was used to simulate soil moisture in the highly urbanized and fragmented Neponset watershed and displayed good correlation with the measured soil moisture values. Another two measures of soil moisture conditions (the topographic moisture index (TMI) and the remotely sensed temperature vegetation dryness index (TVDI)) were also estimated and compared with field measured data. Two nested study areas, the Neponset River Watershed and the Greater Boston Area, were utilized to correspond with two spatial resolutions. The DOC concentration data sampled in the Neponset River Watershed were analyzed and the sensitivity of the DOC simulation in RHESSys was evaluated. The simulated DOC was compared with estuarine results and a good correlation was found to exist between the measured and simulated DOC concentrations and fluxes.

This effort represents the first successful application of RHESSys model to an urbanized New England watershed and not only provided an accurate way to estimate both soil

moisture and DOC flux but also provided a framework to test further hypotheses and future scenarios to benefit global carbon cycle research.

## ACKNOWLEDGEMENTS

First and foremost I would like to express the deepest appreciation to my advisor, Professor Crystal Schaaf, for her support and help. Without her knowledge, guidance and persistent help this dissertation would not have been possible.

I would like to thank the following professors and members of my committee: Professor Christina Tague, Professor David Tenenbaum, Professor Robert Chen, Professor Ellen Douglas and Professor Wei Ding, for their advice, thoughtful scientific discussions, and hard work. I especially want to thank Professor Christina Tague for repeatedly hosting me in UC Santa Barbara, and for her support and scientific insights. It has been a real pleasure and a joy to work with her.

I want to thank members of Schaaf research group for their help and friendship. I would also like to extend my appreciation to people in School for the Environment for creating a great atmosphere to work in.

Last but not least, I would like to thank my family members. I want to thank my husband Zhuosen. He has been with me through my entire graduate career, supported me, helped me and stood by me through the dissertation work. I also want to thank my daughter and my parents for their enormous support and understanding during the completion of the project.

## TABLE OF CONTENTS

ACKNOWLEDGEMENTS .....	vii
LIST OF TABLES .....	x
LIST OF FIGURES .....	xi
LIST OF ABBREVIATIONS .....	xvii
CHAPTER	Page
1. INTRODUCTION .....	1
1.1. Dissolved Organic Carbon .....	2
1.2. Soil Moisture Measurement and Estimation Methods.....	6
1.3. The Regional Hydro-Ecological Simulation System (RHESSys) .....	8
1.4. Research Area .....	11
2. EVALUATING THE SOIL MOISTURE WITH THE TEMPERATURE VEGETATION DRYNESS INDEX (TVDI) ESTIMATED WITH VARIOUS VEGETATON INDICES (VIS) FROM MODIS AND LANDSAT DATA....	15
2.1. Introduction .....	15
2.2. Data and Methodology.....	17
2.3. Results and Discussions.....	29
2.4. Conclusion.....	55
3. DOC CONCENTRATION PATTERNS IN THE NEPONSET RIVER WATERSHED EXPLORED WITH REMOTELY SENSED DATA.....	58
3.1. Introduction .....	58
3.2. Study Area .....	60
3.3. Data .....	61
3.4. Methodology .....	62
3.5 Results and discussions.....	63
3.6. Conclusion.....	89
4. SENSITIVITY ANALYSIS AND SIMULATION OF DOC CONCENTRATION AND FLUX DURING INITIALIZATION OF THE RHESSYS MODEL .....	91

CHAPTER	Page
4.1. Introduction .....	91
4.2. Study Area and Data .....	94
4.3. Methodology .....	102
5. SENSITIVITY ANALYSIS AND SIMULATION OF DOC CONCENTRATIONS AND FLUX USING THE RHESSYS MODEL – THE RESULTS .....	108
5.1. Sensitivity Analysis.....	108
5.2. Neponset Results .....	131
5.3. Conclusion.....	138
6. SUMMARY.....	140
REFERENCE.....	146

## LIST OF TABLES

Table	Page
2.1. Acquisition date of both MODIS NBAR data and LST data. ....	18
2.2. Equations for the vegetation indices that were used to evaluate TVDI. ....	19
3.1. Measured DOC concentration from the Neponset River Watershed. ....	65
3.2. Sub-basins' watershed characteristics list. ....	74
3.3. The correlation between GPP and measured DOC concentration. ....	88

## LIST OF FIGURES

Figure	Page
1.1. The structure of RHESSys model. ....	9
1.2. Greater Boston, Massachusetts, as defined in this study (shown in light blue).....	11
1.3. The Neponset River Watershed. ....	13
2.1. DEM for the Neponset Watershed and the slope map created from the DEM.....	21
2.2. Sampling Locations in the Neponset River Watershed. ....	23
2.3. Sampling locations of the ULTRA-EX project among the two transects (Rao et al. 2013). ....	26
2.4 Simplified Ts/NDVI plot (Sandholt et al. 2002).....	28
2.5. Histogram of the two sub-basins' slope.....	29
2.6. Topographic Moisture Index (TMI) calculated from the 5 m DEM map.....	30
2.7. Histogram of TMI for the two sampling sub-basins.....	31
2.8. Temporal patterns of mean soil moisture in both Milton and Sharon. ....	33
2.9. Boxplot of field measured soil moisture in the Milton area over the sampling period.	34
2.10. Boxplot of field measured soil moisture in the Sharon area over the sampling period. ....	34
2.11. The linear relationship between soil moisture and CV in two sub-basins.....	35
2.12. Coefficient of determination between soil moisture and TMI vs. sampling date in two sub-basins in the Neponset River Watershed and the precipitation data. ....	37

Figure	Page
2.13. TMI of the eastern part of Massachuestts. ....	38
2.14. Slope of VI-LST plot on different days shown with precipitation data. Different lines show slopes using various vegetation indices. ....	40
2.15. The intercept of VI-LST plots on different days shown with precipitation data. Different lines show intercepts using various vegetation indices. ....	41
2.16. Spearman’s test coefficient of TVDI’s using various VIs. ....	42
2.17. TVDI calculated using NDVI and EVI2 from MODIS on day 208 of year 2010. ...	43
2.18. Slope of VI-LST plot on different days shown with precipitation data in 2011. Different lines show slope using various vegetation indices. ....	45
2.19. Intercept of VI-LST plot on different days shown with the precipitation data in 2011. Different lines show intercept using various vegetation indices. ....	46
2.20. Spearman’s test coefficient of TVDI’s estimated using various VIs on different days in 2011. ....	47
2.21. TVDI calculated using NDVI and EVI2 from Landsat data on day 197 of year 2011.	49
2.22. Slope of VI-LST plot on different days shown with precipitation data. Dashed lines show slope using various vegetation indices based on MODIS data. Solid lines show slope using various vegetation indices based on Landsat TM data. ....	50
2.23. Intercept of VI-LST plot on different days shown with precipitation data. Dashed lines show intercepts using various vegetation indices based on MODIS data. Solid lines show intercepts using various vegetation indices based on Landsat TM data. ....	50
2.24. TVDI map created using EVI2 based on Landsat data from July 16 <sup>th</sup> , 2011. ....	51

Figure	Page
2.25. The comparison between TVDI estimated using various VIs and measured soil moisture.....	53
2.26. Plot of TVDI estimated using EVI2 and measured soil moisture in Sharon and Milton. The green dots are samples from Milton and the red dots are samples from Sharon. ....	55
3.1. The Neponset River Watershed. ....	60
3.2. The DOC concentration sampling points throughout the Neponset River Watershed.	64
3.3. Correlation between mean DOC concentration and standard deviation at all sampling points. If P10 is removed, the correlation increases to 0.71. ....	67
3.4. Boxplot of DOC concentrations at each sampling point. ....	68
3.5. Boxplot of DOC concentrations from all sampling points in different years. ....	69
3.6. Boxplot of DOC concentration measurements in different seasons. ....	71
3.7. Comparison of DOC concentrations averaged from all sampling points among different months. ....	72
3.8. Biplot of the scores of the first three principal components. ....	77
3.9. Biplot of the scores of the principal component 1 and principal component 3. ....	77
3.10. Comparison of the precipitation among 118 years' average and from year 2006 to year 2011.....	78
3.11. Comparison of the maximum temperature among 118 years' average and from year 2006 to year 2011.....	79

Figure	Page
3.12. Comparison of the minimum temperature among 118 years' average and from year 2006 to year 2011.....	79
3.13. API estimated from precipitation data. The blue line shows precipitation data and the red line shows the API values. ....	80
3.14 Plot of Average DOC concentrations and API values of samples from the growing season excluding year 2008. ....	81
3.15. Plot of average monthly temperature and measured DOC concentration for all months. Points are numbered with the months in which they were sampled. ....	83
3.16. Plot of DOC concentrations averaged from all sampling sites for December and January to May and corresponding average daily temperature excluding year 2008. The red points represent samplings measured in late April and May. The green points represent samplings measured in December, January, February and March.	83
3.17. The correlation between measured DOC concentration and stream flow larger than 0.35 ft <sup>3</sup> /sec (0.098 m <sup>3</sup> /sec). ....	85
3.18. The correlation between DOC concentration and stream flow during the low flow.	86
3.19. GPP and mean DOC concentration from year 2006 to year 2011. ....	87
3.20. Plot of DOC concentration and 8-day GPP. ....	89
4.1 The Neponset River Watershed with Massachusetts State as the background. The upper right corner is the digital elevation map of the Neponset River watershed.	94
4.2. 100 years' climate data at the Blue Hill weather observation station.....	95
4.3. Location of USGS gauge stations in the Neponset River Watershed and DEM map of the Neponset River Watershed.....	99

Figure	Page
4.4. Input maps for RHESSys of the Neponset River Watershed.....	100
4.5. Patches created from combining DEM, soil type, vegetation type, land use type in the Neponset River Watershed at 30 m resolution .....	101
4.6. The simplified carbon cycle and the DOC production and transportation processes in RHESSys. DOM is dissolved organic matter which includes both dissolved organic carbon and dissolved organic nitrogen in RHESS.....	105
5.1. DOM_decay_rate changes for stream DOC flux when soil depth is 3 m.....	113
5.2. DOM_decay_rate changes for stream DOC concentration when soil depth is 3 m. ....	113
5.3. DOM_decay_rate changes for stream DOC flux when soil depth is 10 m.....	114
5.4. DOM_decay_rate changes for stream DOC concentration when soil depth is 10 m.....	114
5.5. Stream DOC flux changes with DOM_production_rate.....	116
5.6. Stream DOC concentration changes with DOM_production_rate. ....	117
5.7. Plant carbon amount changes with DOM_production_rate.....	117
5.8. Stream DOC flux changes with the DOC_absorption_rate. ....	119
5.9. Stream DOC concentration changes with the DOC_absorption_rate.....	119
5.10. Stream DOC flux changes with nitrogen deposition. ....	123
5.11. Stream DOC concentration changes with nitrogen deposition.....	123
5.12. Plant carbon storage changes with nitrogen deposition changes. ....	123
5.13. Stream DOC flux changes with change in temperature.....	124

Figure	Page
5.14. Stream DOC concentration changes with change in temperature. ....	124
5.15. Plant carbon storage changes with change in temperature. ....	125
5.16. Stream DOC flux changes with soil depth.....	126
5.17. Stream DOC concentration changes with soil depth and plant carbon storage changes with soil depth. ....	127
5.18. The correlation between average daily DOC flux and the proportion of surface water that becomes groundwater. ....	128
5.19. Stream DOC flux changes with the litter composition. ....	129
5.20. Stream DOC concentration changes with the litter composition.....	130
5.21. Plant carbon storage changes with the litter composition.....	130
5.22. Uncertainty assessment of the stream flow simulation. The grey area was defined by using the 5% and 95% confidence levels of the acceptable simulated stream flow. The red line was the observed stream flow at the outlet of the Neponset River Watershed. ....	132
5.23. Uncertainty assessment of logarithms of stream flow simulation. ....	133
5.24. Simulated root zone soil moisture of the whole Neponset River Watershed comparing with average measured soil moisture in Sharon and Milton sub-basins.	134
5.25. Simulated daily DOC concentration compared with observed DOC concentration and simulated daily stream flow compared with observed stream flow. ....	137
5.26. Simulated daily DOC flux compared with observed DOC flux and simulated daily stream flow compared with observed stream flow. ....	137

## LIST OF ABBREVIATIONS

API	antecedent precipitation index
AVHRR	advanced very high resolution radiometer
CDOM	chromophoric dissolved organic matter
CV	coefficient of variation
DEM	digital elevation map
DHSVM	distributed hydrology soils and vegetation model
DN	digital number
DOC	dissolved organic carbon
DOM	dissolved organic matter
DON	dissolved organic nitrogen
DOY	day of year
ET	evapotranspiration
EVI2	two-band enhanced vegetation index
FI	feedback index
GLUE	generalized likelihood uncertainty estimation
GPP	gross primary production
gw	ground water
LAI	leaf area index
LEDAPS	landsat ecosystem disturbance adaptive processing system
LST	land surface temperature
MODIS	moderate resolution imaging spectroradiometer
NASA	national aeronautics and space administration
NBAR	nadir BRDF adjusted reflectance
NDVI	normalized difference vegetation index
NIR	near infrared
NLCD	national land cover dataset
NOAA	national oceanic and atmospheric administration
NRCS	natural resources conservation service

PCA	principal component analysis
RHESSys	regional hydro-ecological simulation system
RVI	ratio vegetation index
SAVI	soil adjusted vegetation index
SD	standard deviation
TM	thematic mapper
TMI	topographic moisture index
TOA	top of atmosphere
TVDI	temperature vegetation dryness index
USDA	united states department of agriculture
USGS	united states geological survey
VI	vegetation index

## CHAPTER 1

### INTRODUCTION

Dissolved organic carbon (DOC) is an important component of the global carbon cycle with variations linked to changes in terrestrial carbon storage. Soil moisture influences the decomposition rate of organic matter in the soil and the amount of available water for vegetation growth and thus DOC in the soil at the land-water boundary. When soil is saturated, lateral flow occurs and carries DOC from the soil into stream channels. This research explored the flux of DOC from a terrestrial urbanized watershed to an estuarine system with a process-based regional hydro-ecological model and remotely sensed data. A special emphasis was placed on the effects of soil moisture on the system and the utility of various remotely sensed indices of soil moisture. The study area encompassed the Neponset River Watershed, one of the main waterways flowing through Boston, Massachusetts and emptying into Boston Harbor. The Regional Hydro-Ecological Simulation System (RHESSys) was used to model the details of the Neponset Watershed

biogeochemistry. Remotely sensed data and field measurements of soil moisture and estuarine DOC are then used to evaluate the modeled results.

### 1.1 Dissolved Organic Carbon Flux

The flux of Dissolved Organic Carbon (DOC) from the terrestrial system to the aquatic system is a fundamental part of the global carbon cycle. The world riverine DOC export to the oceans is 0.2 GtC/year (Smith and Mackenzie 1987). It tightly links terrestrial, estuarine and marine carbon cycling together (Richey et al. 2004b) and contributes to the mechanisms of soil formation by influencing the complexity, solubility, and mobility of metals (Martell et al. 1988; Perdue et al. 1976; Trumbore 1993; Weng et al. 2002). DOC affects the aquatic ecosystem by attenuating radiation to protect the aquatic biota in the surface layer from UV radiation and at the same time serving to shade the aquatic biota in the lower layer of water (Boeing et al. 2004; Williamson and Zagarese 1994). DOC concentrations in riverine stream channels also impact the water quality and thus directly impact the health of both anthropogenic and natural communities in a watershed (Delpla et al. 2009; Siddiqui et al. 1997).

Many studies have been carried out investigating the source, formation, and fate of DOC in soils and flux of DOC from the terrestrial to aquatic systems (Ågren et al. 2010; Chow et al. 2006; Clutterbuck and Yallop 2010; Kicklighter et al. 2013; Mayer 1994; Yano et al. 1998). However, because of the difficulty in obtaining frequent field measurements and lack of consistency between laboratory studies and field measurements, our knowledge of

the DOC in soil and the DOC flux from the terrestrial to aquatic systems is still fragmentary (Kalbitz et al. 2000). DOC in soil originates from the decomposition of plant litter, soil humus, microbial biomass and root matter (Miller 2012; Roulet and Moore 2006). The contact time between soil and soil water is very important for DOC concentrations in soil solution (Borken et al. 2011; Michalzik and Matzner 1999). In the spring, more water passes through the soils in a shorter time, and thus the DOC concentrations in soil pore water is low; the DOC concentrations in soil is higher in summer because less water passes through soils during comparable time periods (Bourbonniere 1989; Dawson et al. 2011; McDowell and Wood 1984). The fate of soil DOC is hydrological flushing, soil absorption and decomposition which relates to the nitrogen status (Boissier and Fontvielle 1993; Boyer et al. 1996; Nelson et al. 1994). Between 12 to 44% of DOC in the forest floor soil is decomposed by indigenous microbes (Yano et al. 1998). Temperature appears to be a key factor that can affect the concentration of DOC in soil with respect to both its source and its fate, making it difficult to discern the effect of increasing temperature on DOC concentrations in soil solution (Preston et al. 2011). Some research shows that increasing temperature increases DOC concentrations in soil solution (Bianchi et al. 2009; Liechty et al. 1995; Luo et al. 2009; Williamson et al. 2008) while other research finds only a weak relationship between temperature and DOC concentrations in soil (Chow et al. 2006; Dosskey and Bertsch 1997; MacDonald et al. 1999).

Hydrological flushing caused by precipitation or snowmelt serves as major method of DOC transport from the terrestrial to aquatic systems (Dyson et al. 2011; Raymond and

Saiers 2010). A high DOC flux into a stream is often observed right after snowmelt and the flux decreases sharply after the first peak (Boyer et al. 1996; Yavitt and Fahey 1985). The timing, duration and amount of precipitation and antecedent soil moisture conditions all influence the processes that transition DOC into streams. Field studies have found high DOC concentrations in stream channels during moist periods following a particularly dry period (Tipping et al. 1997; Zsolnay et al. 1999). Transition of DOC from the terrestrial to aquatic systems is also regulated by mineral soil absorption, a complicated process hard to quantify (Kalbitz et al. 2000). Despite intensive research on DOC in soils and in streams, there appears to be a combination of causes for either higher DOC concentrations in soil or higher DOC flux (Kalbitz et al. 2000; Strohmeier et al. 2013).

The flux of DOC in streams can be estimated using existing field measurements and landscape characteristics. Previous modeling work includes the SPATIally Referenced Regressions On Watershed attributes (SPARROW) model which is an empirical model that uses a nonlinear regression equation describing the transport of contaminants from point sources on land to rivers and through the stream network to relate the water quality measurements of monitoring stations to attributes of the corresponding watersheds (Schwarz et al. 2006). The Load Estimator (LOADEST) regression software (Runkel et al. 2004) is also an empirical model and relates point samples to the whole watershed based on the regression relationship among the point measurements (Huntington and Aiken 2012). A landscape-mixing model was applied to predict DOC concentration from contributing landscape elements (Ågren et al. 2013). Currie and Aber coupled a

decomposition model (DocMod) with a hydrology model that predicts litter production and actual evapotranspiration and applied this to the White Mountain National Forest in 0.1 km<sup>2</sup> grids on a monthly time step (Currie and Aber 1997). Aitkenhead and McDowell used C:N ratio in soil as a predictor to estimate annual DOC flux at both local and global scales (Aitkenhead and McDowell 2000). As a major component of DOC, chromophoric dissolved organic matter (CDOM), absorbing ultraviolet and visible light and plays an important role in both coastal water optical properties and the biogeochemical cycling of various elements, can also be used as a proxy of DOC flux (Bissett et al. 2001; Bricaud et al. 1981; Chen 1999; Chen et al. 2002; Green and Blough 1994; Huang and Chen 2009). While many studies have been developed to estimate DOC fluxes in forested areas, few have been developed for coastal areas and particularly for urbanized coastal areas. Coastal areas connect the terrestrial areas and the oceans, with energy and materials being exchanged frequently and in large amounts. Furthermore, urbanized areas are the places most impacted by human activities. Thus urbanization has the potential to greatly modify soil carbon pools and fluxes (Groffman and Turner 1995; Pouyat et al. 2002). Global deforestation due to land use changes over a 15 year period have been shown to cause a decrease of about  $4 \times 10^{11}$  g of DOC (Hedges et al. 1997). The amount of carbon released from fossil fuels and stored in cement production for urbanized regions is estimated at 5.5 GtC (Beven and Binley 1992). Conversely, urban trees in the conterminous USA are estimated to have stored 700 million tons of carbon in 2001 (Nowak and Crane 2002). However, it must be acknowledged that climate change influences may be exacerbated in urban areas because of the multiple artificial surfaces and the high levels of fossil fuel combustion (Nowak 2000). Therefore, improving our understanding of DOC fluxes in

urbanizing coastal areas will provide more detailed information about the total carbon cycle at both regional and global scales.

## 1.2. Soil Moisture Measurement and Estimation Methods

Soil moisture, the content of water contained in the soil matrix, is an important parameter in the global hydrologic and energy cycles. It influences the partitioning of incoming radiative energy into sensible and latent heat fluxes (Engman 1991). Soil moisture is a key factor regulating DOC export by directly influencing vegetation growth, organic matter decomposition and the amount of water running through soil to carry DOC out from the terrestrial to aquatic systems. Soil moisture is one of the few parameters that both laboratory and field studies show the same and consistent influence on DOC export. DOC concentrations increase during rewetting after dry periods (Chittleborough et al. 1992; Haynes and Swift 1991; Kalbitz and Knappe 1997; Lundquist et al. 1999; McDowell and Wood 1984; Tipping et al. 1999; Zabowski and Ugolini 1990; Zsolnay et al. 1999).

Although soil moisture is a key variable in several land surface processes, it is often not measured with the same accuracy and frequency as other important environmental variables (Houser et al. 1998; Verstraeten et al. 2010). As a crucial input for many climate or water resource management models, increasing our understanding of soil moisture through remotely sensed and *in situ* datasets is necessary (Albergel et al. 2012; Beljaars et al. 1996; Entekhabi et al. 2010). The traditional measurement of soil moisture

using a gravimetric method is time-consuming (including both field work and oven drying in lab) and difficult to extrapolate to larger areas from point samples. Remotely sensed data are widely used to measure surface soil moisture conditions on both regional and global scales (Brocca et al. 2010; Choi and Hur 2012; Draper et al. 2009).

Microwave remote sensing data is one source for retrieval of soil moisture measures (Entekhabi et al. 2010; Njoku and Entekhabi 1996). For instance, active microwave sensors (e.g. the active Advanced Scatter meter (ASCAT)) can measure soil moisture at different spatial scales (on the order of tens of meters), but the temporal resolution is relatively low. Furthermore, active microwave sensors' sensitivity to soil moisture is often impacted by surface roughness, topographic features and vegetation (Engman and Chauhan 1995). Passive microwave instruments (e.g. the passive microwave Advanced Microwave Scanning Radiometer (AMSR-E)) have high temporal resolution, but poor spatial resolution (only on the order of tens of kilometers). Therefore, microwave methods are not appropriate for research that focuses on small spatial scales and high temporal frequency variations.

In contrast, optical passive satellite data can provide high temporal and spatial resolution information to estimate soil moisture conditions, even though optical observations are not a direct measure of soil moisture. Spectral indices are often used to acquire information describing soil moisture status. Beven and Kirkby (Beven and Kirkby 1979) created the topographic moisture index (TMI) to capture the relationship between topographic control and sub-surface hydrology to examine soil moisture patterns. The correlation between near-surface soil moisture and TMI is strong in wet conditions in semi-arid

catchments in Australia (Western and Blöschl 1999). High correlations between near-surface soil moisture and the TMI were also found over a gently sloping and humid Piedmont watershed and an urbanizing watershed in the vicinity of Baltimore, Maryland (Tenenbaum et al. 2006).

Numerous studies (Patel et al. 2009; Sims et al. 2008; Wan et al. 2004) have shown a strong relationship between soil moisture and the Temperature Vegetation Dryness Index (TVDI) especially where the Normalized Difference Vegetation Index (NDVI) is low during growing seasons (i.e. in locations with sparse canopy cover) (Patel et al. 2009). TVDI is based on the relationship between land surface temperature (LST) and NDVI over different land use types (Sandholt et al. 2002). Retrieval methods of soil moisture data using the LST/NDVI relationship have been documented in detail (Carlson 2007; Petropoulos et al. 2009; Sun et al. 2011). TVDI also has been shown to have a relationship with land use type and antecedent precipitation index (API).

### 1.3. The Regional Hydro-Ecological Simulation System (RHESSys)

Remote sensing and *in situ* data can both be used as inputs to simulate watershed dynamics using complex land surface models (e.g. TOPS and the Regional Hydro-Ecological Simulation System (RHESSys)) (Nemani et al. 2009; Tague and Band 2004). RHESSys is a hydro-ecological model which has been developed to simulate water, carbon and nutrient flux cycling and transport in watersheds (Tague and Band 2004). The model is designed as a spatially nested hierarchical representation of the landscape, using

different models to represent processes at different scales. There are five different spatial scales in this model, which are (from largest to smallest) basins, hillslopes, zones, patches and canopy strata. Basins are closed drainage areas that have a single stream network, while areas that drain into one side of a stream reach are defined as hillslopes. Zones are areas having similar climate forcing conditions. Patches, the finest spatial unit of these five scales, are the areas having similar soil moisture and land use characteristics. Canopy strata represent the horizontal spatial variation of vertical layers. The modeling and processing flow in RHESSys is shown in the following diagram (Figure 1.1, <http://fiesta.bren.ucsb.edu/~rhessys/about/about.html#intro>):

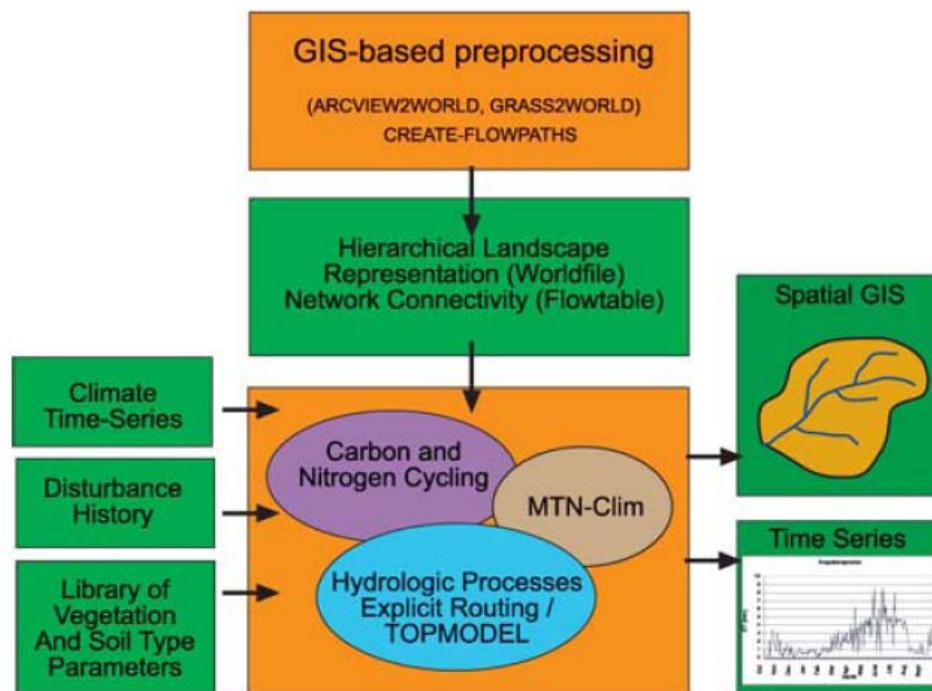


Figure 1.1. The structure of RHESSys model.

RHESSys has been applied to many diverse watersheds under different climate conditions for various research objectives (e.g. a semiarid watershed in California (Shields and Tague 2012), and mountain watersheds in Switzerland (Zierl et al. 2007)). It was used to study nitrogen export at the watershed scale (Band et al. 2001), stream flow feedbacks in response to climate change, parameterizing ungauged watersheds to improve the modeling stream flow feedbacks (Tague et al. 2007; Tague et al. 2009a; Tague et al. 2012), hydrologic vegetation gradient as an indicator for lateral hydrologic connectivity (Hwang et al. 2012), eco-hydrologic response to the combined impacts of projected climate change and altered fire frequencies (Tague et al. 2009b) and snow distribution (Christensen et al. 2008; Hartman et al. 1999). The redistribution of moisture in RHESSys is similar to TOPMODEL (Beven and Kirkby 1979) and the DHSVM explicit routing method (Wigmosta et al. 1994). The vertical soil moisture model includes a variable rooting zone soil moisture store, an unsaturated store and a saturated store. For the carbon cycle, carbon is fixed in the ecosystem by photosynthesis (Farquhar Equation) and then partially consumed by the maintenance respiration (Ryan 1991) and growth respiration. The rest of the carbon is allocated to different tissues in vegetation based on fixed allocation ratios. Carbon is lost from the system by decomposition (Parton et al. 1996) and leaching as DOC. Nitrogen is mainly from atmosphere nitrogen deposition (including both dry and wet deposition) and also from plants which are able to fix nitrogen. The nitrogen cycle includes mineralization (Parton et al. 1996) and denitrification (Parton et al. 1996). Nitrogen is lost from the terrestrial system by leaching of water as  $\text{NH}_4$ ,  $\text{NO}_3$  and DON. Although RHESSys has been applied successfully in many climate types, it has not been used in the New England area for the study of DOC

flux from terrestrial to coastal aquatic environments. Thus this present effort applied RHESSys to an urbanized coastal watershed located south of City of Boston to simulate the DOC export from the terrestrial to aquatic systems.

#### 1.4. Research Area

##### 1.4.1 The Greater Boston Area

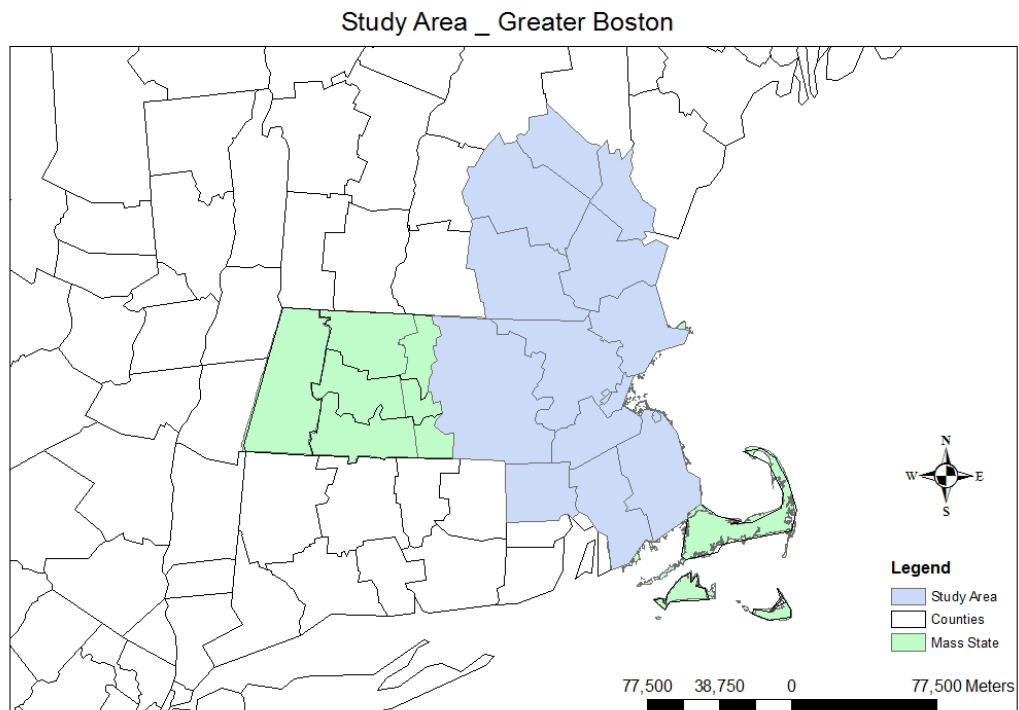


Figure 1.2. Greater Boston, Massachusetts, as defined in this study (shown in light blue).

To capture a gradient from drier urban pixels to wetter suburban/rural pixels, the Greater Boston Area, was defined for this research project (Figure 1.2), and included counties

from three New England states, Massachusetts, Rhode Island and New Hampshire. These counties were Essex, Middlesex, Worcester, Suffolk, Plymouth, Norfolk and Bristol in Massachusetts, Providence in Rhode Island, and Belknap, Merrimack, Stafford, Rockingham and Hillsborough in New Hampshire. A few separate regions (the Interstate 495 corridor, Downtown Boston, etc.) were also tested to see if these were areas which would capture sufficient values along the full range of moisture (TVDI values) expected in an urban-rural gradient. The soil type in this region is typical New England soil; rocky, hard-packed and generally poor for agriculture, especially across the eastern half of Massachusetts (NOAA, 2005). There are over six million residents in Massachusetts, about half of which reside within a 50-mile radius of Boston (inside the Interstate 495 corridor) (NOAA, 2005). The study area in New Hampshire has a much higher population density than the rest of the New Hampshire State. While the study area is predominantly residential, forest is an important component of the land cover in New England.

#### 1.4.2 The Neponset Watershed

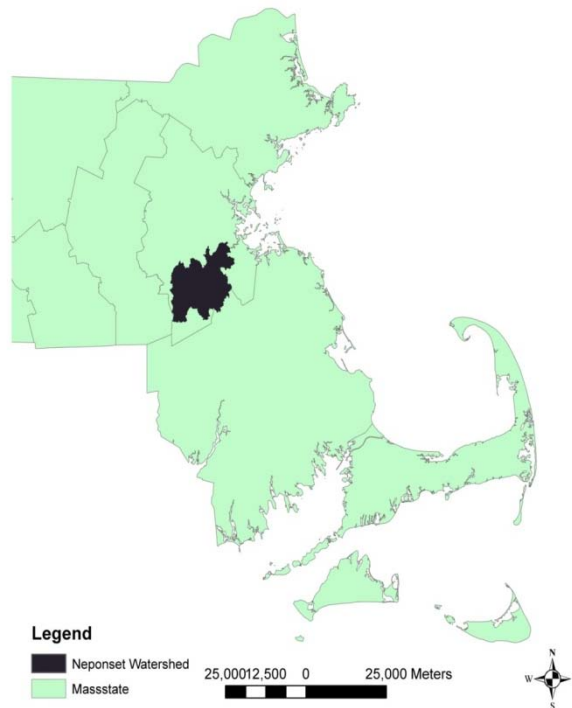


Figure 1.3. The Neponset River Watershed.

The Neponset River Watershed (Figure 1.3) lies south of the City of Boston. It covers parts of 14 cities and towns southwest of Boston. The watershed area is roughly 300 km<sup>2</sup> and includes about 330,000 residents. The Neponset River exits over the Lower Mills Dam into Boston Harbor, after running approximately 48 km throughout the watershed (NepRWA, 2004). It has a long history of scientific study. As early as 1873, the Neponset Watershed was chosen as the nation's first publicly funded water quality study site. Research under the Federal Clean Water Act was carried out in the Neponset Watershed from 1972 onward. In the 1990s, the EPA chose this watershed as a test basin for the Water Evaluation and Planning Model (WEAP), a practical yet robust tool to incorporate water demand, water supply, water quality and ecological considerations for integrated

water resources planning (Gao et al. 2012). The size of Neponset River Watershed was selected for this study because it is big enough to develop TVDI and other remotely sensed datasets from Landsat data but not too large to efficiently run the RHESSys model. Urban land occupies a large proportion of the Neponset Watershed (around 40%). Forest and wetland land covers comprise most of the rest of the watershed (about 40% and 20% respectively). The average annual precipitation was 1054 mm from 1971 to 2000 (NOAA, 2005). The Neponset Watershed is located in close enough proximity to the University of Massachusetts Boston to allow for frequent field samples. Furthermore long-term measurements of DOC and CDOM are also available from 2006 to present in this watershed (Huang and Chen, 2010).

## CHAPTER 2

### EVALUATING THE SOIL MOISTURE WITH THE TEMPERATURE VEGETATION DRYNESS INDEX (TVDI) ESTIMATED WITH VARIOUS VEGETATION INDICES (VIS) FROM MODIS AND LANDSAT DATA

#### 2.1. Introduction

Appropriate estimates of soil moisture are necessary for the accurate hydrologic and biogeochemical modeling of a watershed and satellite based measures offer the best opportunity to capture high temporal and spatial resolution soil moisture in a regional fashion. The Temperature Vegetation Dryness Index (TVDI) calculated from Pathfinder, AVHRR and MODIS data has been shown to have a strong relationship with soil moisture (Patel et al. 2009; Wang et al. 2004; Xin et al. 2006). However, few studies have been conducted using Landsat data (with its higher spatial resolution) to calculate TVDI. In these earlier studies, a strong negative relationship between TVDI and in-situ soil moisture was found when vegetation cover is sparse (Patel et al. 2009). However the

relationship is less clear over thick canopy cover. This is because the NDVI (used to compute the TVDI) reaches saturation over dense vegetation when the biomass exceeds a threshold, and can even apparently decrease when dense biomass increases because of the effects of canopy shadowing. This makes it difficult to detect changes in land cover (Huete et al. 1997). While NDVI is the traditional satellite index used for TVDI, various other common vegetation indices (Table 2.2), including the two-band enhanced vegetation index (EVI2) (Jiang et al. 2008), the ratio vegetation index (RVI) (Pearson and Miller 1972), and the soil adjusted vegetation index (SAVI) (Huete 1988) were also analyzed here at both medium and fine scales. Each vegetation index formulation focuses on different properties of vegetation conditions; for example, some of them include the influence of background soil, while others are more sensitive in dense vegetation. By exploring the various vegetation indices, an attempt was made to improve our understanding of how TVDI functions and also how the various indices might work for different land use types. This research used both MODIS data (500m) and Landsat data (30m) to calculate TVDI for the Greater Boston Area and the Neponset River Watershed respectively. Field sampled soil moisture data collected in the Greater Boston Area and the Neponset River Watershed are used to validate the TVDI patterns.

Near-surface soil moisture has also been proved to relate to the Topographic Moisture Index (TMI) in some study areas (Tague et al. 2010; Tenenbaum et al. 2006; Western et al. 1999; Western et al. 2004). Many studies have used TMI to study variables that are indirectly influenced by hydrological processes, such as soil chemistry (Band et al. 1993; Whelan and Gandolfi 2002) and plant species richness (Hwang et al. 2011; Zinko et al.

2005). TMI has been shown to be an effective proxy for depth to water table and the distribution of vadose zone soil moisture for the eastern U.S., if sufficient samples in each sampling locations are obtained and appropriate scales of DEM data are used (Tague et al. 2010; Tenenbaum et al. 2006). Therefore TMI was also estimated at both MODIS and Landsat scales using DEM data and was compared with field measured soil moisture to evaluate the ability of TMI to measure soil moisture conditions in the New England area.

## 2.2. Data and Methodology

### 2.2.1 MODIS Data and Processing

This study incorporated a variety of satellite data sources, including 8-day standard V005 MODIS Nadir BRDF-Adjusted reflectance (NBAR) (MCD43A4) (Schaaf et al. 2002; Schaaf et al. 2011) and daytime land surface temperature (LST) (MOD11A1) (Wan et al. 2002). The spatial resolution of the NBAR data is 500 m, while LST is provided at 1 km. The MODIS products were downloaded from the NASA Reverb website (<http://reverb.echo.nasa.gov/reverb>). High quality remotely sensed data were filtered based on the data quality flags. All of the MODIS data were originally in a Sinusoidal (SIN) projection, and reprojected into NAD\_1983\_StatePlane\_Massachusetts\_Mainland\_FIPS\_2001. TVDI was estimated using the multiday NBAR data and the daily LST that fell within the retrieval range.

Table 2.1 lists all the NBAR and LST data selected (based on data quality) in 2010 and 2011 and used to estimate TVDI.

Table 2.1. Acquisition date of both MODIS NBAR data and LST data.

Year	Type	DOY	Type	DOY
2010	MCD43A4	97	MOD11A1	104
	MCD43A4	145	MOD11A1	145
	MCD43A4	145	MOD11A1	146
	MCD43A4	169	MOD11A1	172
	MCD43A4	201	MOD11A1	208
	MCD43A4	209	MOD11A1	213
	MCD43A4	225	MOD11A1	231
	MCD43A4	233	MOD11A1	239
	MCD43A4	241	MOD11A1	242
	MCD43A4	241	MOD11A1	243
2011	MCD43A4	193	MOD11A1	197
	MCD43A4	225	MOD11A1	225
	MCD43A4	225	MOD11A1	229
	MCD43A4	241	MOD11A1	241
	MCD43A4	281	MOD11A1	281
	MCD43A4	305	MOD11A1	309

NDVI values calculated from NBAR were resampled to 1 km to be comparable with the 1 km surface temperature data. Since NDVI usually saturates in dense vegetation (Huete et al. 1997); as an alternative, a few additional vegetation indices (Table 2.2), including Ratio Vegetation Index (RVI) (Pearson and Miller 1972), Soil-Adjusted Vegetation Index (SAVI) (Huete 1988) and the two band Enhanced Vegetation Index (EVI2) (Huete et al. 1994; Jiang et al. 2008) were also used to calculate TVDI. RVI was calculated as the ratio of near infrared and red band which is not normalized like the other three indices. SAVI

was created in order to remove the influence of a soil background, especially when the canopy coverage is around 0.5 (Huete 1988). EVI2 also considers the influence from a soil background and resolves the problem of using the noisy blue band in the traditional EVI (Jiang et al. 2008). EVI2 has been proved to effectively deal with index saturation in full canopy coverage locations (Jiang et al. 2008).

Table 2.2. Equations for the vegetation indices that were used to evaluate TVDI.

Index	Equation	Reference
Normalized difference vegetation index (NDVI)	$NDVI = \frac{NIR - RED}{NIR + RED}$	(Inamdar and Mitchell 2006)
Two-band Enhanced vegetation index (EVI2)	$EVI2 = \frac{2.5 \times (NIR - RED)}{NIR + 2.4 \times RED + 1}$	(Jiang et al. 2008)
Ratio vegetation index (RVI)	$RVI = \frac{NIR}{RED}$	(Pearson and Miller 1972)
Soil-adjusted vegetation index (SAVI)	$SAVI = \frac{NIR - RED}{NIR + RED + L} (1 + L)$	(Huete 1988)

### 2.2.2 Landsat Data and Processing

The Landsat5 Thematic Mapper (TM) has six bands in the visible and near infrared and one band (band 6) in the thermal infrared region. The spatial resolution is 30 m for band 1-5 and is 120 m for band 6. All Landsat TM data were downloaded from USGS GLOVIS website (<http://glovis.usgs.gov/>). The Landsat Ecosystem Disturbance Adaptive

Processing System (LEDAPS) (Masek et al. 2006) was used to convert the digital number (DN) value into the corresponding Top of Atmosphere (TOA) radiance and to do the atmosphere correction to surface reflectance. Valor and Caselles' method of calculating emissivity, which relates emissivity to the NDVI of a given land surface, was used to convert brightness temperature to real temperature (Valor and Caselles 1996). Because of the cloud effect and the long revisiting time of Landsat data, the data that can be used is limited. Only day of Year (DOY) 197, 229 and 309 in 2011 were selected based on their quality and the consideration of corresponding with selected MODIS data acquisition date.

2.2.3 The Digital Elevation Map (DEM) and the Topographic Moisture Index (TMI)  
DEM data (Figure 2.1 left) for the State of Massachusetts available from the MassGIS (<http://www.mass.gov/mgis/>) with a scale of 1:500 were used to create the Neponset Watershed slope map (Figure 2.1 right) based on the location of USGS gauge station in Milton Village.

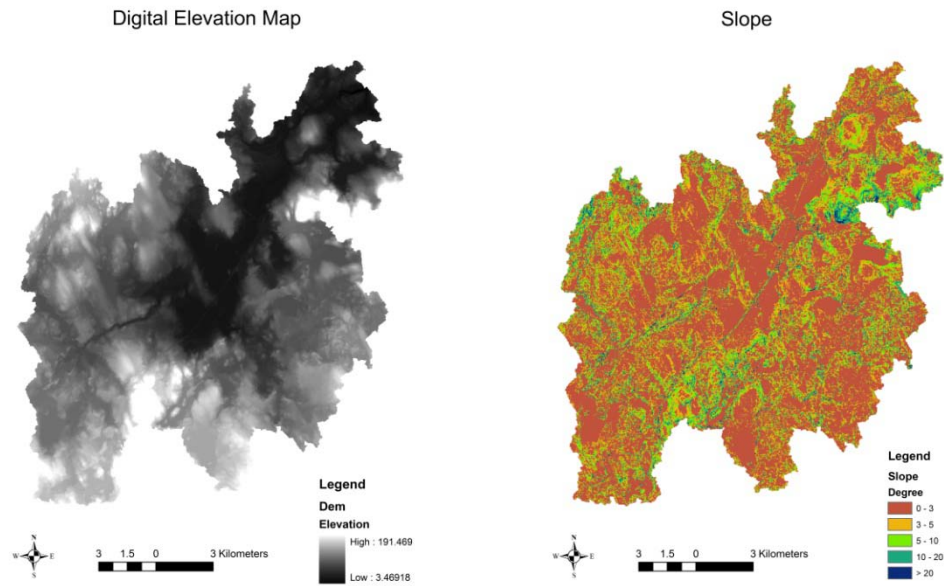


Figure 2.1. DEM for the Neponset Watershed and the slope map created from the DEM.

Topographic Moisture Index (also called Topographic Wetness Index) (Beven and Kirkby (1979)) which shows topographic conditions as a first-order control over hydrology was used in the TOPMODEL. It highly relates not only to wetness status but also indirectly to groundwater levels, soil pH and species distribution (Giesler et al. 1998; Moore et al. 1993; Rodhe and Seibert 1999; Tenenbaum et al. 2006; Zinko et al. 2005).

TMI is calculated by the following equation:

$$\text{TMI} = \ln(\alpha/\tan\beta) \quad (1)$$

where  $\alpha$  is the drainage area that all water flow through one point per unit contour line length and  $\tan\beta$  is the slope.

#### 2.2.4 Field Sampling of Soil Moisture in the Neponset Watershed

Soil moisture data were measured using a portable soil moisture impedance probe (ThetaProbe ML2x by Delta-T Inc.) over the Neponset Watershed. This device has an array of four steel pins, which are 6 cm in length and are inserted into the soil to measure soil moisture. Soil moisture is measured depending on the changes in the apparent dielectric constant. Systematic soil moisture measurements were performed at stratified selected sample locations (Figure 2.2), primarily during the vegetation growing season (April, 2011 to November, 2011). TVDI reflects the dryness condition mostly for the root zone, which varies with study area and seasons (Sims et al. 2008). Earlier research indicated that TVDI is more related to the soil moisture at 0-10 cm depth by comparing the relationship between TVDI and 10 cm, 20 cm and 30 cm soil moisture measurements (Patel et al. 2009). The soil depth of the study area is shallow, so they are still comparable even though the field measured soil moisture is from the surface 6 cm.

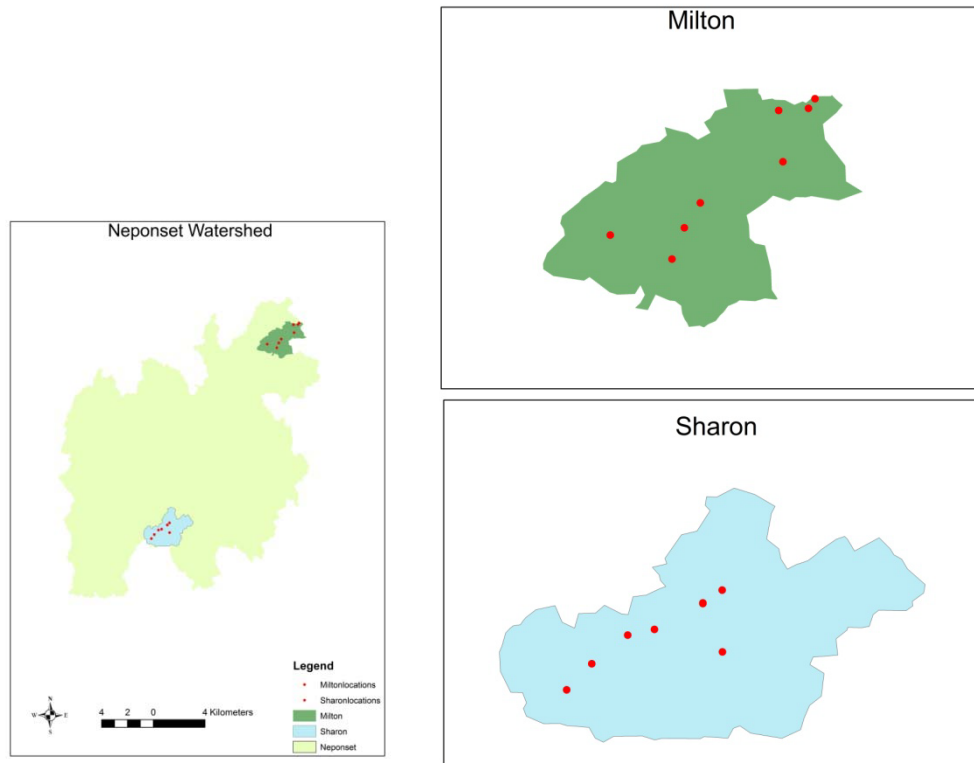


Figure 2.2. Sampling Locations in the Neponset River Watershed.

Sampling was conducted in two sub-basins of the Neponset River Watershed. One is in the Milton area, which represents more of an urban environment, and the other is in the Sharon region, which represents more of a forest environment. They will be referred later in the dissertation as Milton and Sharon respectively. Eight sampling locations were chosen based on the Topographic Moisture Index (TMI) gradient in each sub-basin. Six of the eight Milton urban sampling locations were in residents' back yards and the other two were in two schools' playgrounds. Seven of the eight forest sampling locations were in dense forest and one was in grassland. The sampling locations were chosen to be representative and homogeneous within each 5 m by 5 m sampling plot. Tague et al. (Tague et al. 2010) indicated that sufficient samples within a plot can avoid problems

associated with fine scale spatial heterogeneity and improve the accuracy of field measurements. 25 samples were collected and averaged in each sampling plot. Cylindrical soil cores (10 cm long, 5 cm diameter) were also collected from sampling sites and then analyzed in lab to measure the gravimetric soil moisture to calibrate the Theta Probe.

The errors from the Theta probe itself are  $\pm 0.01 \text{ m}^3/\text{m}^3$  and vary depending on the calibration method applied. If the generalized calibration is used, the errors associated with this are  $\pm 0.04 \text{ m}^3/\text{m}^3$  (Theta probe user manual). The soil-specific calibration method was tested to see whether it is acceptable to use the generalized calibration. The soil-specific calibration method is based on the following two equations:

$$\sqrt{\varepsilon} = 1.07 + 6.4V - 6.4V^2 + 4.7V^3 \quad (2)$$

$$\sqrt{\varepsilon} = a_0 + a_1 \times \theta \quad (3)$$

where  $\varepsilon$  is the dielectric constant,  $V$  is the Theta probe output,  $a_0$  and  $a_1$  are the soil specific parameters that need to be calibrated. The Theta probe output is converted to dielectric constant (Equation 1) to calculate the soil specific parameters (Equation 2).

The soil at most of the urban sampling locations was mineral soil while organic soil dominated the forest sampling locations. Cylindrical soil cores were collected for each of the sampling locations (except one site due to the resident declining permission) and they were grouped into two types: mineral and organic soils. All of the soil cores were weighed and measured with the millivolt output using the Theta probe first, and then dried down in an oven at a relatively high temperature. The average difference between

the true soil moisture and the generalized calibrated soil moisture is around 0.03 which is at the same order of magnitude as the sampling uncertainty for estimating the plot mean. This is also consistent with earlier research results (Tague et al. 2010). So the generalized calibrations for soil moisture were used in this study.

#### 2.2.5 Field Sampling of Soil Moisture in the Greater Boston Area

Soil moisture samples collected in the Greater Boston Area were provided by Professor Lucy Hutyra's group working on the Ultra-Ex Boston project (Rao et al. 2013). The sampling period was between June and August 2010. Two transects (Figure 2.3) were established across the Greater Boston Area. Both of them extend from the downtown Boston to the west. The northern transect starts from the downtown core, and passes through high density suburbs, low density suburbs and into rural areas. The southern transect follows a major transportation corridor from the City of Boston, through Framingham to Worcester, MA. Three land use classes (forest, residential, other developed) based on 30 m NLCD and three urban classes (high population urban, lower population urban and rural) were chosen and at least 15 plots were sampled for any given combination of land use and urban classes. Within a 990 x 990m neighborhood around a cell, places with more than 25% impervious surface area were classified as urban areas. Population density was further used to classify urban areas to high population urban and low population urban classes. The soil moisture samples collected between DOY 213 and 221 were used to compare with TVDIs calculated from MODIS data based on the availability of MODIS data.

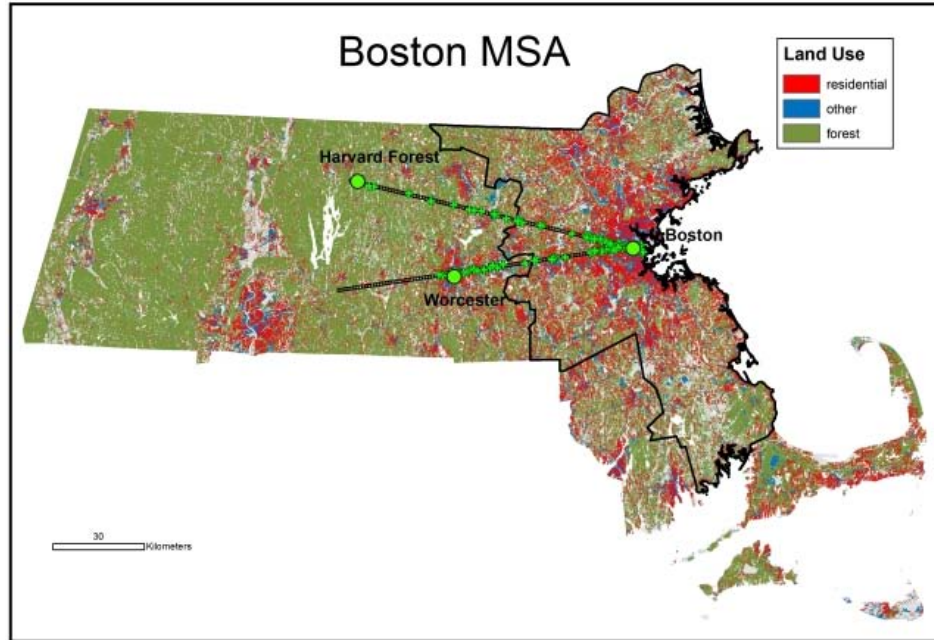


Figure 2.3. Sampling locations of the ULTRA-EX project among the two transects (Rao et al. 2013).

### 2.2.6 TVDI

Theoretically, the plot of the vegetation index and land surface temperature forms a triangle shape in a heterogeneous landscape (Sandholt et al. 2002). The estimation of the hypotenuse is a key process of the TVDI calculation. The NDVI-LST slope relates to the dryness conditions and has been used in land use change mapping, land use classification, and ET estimation (García et al. 2013; Julien et al. 2011; Nemani and Running 1988; Sobrino and Raissouni 2000). TVDI was calculated from an empirical interpretation of the  $VI - T_s$  space (Figure 2.4), which is normally triangular if the land cover of the area is heterogeneous enough (Sandholt et al. 2002). TVDI can be calculated using the following equation (5):

$$TVDI = \frac{T_s - T_{s-\min}}{T_{s-\max} - T_{s-\min}} \quad (5)$$

where  $T_s$  is the observed surface temperature at a given pixel, and  $T_{s-\min}$  is the minimum surface temperature (at a given VI) from the wet edge of the VI-  $T_s$  triangle space.  $T_{s-\max}$  is the maximum surface temperature (at a given VI) from the dry edge of the NDVI- $T_s$  triangle space. Estimating the dry edge is most important for the TVDI calculation; the automatic envelope method developed by Nemani and Running was used (Nemani et al. 1993; Nemani and Running 1988). The equation (6) of  $T_{s-\max}$  is:

$$T_{s-\max} = a + b \times NDVI \quad (6)$$

where  $a$  and  $b$  are the slope and the intercept of the regression line of the dry edge, respectively. The values that construct the dry edge are selected by data sorting, and then linear regression is applied to these selected data to obtain the slope and the intercept.

This process is repeated until the following criteria are satisfied simultaneously:

- (1) The  $R^2$  value of the linear regression is larger than 0.70
- (2) The change of the slope (from the previous iteration) is less than 10%
- (3) The change of the intercept (from the previous iteration) is less than 10%

Thus, equation (7) can be rewritten as:

$$TVDI = \frac{T_s - T_{s-\min}}{a + b \times NDVI - T_{s-\min}} \quad (7)$$

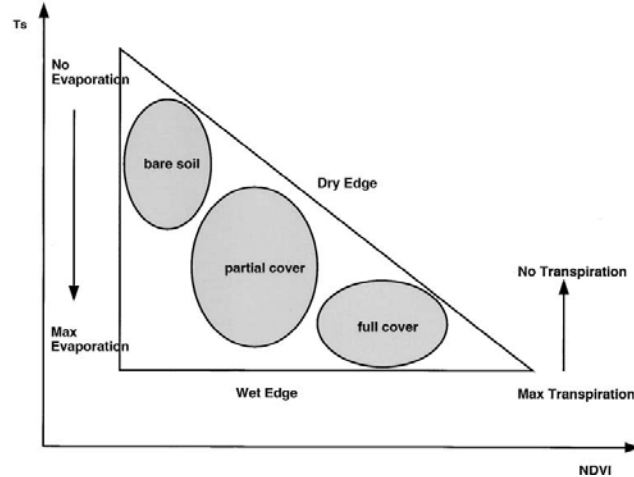


Figure 2.4 Simplified Ts/NDVI plot (Sandholt et al. 2002).

### 2.2.7 Statistical methods

When analyzing field measured soil moisture, the following statistical methods were used: mean, standard deviation (SD), coefficient of variation (CV) and the nonparametric Spearman's test.

The nonparametric Spearman's test was applied to evaluate the difference between TVDI values calculated using different VIs. The Spearman's rank correlation coefficient is expressed as equation (4):

$$R_s = 1 - \frac{6 \sum_{i=1}^N (R_{ij} - R_{ij'})^2}{n(n^2 - 1)} \quad (4)$$

Where  $R_{ij}$  is the rank of TVDI value of one pixel when using one VI and  $R_{ij'}$  is the rank of TVDI value of the same pixel when using another VI.

## 2.3. Results and Discussions

### 2.3.1 Analysis of the Slope Data and TMI of the Two Sub-basins

The Neponset Watershed is flat, especially near the main Neponset river channel. More than half of the Neponset Watershed's slope is less than 3 degrees. The elevation difference along 20 miles of river channel is just 2 feet at the middle of the Neponset River. Most of the steep slope area is located around the Blue Hill. The slope of the two sample sub-basins is also low. The forest sub-basin has more area with a slope greater than 7 degrees and the maximum slope in the forest sub-basin is also larger than the urban sub-basin (Figure 2.5).

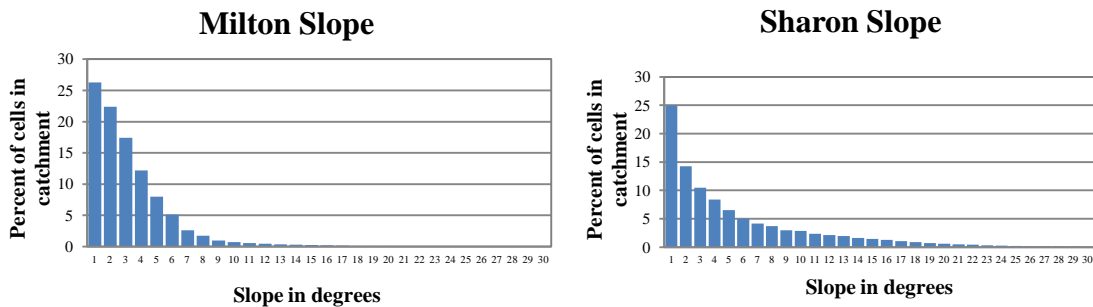


Figure 2.5. Histogram of the two sub-basins' slope.

The urban sub-basin is urbanized with 71.71% of the area classified as developed, while the forest sub-basin has only 22.98% developed area and 68.68% vegetation area (dominated by deciduous forest).

## Topographic Moisture Index

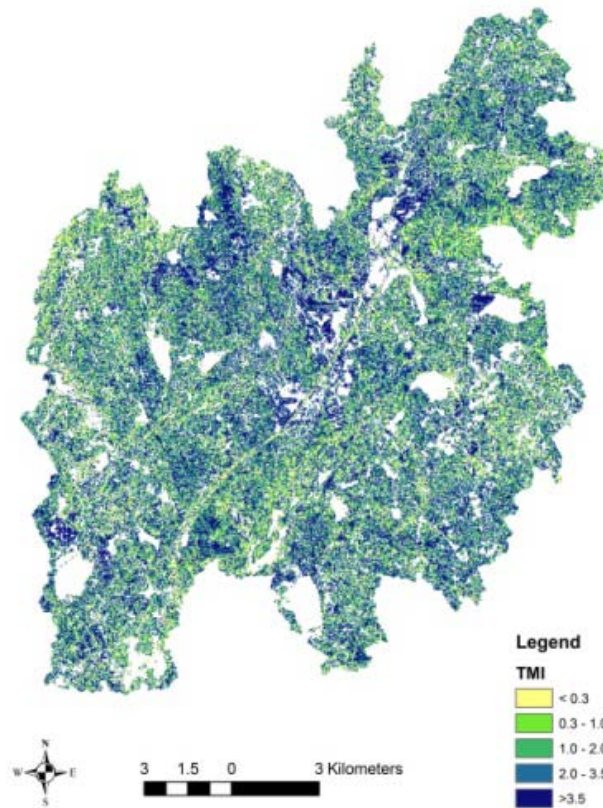


Figure 2.6. Topographic Moisture Index (TMI) calculated from the 5 m DEM map.

TMI, a relative index of the wetness status, is estimated based on the contributing drainage area and slope. The flatter areas are wetter (higher TMI value) than the steeper areas with the same drainage area. However, this method cannot work when the slope goes to zero. The white space in Figure 2.6 represents this case and indicates very wet conditions.

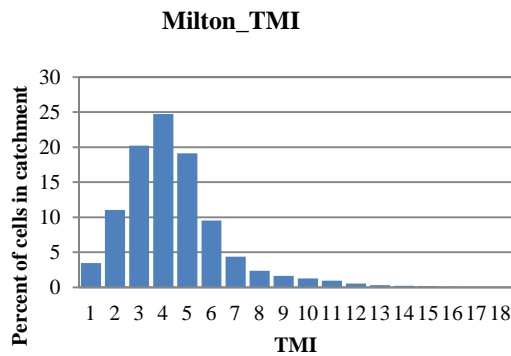
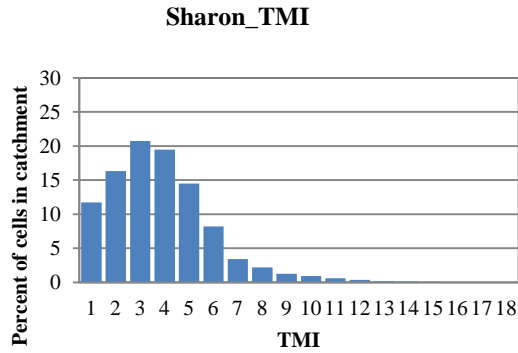


Figure 2.7. Histogram of TMI for the two sampling sub-basins.

The Milton area is wetter than the Sharon area (Figure 2.7) because Sharon has steeper slopes, and Milton is closer to the outlet of the Neponset River, while Sharon lies in the head of the basin.

### 2.3.2 Analysis of the Field Sampled Soil Moisture Data

Field measured soil moisture apparently follows precipitation variation, with relatively low soil moisture condition during less precipitation period in summer (Figure 2.8). The highest soil moisture over the sampling period is in late September and October while the

lowest soil moisture happened in late July and early August. However, the highest soil moisture did not occur after the highest precipitation event (August 19, 2011) in the sampling period because of a relatively long dry period and low antecedent moisture condition before the precipitation. The soil moisture measured from the forest sub-basin (standard deviation is 0.07) has higher temporal variation than that in the urban sub-basin (standard deviation is 0.05). The soil moisture in the forest sub-basin is higher than that in the urban sub-basin, except in July and August because of irrigation in the summer in the urban area. During the dry period in late July, soil moisture in both sub-basin decreases gradually while the soil moisture in the urban sub-basin is higher than that in the forest sub-basin.

#### 2.3.2.1 Variation of Soil Moisture in Plot and in the Watershed

Figure 2.9 and Figure 2.10 are box plots of field measured soil moisture over the sampling period. Each box is based on soil moisture measured from the eight sampling plots. Soil moisture in the urban sub-basin is more variable among different sampling plots than in the forest sub-basin. Spatial variation among various sampling sites is usually greater than temporal variation among different sampling dates, especially for the urban sub-basin. The high spatial variation observed in this study area is consistent with earlier studies (Brocca et al. 2010; Tague et al. 2010). The mean CV is 0.27 for the urban sub-basin and 0.18 for the forest sub-basin. A one-way Anova test shows the CV in Milton is significantly higher than the CV in Sharon (p-value= 0.0002).

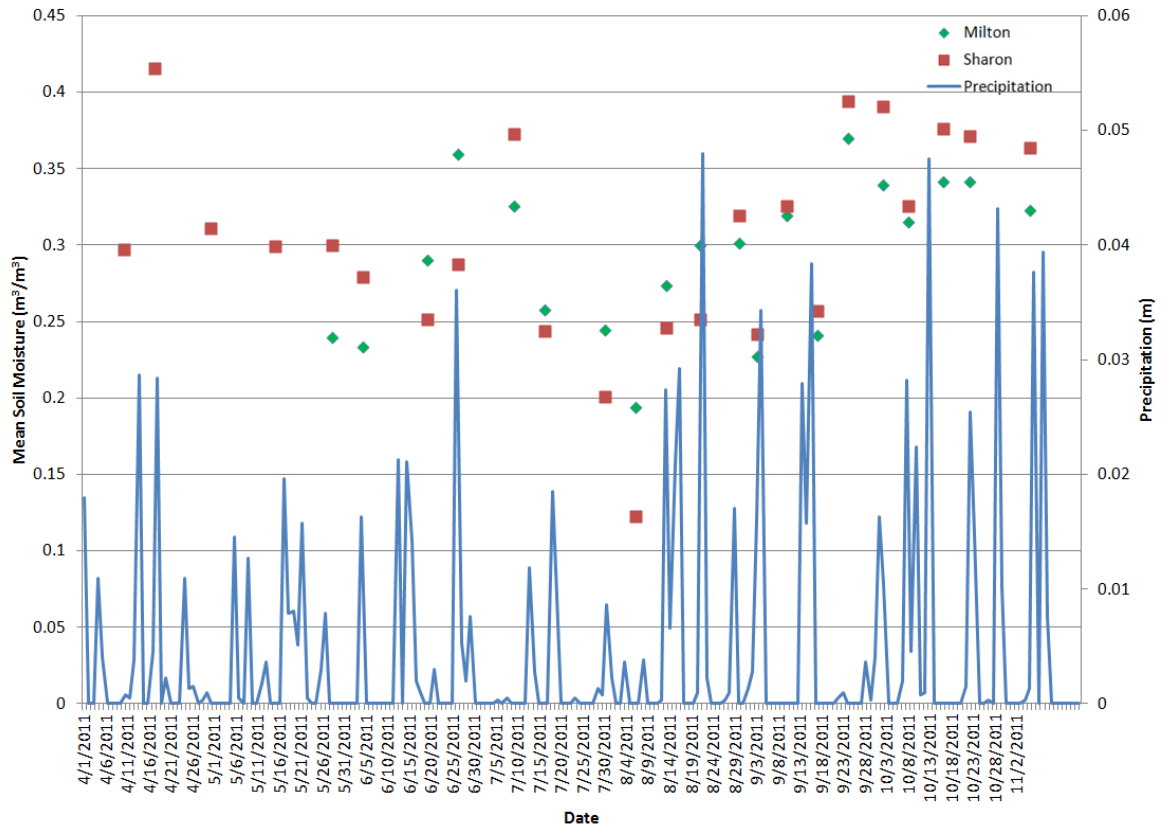


Figure 2.8. Temporal patterns of mean soil moisture in both Milton and Sharon.

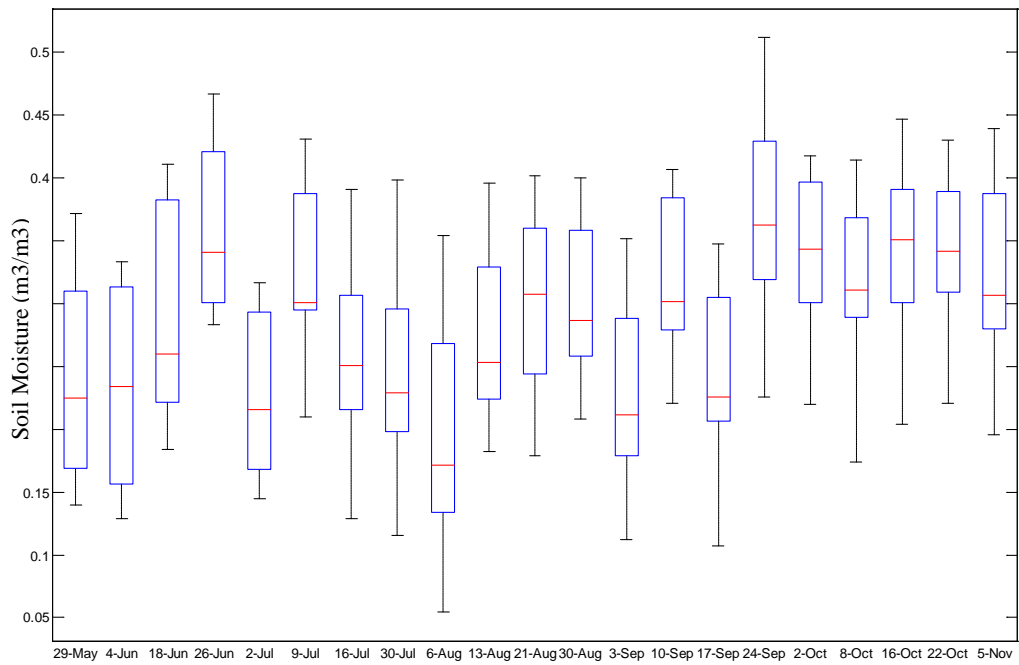


Figure 2.9. Boxplot of field measured soil moisture in the Milton area over the sampling period.

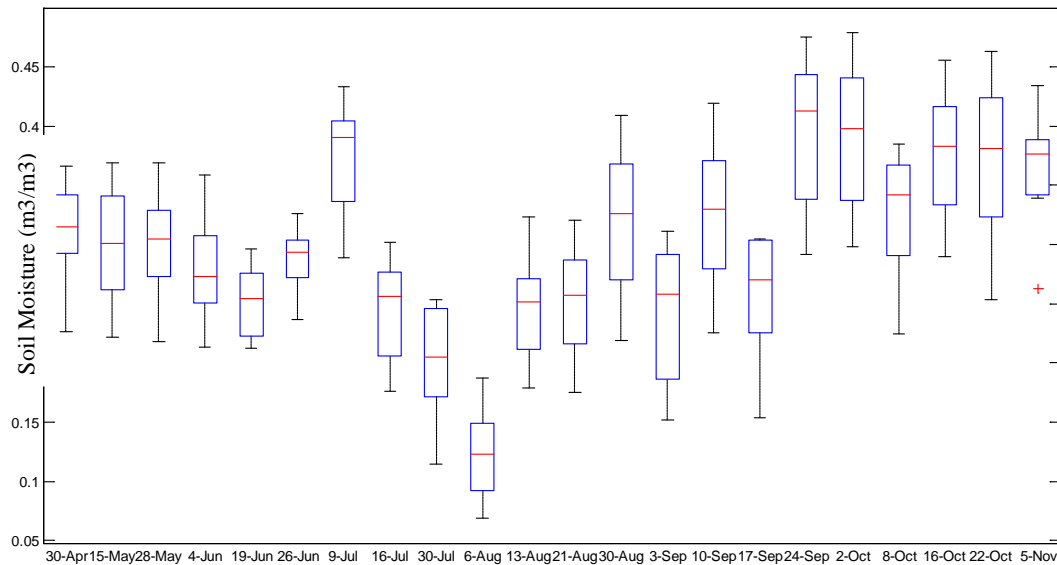


Figure 2.10. Boxplot of field measured soil moisture in the Sharon area over the sampling period.

Several studies indicate a strong negative correlation between the soil moisture and CV, meaning soil moisture is more variable in drier conditions (Brocca et al. 2007; Famiglietti et al. 2008; Penna et al. 2009; Tague et al. 2010), which is also observed in this study area (Figure 2.11). The CV in the urban sub-basin has a steeper and stronger negative relationship with soil moisture ( $R^2=0.79$ ) than that in the forest sub-basin ( $R^2=0.43$ ). The stronger negative relationship between CV and soil moisture in urban sub-basin is caused by the irrigation during the summer dry period which decreased the variance of soil moisture among various sampling sites. The value of CV in both the urban and forest sub-basin is relatively lower than the CV range reported by Famiglietti et al. [2008] and is similar to those observed by Brocca et al. [2007] and Tague et al. [2010].

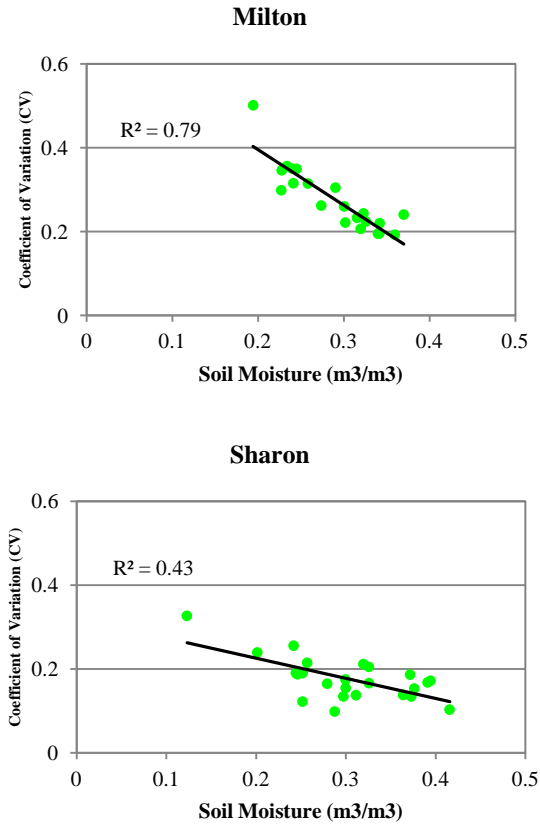


Figure 2.11. The linear relationship between soil moisture and CV in two sub-basins.

### 2.3.2.2 Spatial Patterns of Measured Soil Moisture in Relation to TMI

Figure 2.12 shows the correlation between TMI and measured soil moisture on each sampling date. The average  $R^2$  for all the sampling dates between TMI and measured soil moisture is 0.28 in Milton and 0.32 in Sharon. In Milton, the highest correlation between measured soil moisture and TMI happens in July with an  $R^2$  of 0.68. This high correlation may be introduced by irrigation because this is a dry season and the soil moisture from Milton is consistently higher than in Sharon. The  $R^2$  is less than 0.5 during all the other dates and is especially low in the fall in Milton. The  $R^2$  varies from 0.43 to 0.15 in

Sharon and is more stable than Milton. The overall  $R^2$  values in both sub-basins are lower than those found by several other studies. In a mountain area in central-eastern Italian Alps,  $R^2$  was reported as 0.58 and 0.64 (Penna et al. 2009). In an undeveloped watershed,  $R^2$  between measured soil moisture and TMI was observed as high as 0.74. In a developed watershed close to the undeveloped watershed, the highest  $R^2$  was 0.32 (Tenenbaum et al. 2006). The results from this study area are more similar to the  $R^2$  reported from an arid watershed in Australia, in which the highest  $R^2$  was 0.54 and the average  $R^2$  is about 0.3 (Western et al. 1999). Several studies reported higher  $R^2$  values during wetter conditions (Tenenbaum et al. 2006; Western et al. 1999). However, this was not found in this study area. For the urban sub-basin, the main reason for this may be the irrigation during dry season which could have dampened the pattern. For the forest sub-basin, the small variation of slope may be the reason. The relatively low correlation overall may be caused by the flat sub-basins such that TMI can not distinguish the small difference among sampling plots. No significant relationship can be observed between TMI and measured soil moisture over these field sites in the Greater Boston Area (Figure 2.13). This may also be due to the lack of gradient of both measured soil moisture and TMI.

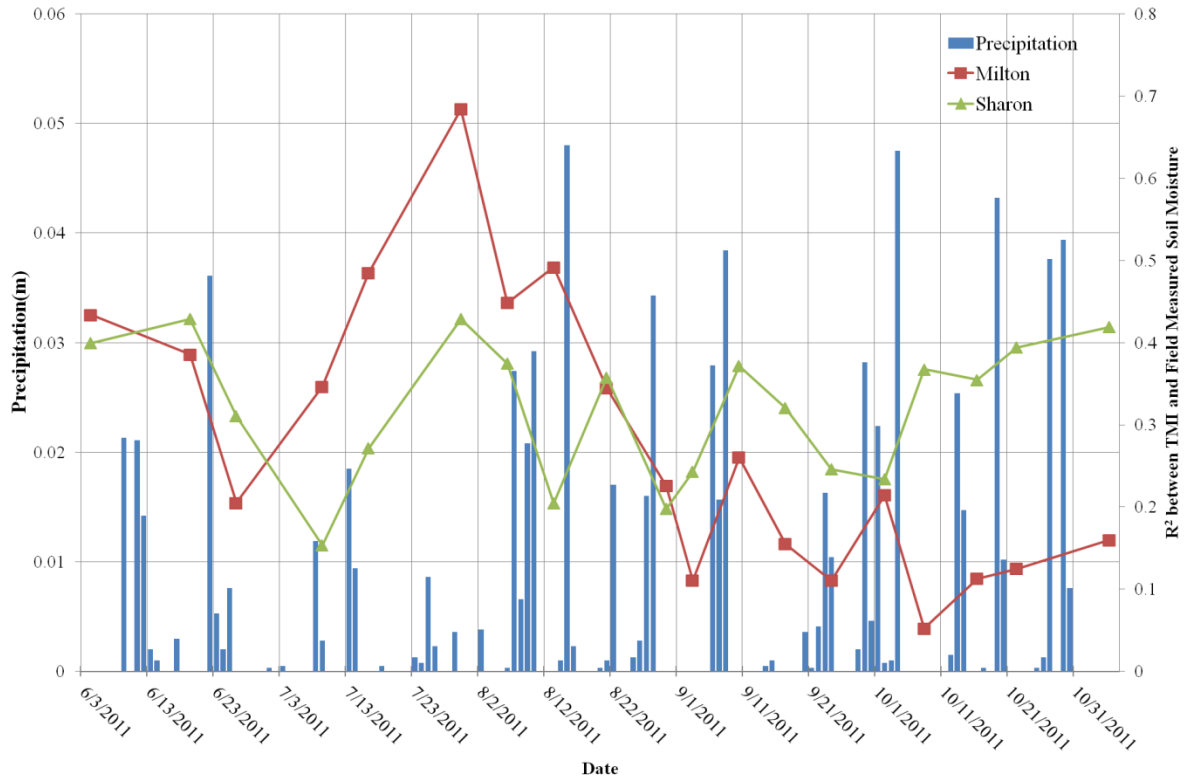


Figure 2.12. Coefficient of determination between soil moisture and TMI vs. sampling date in two sub-basins in the Neponset River Watershed and the precipitation data.

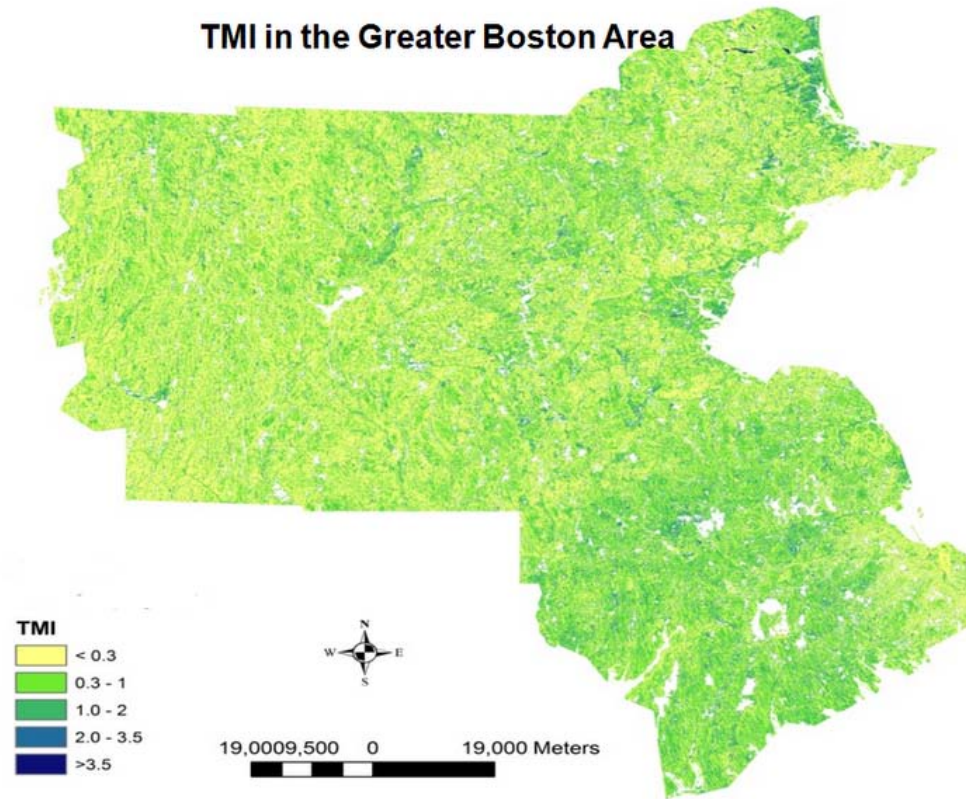


Figure 2.13. TMI of the eastern part of Massachusetts.

### 2.3.3 TVDIs calculated from MODIS data

Based on the quality of both MODIS NBAR and surface temperature data, ten combinations of MOD43A4 and MOD11A1 from 2010 and six combinations from 2011 were selected to calculate TVDI using the four VIs over the Greater Boston Area.

#### 2.3.3.1 TVDIs calculated from 2010 MODIS data

Figure 2.14 shows the slopes of the VI-LST dry edges on multiple dates. Higher slopes mean flatter regression lines while lower slopes mean steeper regression lines. The slopes of NDVI-LST dry edges in this study are comparable with the range of slopes reported by *Chen et al.* (Chen et al. 2011). Research conducted in Vietnam also reported a similar slope during October, however, a much steeper slope during April (Patel et al. 2009). Slopes of RVI –LST plots are always the highest among all the VIs for all the 10 days, which suggests that RVI works differently as the other three normalized VIs. The slopes of EVI2-LST plots are almost parallel with SAVI-LST plots with the slope of EVI2-LST consistently higher. The slopes of NDVI-LST plot are higher than those of EVI2-LST and SAVI-LST during most days among the 10 days, except on June 21<sup>st</sup>, 2010. Although the slopes of NDVI-LST plots show different trends from April to early August, they are parallel with the EVI2-LST and SAVI-LST in late August. All slopes using NDVI, EVI2 and SAVI are related to recent precipitation, which can be clearly seen from August 19<sup>th</sup> 2010 which is before a storm, and August 27<sup>th</sup>, 2010 which is after that storm.

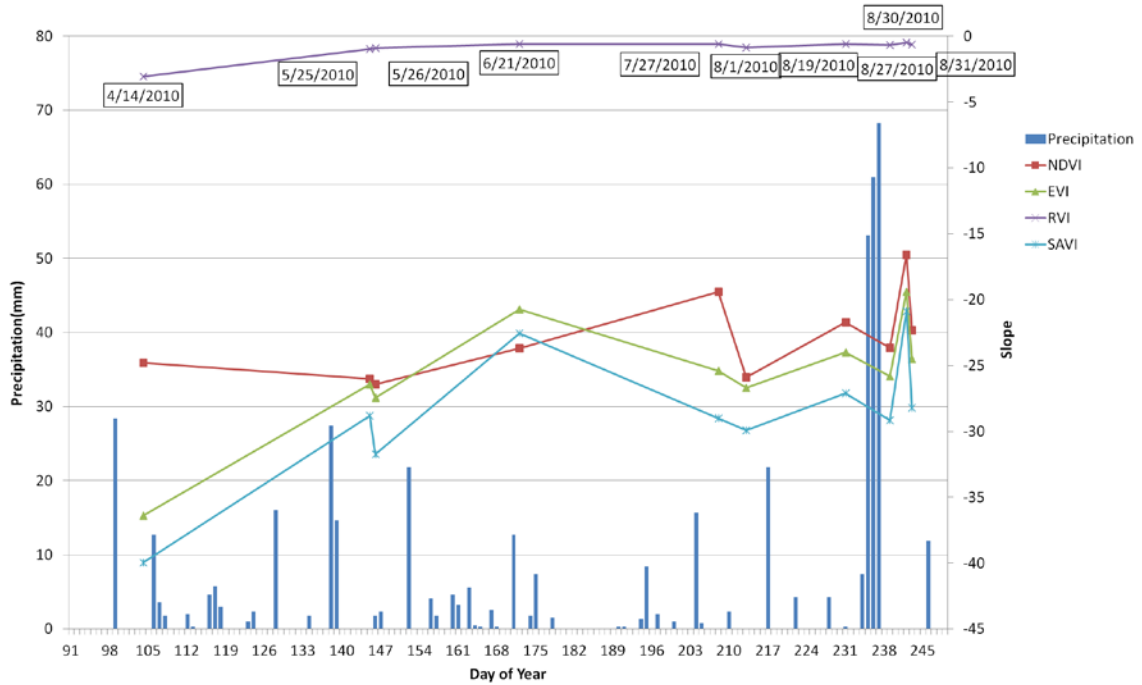


Figure 2.14. Slope of VI-LST plot on different days shown with precipitation data.

Different lines show slopes using various vegetation indices.

Figure 2.15 shows the intercepts of the VI-LST plots' dry edges. The range of intercepts of the VI-LST plots is comparable with earlier studies (Chen et al. 2011; Patel et al.

2009). Intercepts of NDVI-LST plots are the highest among all the four VIs and

intercepts of EVI2-LST plots and SAVI-LST plots still follows a similar trend, while the

intercepts of EVI2-LST plots are a little higher. Intercepts of RVI-LST plots are always

lower than the other three and have similar trends to the intercepts of NDVI-LST plots.

April 14<sup>th</sup>, 2010 is before the growing season, so TVDI estimated using LST and VIs

does not properly show the surface soil moisture status on that day. On June 21<sup>st</sup>, 2010,

however the NDVI-LST plot has a steeper slope and a higher intercept than the EVI2-

LST plot and the SAVI-LST plot. On July 27<sup>th</sup>, 2010, the slope of NDVI-LST plot is less

than that of the EVI2-LST and SAVI-LST plots, and the intercept of the NDVI-LST plot is the same as the SAVI-LST plot and larger than the EVI2-LST plot. The slope of the NDVI-LST plot is flatter and has a larger intercept than EVI2-LST and SAVI-LST on August 1<sup>st</sup>, 2010. These differences indicate that NDVI works differently from EVI2 and SAVI in the development of TVDI values. The steeper slope of the SAVI-LST plot than that of the EVI2-LST plot is mainly due to the larger EVI2 value than SAVI under the same amount of leaf area index.

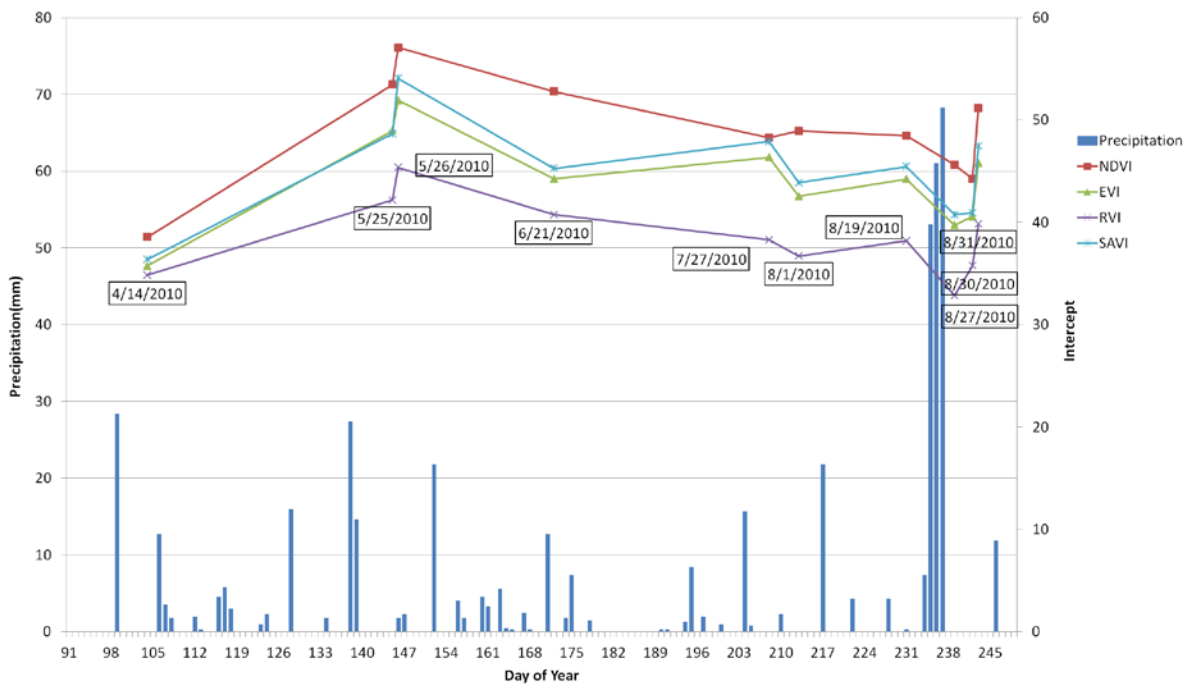


Figure 2.15. The intercept of VI-LST plots on different days shown with precipitation data. Different lines show intercepts using various vegetation indices.

The Spearman test was used to estimate the correlation of the rank of each pixel's TVDI value among the four VIs because TVDI is calculated as a scaled value (Figure 2.16).

TVDIs calculated using EVI2 and SAVI always have the highest correlation while RVI derived TVDIs has the lowest correlation especially on August 31<sup>st</sup>, 2010. All the comparisons are statistical significant (p-value <0.005). This is consistent with the earlier statement that RVI functions differently from the other three VIs. Figure 2.17 shows the comparison of TVDIs calculated using NDVI and EVI2. TVDI calculated using NDVI tends to be higher than TVDI calculated using EVI2, especially in the drier areas (e.g. the Boston Downtown core).



Figure 2.16. Spearman's test coefficient of TVDIs using various VIs.

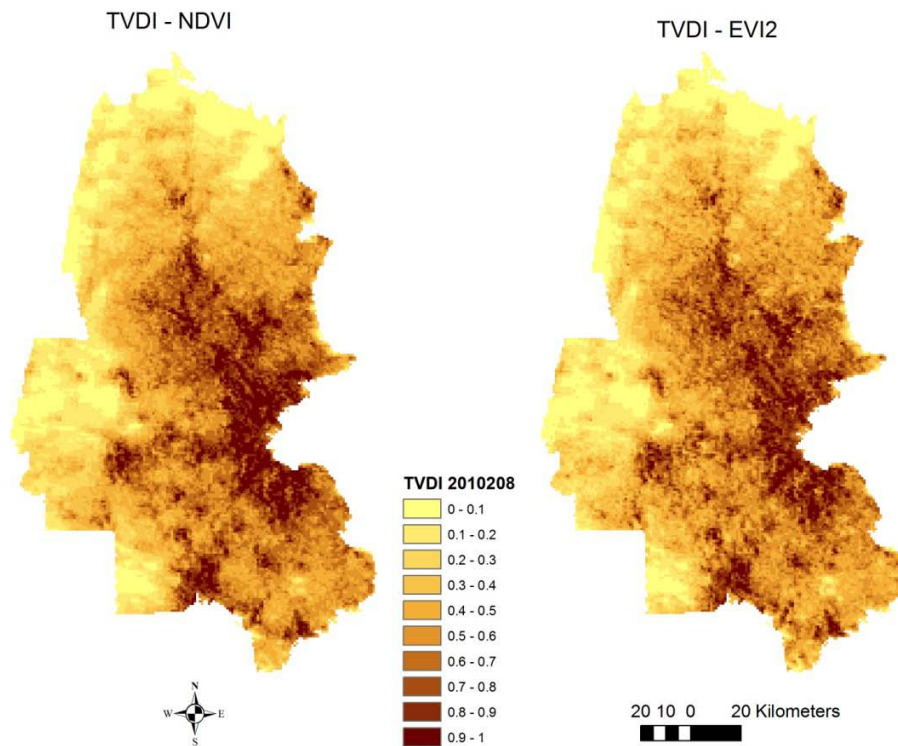


Figure 2.17. TVDI calculated using NDVI and EVI2 from MODIS on day 208 of year 2010.

### 2.3.3.2 TVDIs calculated from 2011 MODIS data

Six combinations of MODIS NBAR and LST data were selected to calculate TVDI in 2011 based on data quality and cloud coverage. All TVDIs using various VIs show similar rural-to-urban dryness trends on different days. They all show that the City of Boston is consistently drier than the rural area surrounding it. NDVI derived TVDI has more dry area than all of the other three VI derived TVDI methods on July 7<sup>th</sup>, 2011. The intercept of the NDVI-LST plot is lower than that of the SAVI-LST plot and the same as that of the EVI2-LST plot on July 16<sup>th</sup>, 2011 (Figure 2.19). The dry edge of the NDVI-

LST plot is lower than that of the other two, which produces the even drier condition in dry areas in NDVI derived TVDI.

The slopes of RVI-LST are very flat and close to zero, which is consistent with the results in 2010 (Figure 2.18 and Figure 2.14). Slopes of the other VI-LST plots have similar trends, with the slope of the NDVI-LST plot being the highest. They all drop in late August which is the same as the results from August 2010. This may be due to the high evapotranspiration during late summer, which increases the land surface temperature differences among different canopy coverages. The decreasing trend of intercepts (Figure 2.19), which can be interpreted as a dropping of bare soil temperature, shows the opposite of the the change of slopes, which is also similar to the results from 2010 (Figure 2.15). The intercepts of NDVI-LST are higher than all the other VI-LST plots, except on July 16<sup>th</sup>, 2011. The dry edges of TVDI on the MODIS scale have similar seasonal trends between the two years, suggesting the importance of vegetation on soil moisture status.

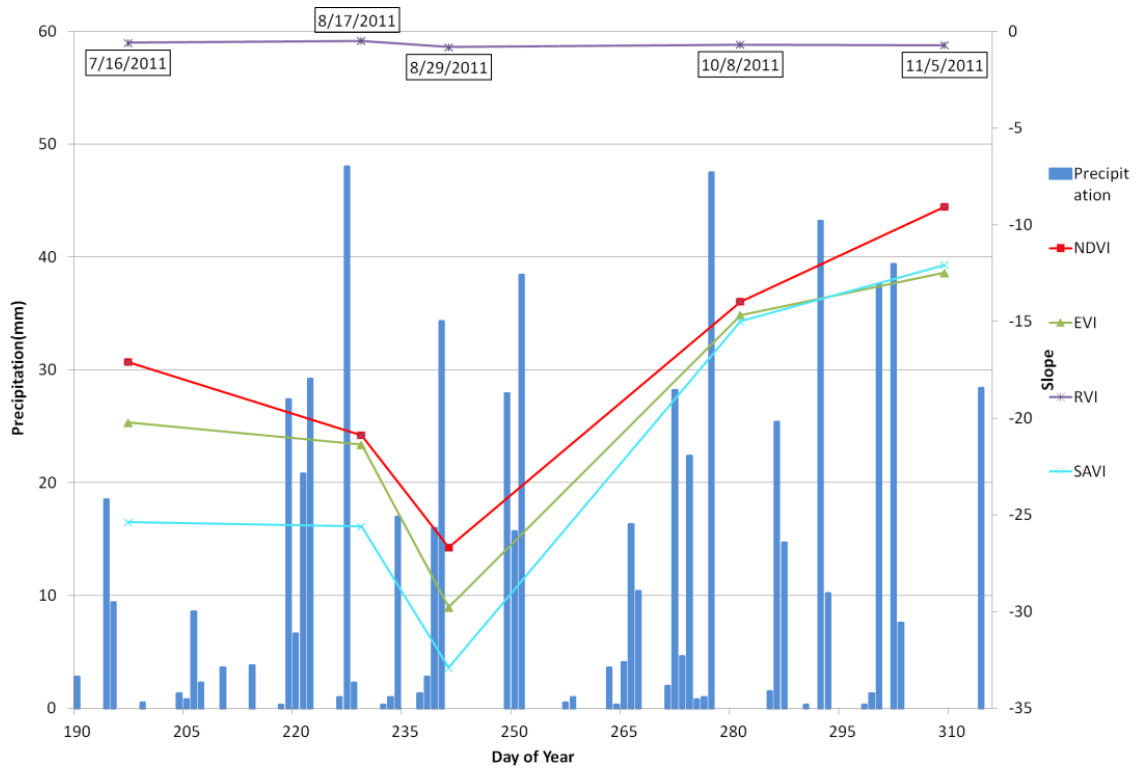


Figure 2.18. Slope of VI-LST plot on different days shown with precipitation data in 2011. Different lines show slope using various vegetation indices.

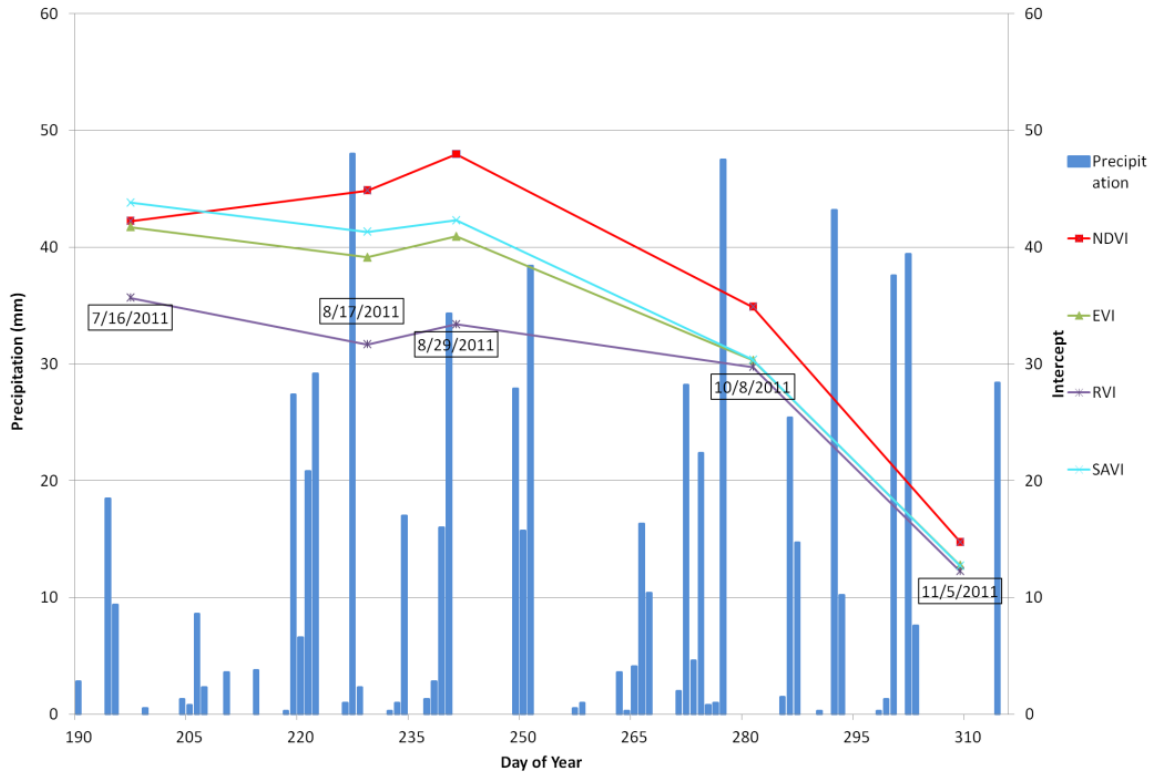


Figure 2.19. Intercept of VI-LST plot on different days shown with the precipitation data in 2011. Different lines show intercept using various vegetation indices.

The Spearman's test (Figure 2.20) shows that EVI and SAVI derived TVDIs always have the highest correlation among the six days sampled while RVI derived TVDIs have a lower correlation than NDVI, EVI and SAVI derived TVDIs. However, the correlation of RVI derived TVDIs is almost the same as the correlation of NDVI derived TVDIs on October 8<sup>th</sup>, 2011 and November 5<sup>th</sup>, 2011. The rank correlation coefficients are very high (close to 1) on these two days, suggesting that there is not much difference between the four VIs during the leaf secession period.

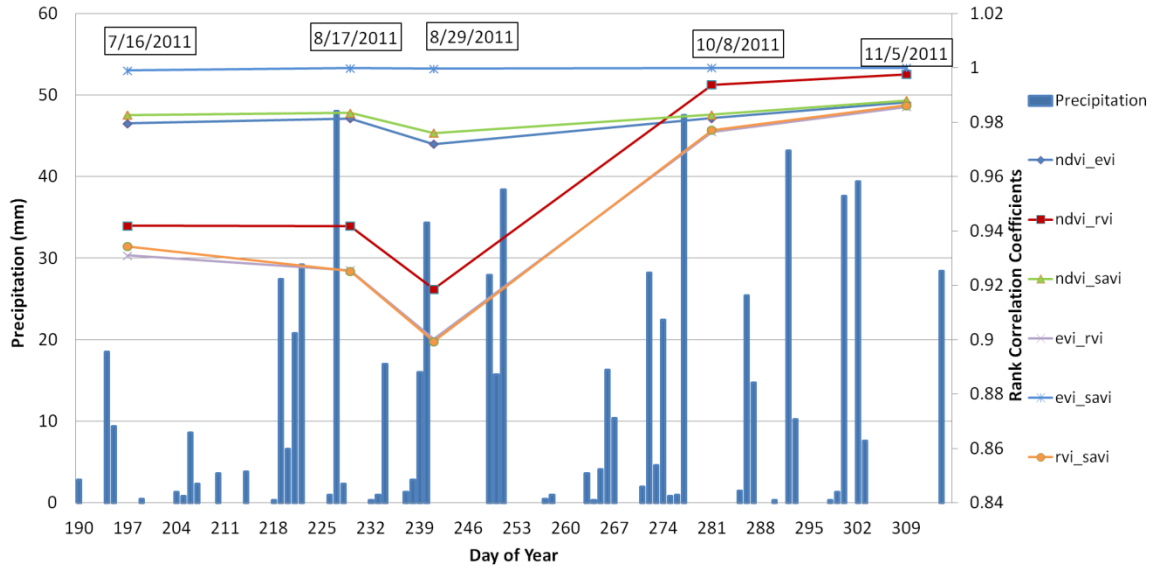


Figure 2.20. Spearman's test coefficient of TVDIs estimated using various VIs on different days in 2011.

### 2.3.4 TVDIs from Landsat data

RVI was not used for TVDI calculation using Landsat data because RVI is not an appropriate vegetation index for TVDI estimation during the green season, based on the above analysis. The comparison between TVDIs in Figure 2.21 also shows a similar trend in MODIS TVDIs; that TVDI calculated from NDVI tends to be higher than TVDI calculated from EVI2 (Figure 2.21).

Slopes of VI-LST derived from Landsat data are flatter than the slopes of VI-LST derived from MODIS data, which means a higher VI value was found at the same temperature for Landsat data (Figure 2.22). This flat slope was also reported by Wang *et al.* in an urbanized watershed in north China (Wang *et al.* 2010). The flatter slope is likely due to

the scale effect that occurs when the moderate spatial resolution MODIS data mixes the reflectance characteristics of vegetated areas with non-vegetated areas, while the fine resolution Landsat data has less mixed pixels. Since the Landsat TM only has one thermal band, which makes the split window method not suitable to calculate land surface temperature, the land surface temperature estimation method used here may also introduce some noise into the analysis.

There is no big difference among the intercepts of VI-LST plots using MODIS and Landsat data, except on August 17<sup>th</sup>, 2011 (Figure 2.23). This suggests that the scale effects of MODIS and Landsat on temperature for less canopy covered areas is not apparent in the resulting vegetation indices.

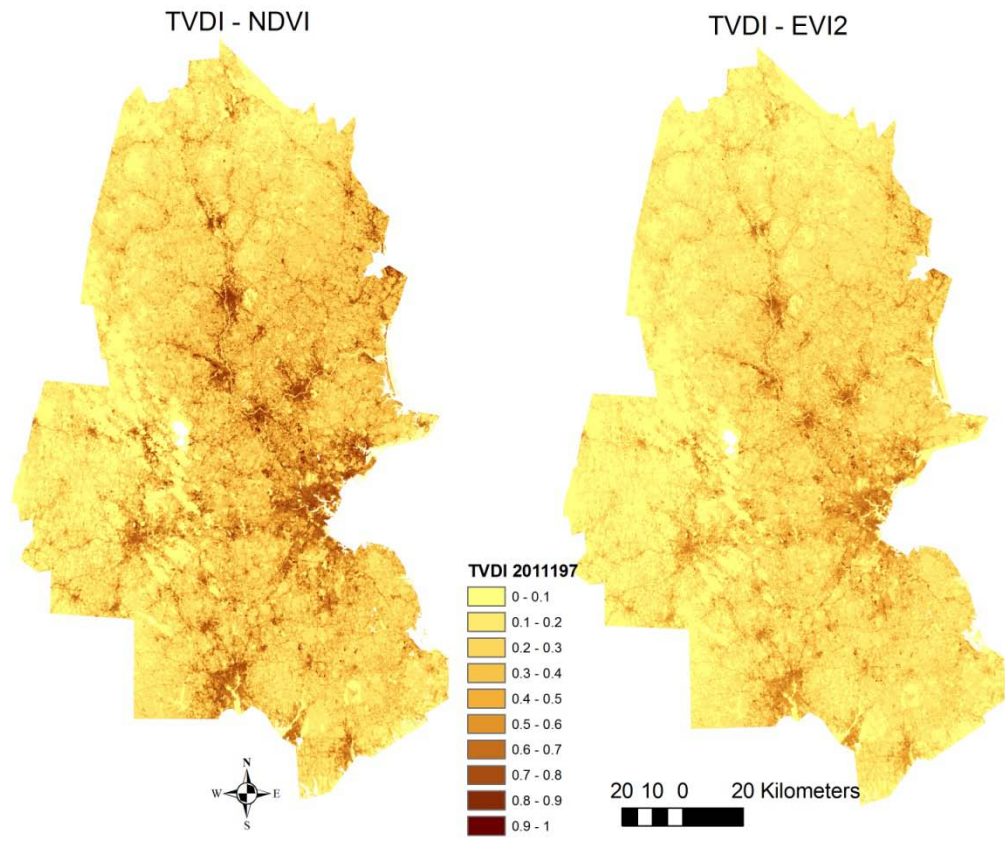


Figure 2.21. TVDI calculated using NDVI and EVI2 from Landsat data on day 197 of year 2011.

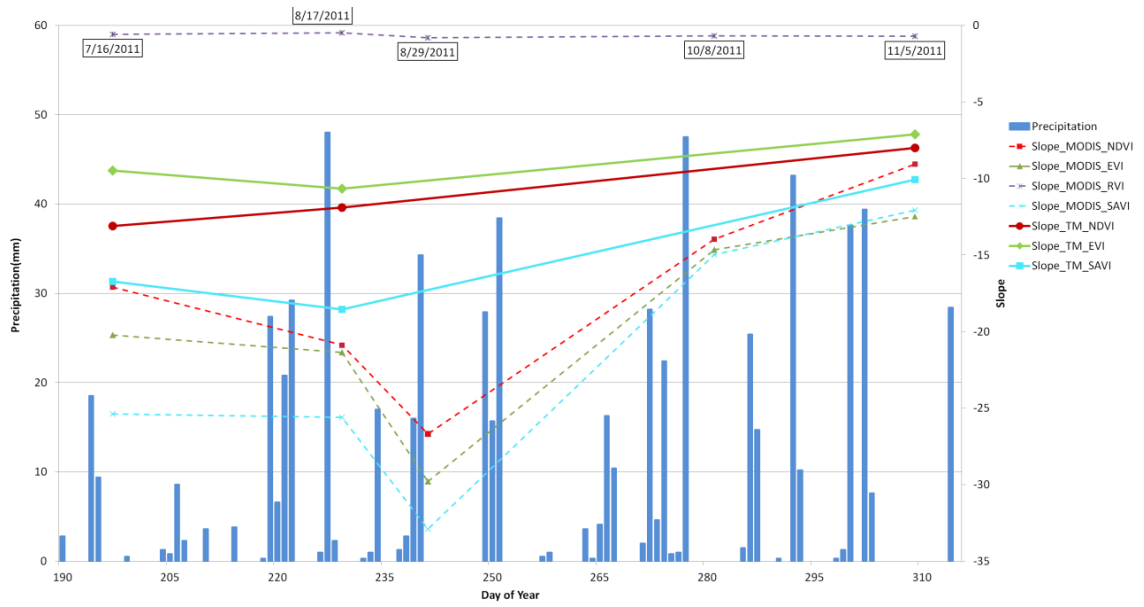


Figure 2.22. Slope of VI-LST plot on different days shown with precipitation data. Dashed lines show slope using various vegetation indices based on MODIS data. Solid lines show slope using various vegetation indices based on Landsat TM data.

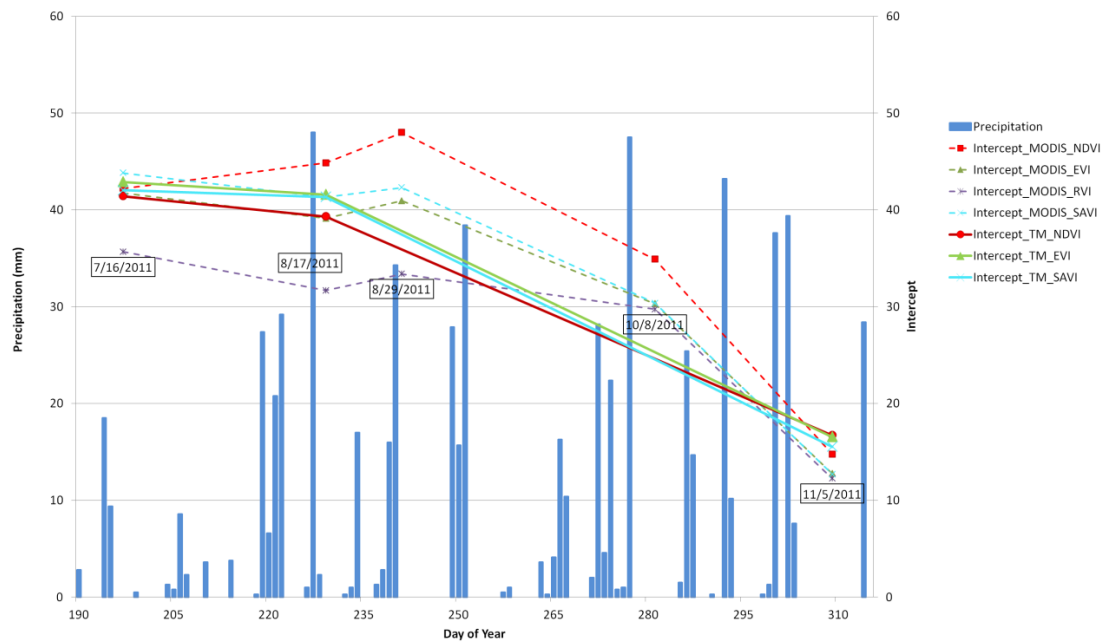


Figure 2.23. Intercept of VI-LST plot on different days shown with precipitation data. Dashed lines show intercepts using various vegetation indices based on MODIS

data. Solid lines show intercepts using various vegetation indices based on Landsat TM data.

TVDI Estimated Using EVI Based on Landsat TM Data

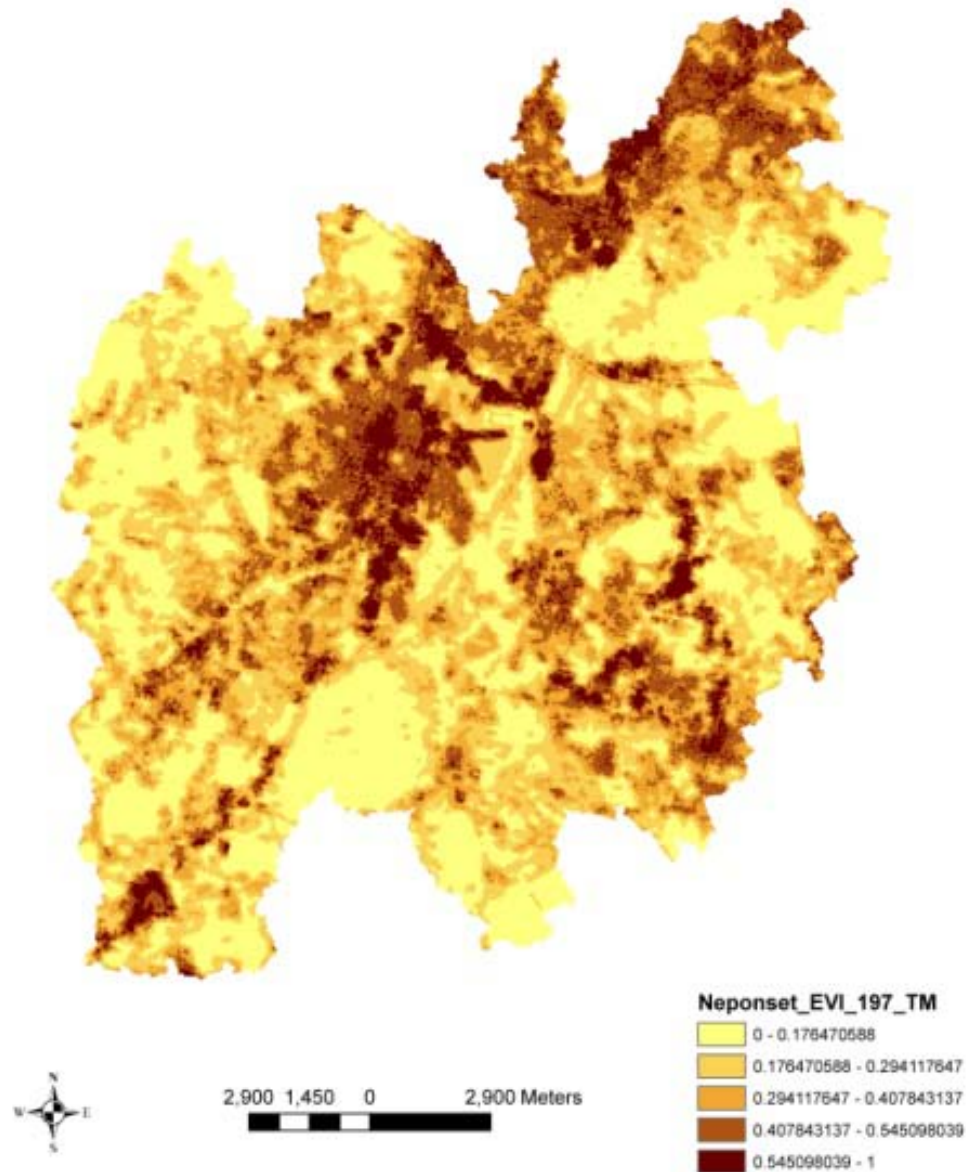


Figure 2.24. TVDI map created using EVI2 based on Landsat data from July 16<sup>th</sup>, 2011.

### 2.3.5 Comparison between TVDI<sub>s</sub> and Measured Soil Moisture

TVDI<sub>s</sub> calculated using various VIs from MODIS data in the Greater Boston Area were compared with field measured soil moisture in 2010 and TVDI<sub>s</sub> calculated using various VIs from Landsat data in the Neponset River Watershed were compared with field measured soil moisture on July 16<sup>th</sup>, 2011 based on the data quality and available field measurements.

#### 2.3.5.1 Comparison between TVDI<sub>s</sub> and Soil Moisture Measured in Greater Boston Area

The correlations are strong between TVDI<sub>s</sub> calculated from MODIS data (MOD43A4 DOY 209 and MOD11A1 DOY 213) using various VIs and the soil moisture measured in the Greater Boston Area. EVI2-TVDI and SAVI-TVDI have high correlations with measured soil moisture and the  $R^2$  values are 0.69 and 0.68 respectively (Figure 2.25). The  $R^2$  of NDVI-TVDI with measured soil moisture is 0.63. The RVI-TVDI has the lowest correlation with measured soil moisture ( $R^2 = 0.46$ ). The  $R^2$  value of measured soil moisture and NDVI estimated TVDI is consistent with the value (0.62) reported by *Patel et al.* (Patel et al. 2009) and is higher than the value (0.43 for 10 cm-20 cm layer) reported by *Chen et al.* (Chen et al. 2011).

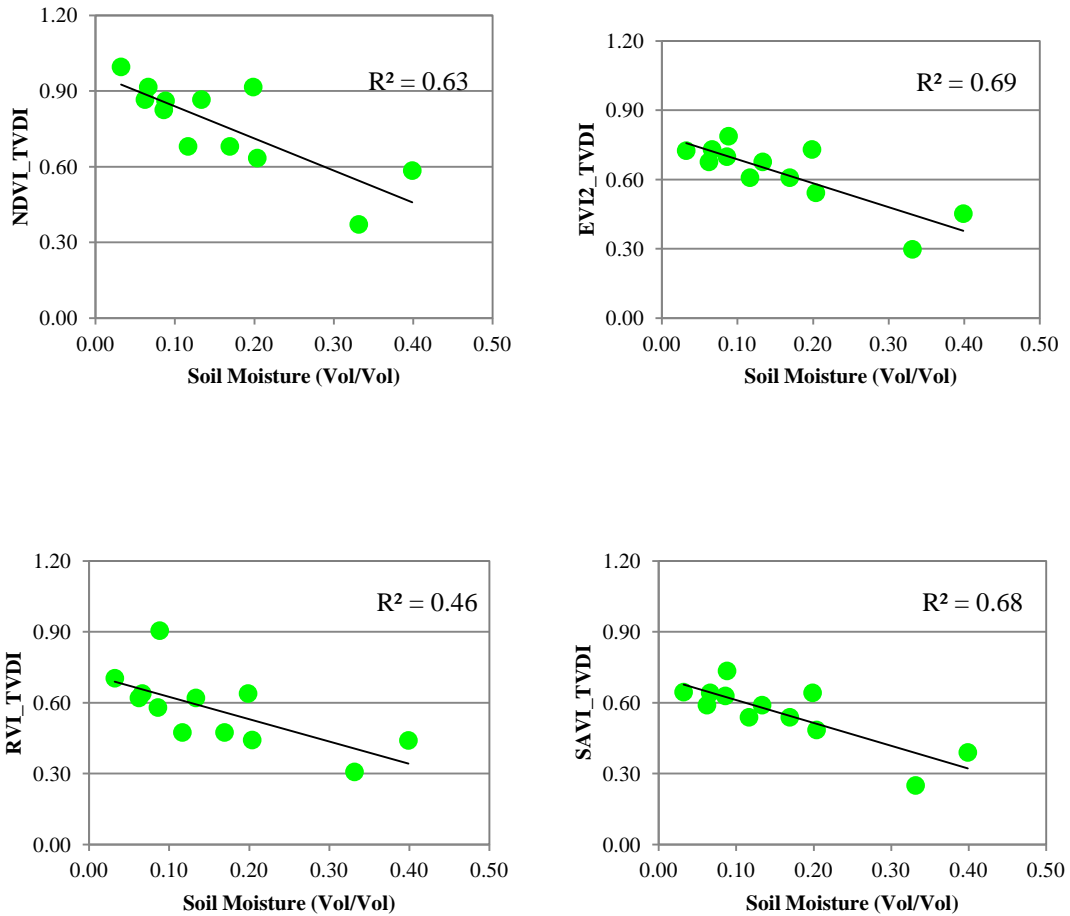


Figure 2.25. The comparison between TVDI estimated using various VIs and measured soil moisture.

### 2.3.5.2 Comparison between the TVDIs estimated using Landsat Data and Field

#### Measured Soil Moisture in the Neponset River Watershed

Earlier analysis indicated that EVI2 and SAVI work very similarly in the calculation of TVDI. Only NDVI and EVI2 derived TVDIs from the Landsat data were compared with field measured soil moisture. The correlations between NDVI and EVI2 derived TVDIs and field measured soil moisture are different in the forest and urban sub-basins. The

correlations between NDVI and EVI2 derived TVDI are 0.32 and 0.34 respectively in the Sharon sub-basin on July 16<sup>th</sup>, 2011. The correlations between NDVI and EVI2 derived TVDI are 0.20 and 0.28 respectively in the Milton sub-basin. Figure 2.28 shows the correlation between TVDI calculated using EVI2 at the two sub-basins. Another study using Landsat data to estimate TVDI also reported a similar result, the  $R^2$  between NDVI estimated TVDI using Landsat data was 0.25 for surface soil layer (Wang et al. 2010). TVDI correlation with field sampling of soil moisture from the Milton sub-basin is higher than that from the Sharon sub-basin. The poor correlation results may be due to the scale effect and the more heterogeneous landscapes in the urban area. Sharon, as the forest sub-basin, has little variation in both measured the soil moisture and TVDI. The lack of range in the soil moisture values can limit the  $R^2$  of the linear regression. The only thermal band of TM data is also a limitation in estimating land surface temperature which eventually affects the TVDI estimation.

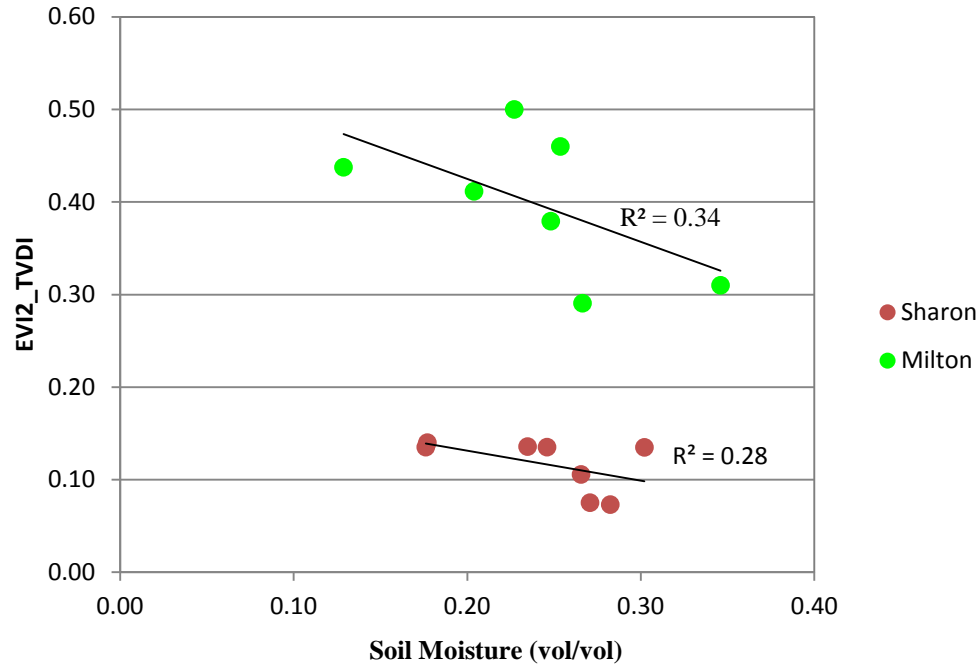


Figure 2.26. Plot of TVDI estimated using EVI2 and measured soil moisture in Sharon and Milton. The green dots are samples from Milton and the red dots are samples from Sharon.

#### 2.4. Conclusion

Weekly soil moisture sampling over both the urban sub-basin and forest sub-basin during the growing season of 2011 shows that soil moisture in the forest sub-basin is higher than that in the urban sub-basin, except during the summer when most of the irrigation happens. The CV and soil moisture are correlated in this research area, which is consistent with earlier studies. The average correlation between TMI and measured soil moisture in the Neponset River Watershed is around 0.3. However, this can be lower than 0.1 during late Fall in the urban sub-basin. The ascending pattern of the correlations between soil moisture and TMI in wetter conditions was not observed in this study area.

The influence of various VIs in estimating TVDI using both MODIS and Landsat data show RVI does not work as effectively as NDVI, EVI2 and SAVI. EVI2 and SAVI work similarly and give slightly better estimates of the dryness condition. NDVI derived TVDI does not follow the same trend as EVI2 and SAVI derived TVDI during the peak growing season. This suggests a careful usage of NDVI when estimating TVDI during full canopy coverage period. TVDI estimated from MODIS data gives a good correlation with measured soil moisture in the Greater Boston Area. The relatively weak correlation between field measured soil moisture and TVDI estimated from Landsat data may due to the highly heterogeneous land cover of the study area, the small range of soil moisture and the limitation of the TM thermal band. Further research is needed, especially with the new Landsat 8 and mid-resolution Aster data.

Therefore, with the good correlation with field measured soil moisture, the EVI2 estimated TVDI can also be used as an evaluation tool for model simulated soil moisture at the MODIS resolution and even at the Landsat resolution if no field measurements are available.



## CHAPTER 3

### DOC CONCENTRATION PATTERNS IN THE NEPONSET RIVER WATERSHED EXPLORED WITH REMOTELY SENSED DATA

#### 3.1. Introduction

DOC critically links terrestrial, estuarine, and marine carbon cycling (Richey et al. 2004a) and may indicate changes in the storage of terrestrial carbon (Bianchi et al. 2009; Williamson et al. 2008). Increasing DOC concentrations have been reported all over the world in the last decade which have important effects on the quality of drinking water (Haaland and Mulder 2009), and on ecological processes and mercury dynamics (Forsius et al. 2010). Despite recent major improvements in the understanding of how DOC is influenced by climate indices, watershed topographic characteristics and human-induced change, significant uncertainty still exists.

A number of researchers have focused on identifying relationships between DOC concentration and potential parameters. *Tian et al.* used a few landscape characteristics and SWAT modeled daily runoff to explain DOC concentration in the Neponset Watershed located south of the City of Boston (Tian et al. 2013). *Xenopoulos et al.* analyzed the effect of nine catchment characteristics on DOC concentration in lakes in North American temperate forests (Xenopoulos et al. 2003). *Strohmeier et al.* reported that DOC export in runoff originated mainly from the wetland area in a catchment (Strohmeier et al. 2013). *Findlay et al.* concluded land use can affect both the quantity and quality of DOC exported into rivers from surrounding terrestrial sources. (Findlay et al. 2001). *Huntington and Aiken* reported that DOC concentration in the Penobscot River in Maine can be primarily explained by the abundance of wetlands and water yield (Huntington and Aiken 2012). Other than landscape characteristics and hydrological processes, many studies have also tried to link DOC with the chemistry of the atmosphere and soil. Rising temperature and declining sulphur deposition are suggested as some of the major reasons for the increasing DOC concentration trend (Evans et al. 2006; Evans et al. 2005). *Aitkenhead and McDowell* were able to estimate the annual riverine DOC flux using soil C:N as a predictor (Aitkenhead and McDowell 2000).

While a number of studies have focused on investigating how streamflow and precipitation regulate DOC concentration in streams, fewer studies have focused on the extent of how remotely sensed data can be used to explain DOC concentrations in streams, rivers, and estuaries. Remotely sensed data is relatively easily accessed and can provide information for the whole watershed rather than point measurements. As the

source and pathway for DOC, understanding the linkage between remotely sensed watershed information and DOC in streams can help us better monitor and estimate DOC patterns. This study used a variety of remotely sensed data (Land use data, impervious data, wetland type data, and terrestrial gross primary production data) and inventory soil type data to analyze their relationship with measured DOC concentrations.

### 3.2. Study Area

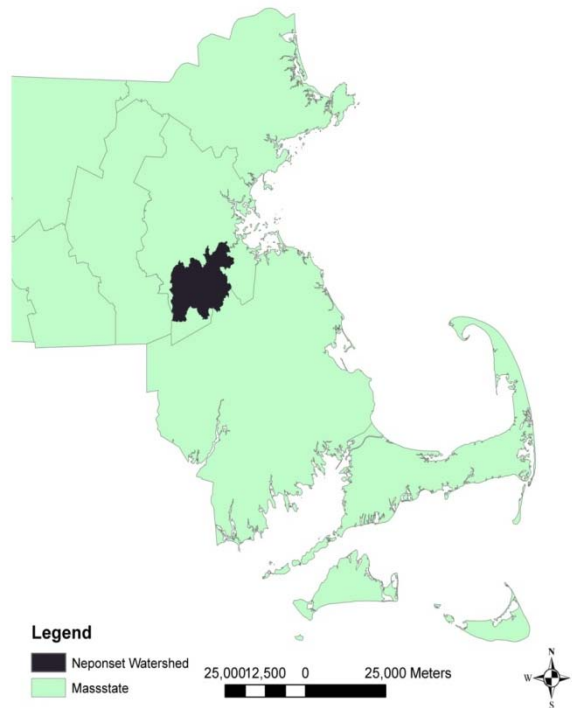


Figure 3.1. The Neponset River Watershed.

The Neponset River Watershed (Figure 3.1) lies south of the City of Boston. The watershed is roughly 300 km<sup>2</sup> and contains approximately 330,000 residents. The

Neponset River exits over the Lower Mills Dam into Boston Harbor after running approximately 48 km throughout the watershed (NepRWA, 2004). Urban land occupies a large proportion of the Neponset Watershed, around 40%. Forest and wetland land covers comprise most of the rest of the watershed, about 42% and 10% respectively. The average annual precipitation from 1971 to 2000 was 1054 mm (NOAA, 2005).

### 3.3. Data

Field measured DOC concentration data, USGS gauge station stream flow data, climate data, and remotely sensed data were used in this study. The DOC concentration data was collected from 11 sampling locations throughout the Neponset River Watershed on a monthly basis from March 2006 to present. DOC sampling, filtration, and analysis was conducted by Wei Huang, Keith Cialino, and Hayley Schiebel in Dr. Robert F. Chen's lab at University of Massachusetts Boston (unpublished). The data analyzed in this study includes the DOC concentration data measured from March 2006 to December 2011. More details about the measurement of DOC concentration data in the Neponset River Watershed can be found in Huang and Chen (Huang and Chen 2009). Daily stream flow data at Milton Village and Mother Brook were downloaded from the United States Geological Survey (USGS). Daily stream flow data were derived from the USGS gauge stations at Milton Village, with values reduced by subtracting flow derived from Mother Brook. Climate data from the Blue Hill Observatory station were downloaded from NOAA, including maximum daily temperature, minimum daily temperature and daily precipitation data. Datasets derived from remote sensing includes DEM, land use type,

wetland type, and GPP data. 1 km spatial resolution 8-day MODIS gross primary production (MOD17A2) (Running et al. 2004) from 2006 to 2011 was downloaded from the REVERB website ([www.reverb.echo.nasa.gov/reverb/](http://www.reverb.echo.nasa.gov/reverb/)). Since there is no GPP value over urban areas, only sampling locations that have more than half of the drainage area with good quality value were chosen in this study.

### 3.4. Methodology

#### 3.4.1 Statistical Analysis

One-way analysis of variance (ANOVA) was used to test for differences among measured DOC concentrations at different sampling points and at different temporal scales. P-values that were smaller than 0.05 were accepted as the significant level.

Regression analysis was used to examine relationships between measured DOC concentrations and other data, such as precipitation, temperature, streamflow, and GPP values.

Principal component analysis (PCA) was used to analyze the various watershed characteristics. PCA is a mathematical procedure which converts a set of variables into a new set of linearly uncorrelated variables (principal components) to extract the domain patterns. The first three principal components extracted from 31 original watershed

parameters were further analyzed using regression analysis to understand the most important watershed parameters that influence DOC concentration.

### 3.4.2. Antecedent Precipitation Index (API)

API was used to represent soil moisture conditions that may predict the impact of precipitation on watersheds. This index is based on the theory that the influence of precipitation on the current soil moisture condition decreases with the time since that precipitation occurred (Fedora and Beschta 1989; Kohler and Linsley 1951). API reflects seasonal soil moisture status over the long term, while it reflects rainfall intensity in short term. The universal equation for calculating API is as follows:

$$API_t = API_{t-1}K + P_{\Delta t}$$

Where  $API_t$  is the API at time  $t$ ,  $API_{t-1}$  is the API at time  $t-1$ ,  $K$  is the recession coefficient, and  $P_{\Delta t}$  is the precipitation occurring between times  $t-1$  and  $t$ .  $K$  dictates the degree of decay rate of the previous API and is normally a value between 0.85 to 0.95 (Leopold and Dunne 1978).

## 3.5 Results and discussions

### 3.5.1 Measured DOC Concentration Data

DOC sampling locations that locate in stream channels were selected. Based on the drainage area of each sampling location, the data from eleven locations were further chosen (Figure 3.2).

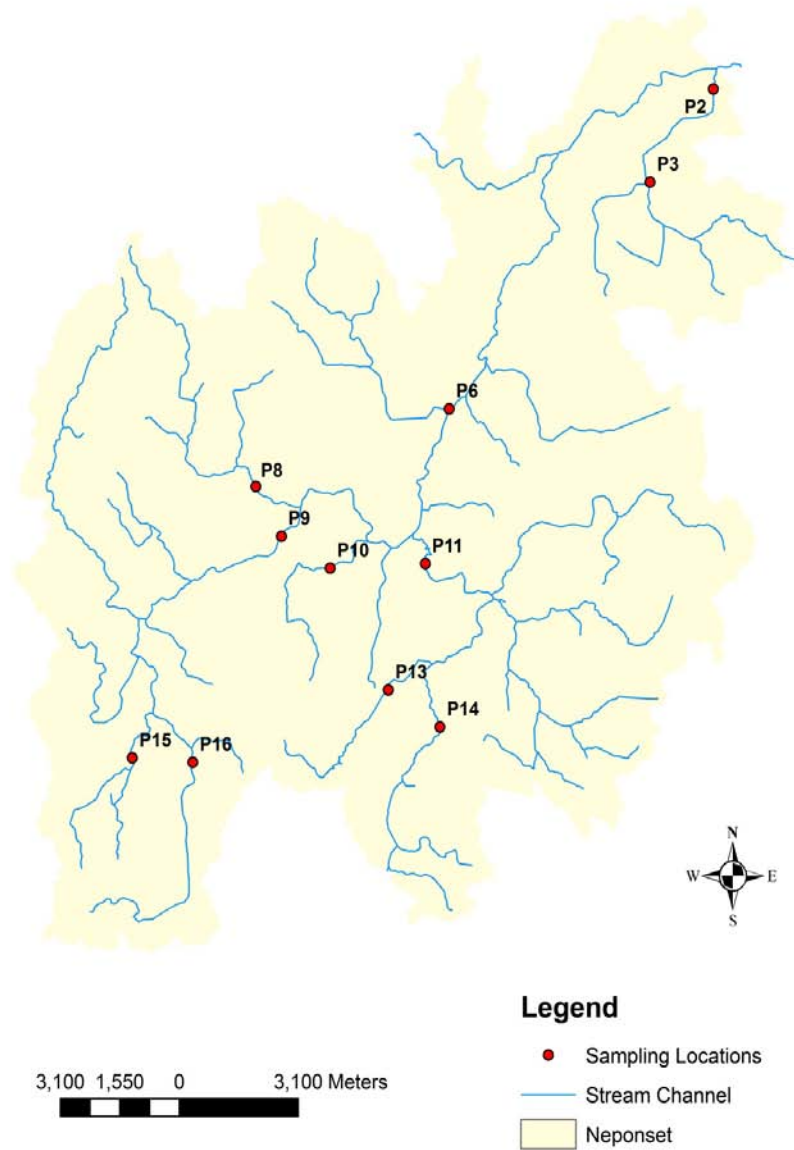


Figure 3.2. The DOC concentration sampling points throughout the Neponset River Watershed.

Note the drainage area of P3 is also part of P2. The drainage area of P9 includes the drainage area of both P15 and P16. P13 and P14 are within the P11 drainage area. P6 covers the largest area among all sampling locations, which includes P8, P9, P10, P11, P13, P14, P15 and P16.

Table 3.1. Measured DOC concentration from the Neponset River Watershed.

<b>Sampling Location</b>	<b>Mean (μmol)</b>	<b>Standard Deviation</b>	<b>Coefficient of Variation</b>	<b>Minimum (μmol) and Date</b>	<b>Maximum (μmol) and Date</b>	<b>Sampling Numbers</b>
<b>P2</b>	482	207	0.43	213 (9/26/2010)	993 (3/29/2008)	79
<b>P3</b>	575	366	0.64	258 (3/24/2006)	2441 (8/27/2010)	75
<b>P6</b>	588	314	0.53	296 (12/08/2007)	2036 (4/25/2010)	78
<b>P8</b>	493	218	0.44	265 (4/01/2011)	1682 (2/23/2008)	77
<b>P9</b>	557	320	0.57	260 (3/24/2006)	2270 (2/23/2008)	69
<b>P10</b>	396	348	0.88	107 (7/17/2007)	2400 (10/27/2008)	78
<b>P11</b>	478	281	0.59	230 (12/08/2007)	2221 (4/12/2008)	79
<b>P13</b>	424	219	0.52	120 (12/08/2007)	1120 (8/27/2010)	76
<b>P14</b>	375	165	0.44	195 (3/24/2006)	1016 (2/28/2010)	76
<b>P15</b>	574	278	0.48	251 (2/18/2007)	1772 (4/12/2008)	75
<b>P16</b>	474	273	0.58	79 (9/26/2010)	1395 (4/12/2008)	75

The maximum mean value over the sampling period happens at P6 (588  $\mu\text{mol}$ ) and the minimum mean value over the sampling period happens at P14 (375  $\mu\text{mol}$ ) (Table 3.1). Standard deviations for all sampling points are high. P3 has the largest standard deviation (366) and P14 has the lowest (165). The mean DOC concentration has a positive relationship ( $R^2=0.28$ ) with standard deviation (Figure 3.3). The correlation reaches up to 0.71 if P10 is removed. This positive relationship between standard deviation and mean DOC concentration indicates that the sub-basins with higher average DOC concentration tends to export more DOC during large precipitation events and tends to trap DOC during small precipitation events. It also indicates that sub-basins with lower average DOC concentration export DOC more evenly among various precipitation events. The minimum DOC concentration measured from all sampling points throughout the sampling period is 79  $\mu\text{mol}$  measured on 9/26/2010 at P16. The maximum DOC concentration is 2441  $\mu\text{mol}$  measured on 8/27/2010 at P3 from all sampling points throughout the sampling period. More than half of the maximum DOC concentration happened in the early spring of 2008.

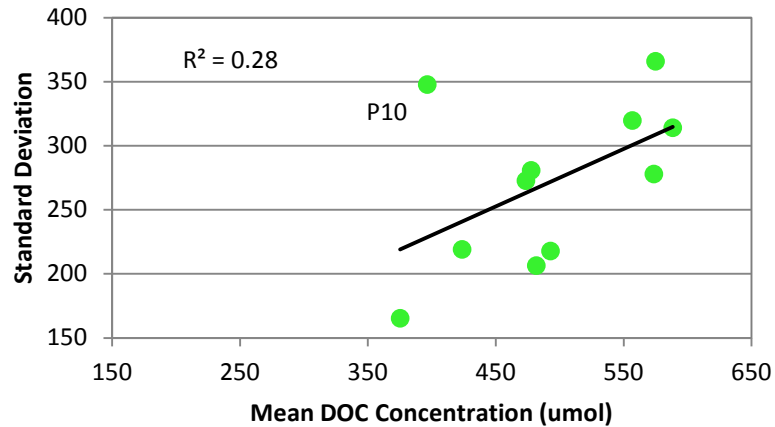


Figure 3.3. Correlation between mean DOC concentration and standard deviation at all sampling points. If P10 is removed, the correlation increases to 0.71.

#### 3.5.1.1 Spatial Variance of the Measured DOC Concentration Data

The average DOC concentration values over the study period from the 11 sampling locations are significantly different (Oneway ANOVA p-value<0.001). Multi-comparisons among these averages show that average DOC concentrations of P10 and P14 are significantly lower than P3, P6, P9 and P15. The largest coefficient of variation (CV) of DOC concentration happens at P10 and the least variance occurs at P2 (Figure 3.4).

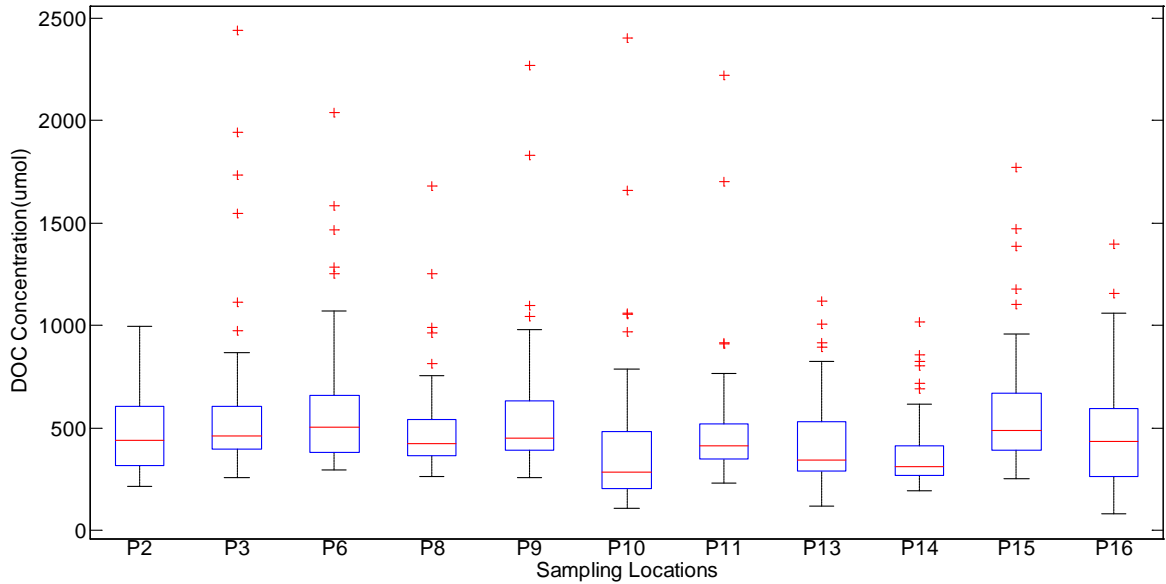


Figure 3.4. Boxplot of DOC concentrations at each sampling point.

### 3.5.1.2 Temporal Variance of the Measured DOC Concentration Data

The annual average DOC concentration values from all 11 sampling locations are significantly different (Oneway ANOVA test,  $p$ -value=0.0002). The average DOC concentration in 2008 is significantly larger than other years' mean DOC concentration ( $p$ -value=0.0015) and the average DOC concentration in 2007 is significantly low ( $p$ -value=0.0012). The low DOC concentration in 2007 was caused by less precipitation during the autumn of 2007 fall. Normally there are a few storms in fall following after the relatively dry summer, but there were no storms in fall of 2007. Correspondingly, high DOC concentration was observed at the beginning of 2008 due to the DOC accumulation in soil during the dry period of the second half of year 2007. This phenomenon is consistent with other studies which describe this as the wet-dry cycle effect on increasing DOC concentration (Chow et al. 2006; Kalbitz et al. 2000). Also year 2008 was the

strongest La Nina year since 1988 which brought a large amount of precipitation and leached out a large amount of DOC out from the terrestrial system.

The DOC concentrations show various trends among different seasons (Figure 3.6).

Spring has the most outliers for all sampling locations and the average DOC concentration is 467  $\mu\text{mol}$ . The DOC concentration is the largest in summer with the value of 539  $\mu\text{mol}$ . The least outliers were found in fall. Winter has the lowest DOC concentration; the value is 433  $\mu\text{mol}$ . The average DOC concentration of the samples is 524  $\mu\text{mol}$  during the growing season (summer and fall) and 470  $\mu\text{mol}$  over the leaf-off season (winter and spring). The average DOC concentrations during the growing and leaf-off seasons are as low as 509  $\mu\text{mol}$  and 405  $\mu\text{mol}$ , if year 2008 is excluded.

The monthly average DOC concentration is the highest in August. March and December have the lowest monthly average DOC concentration.

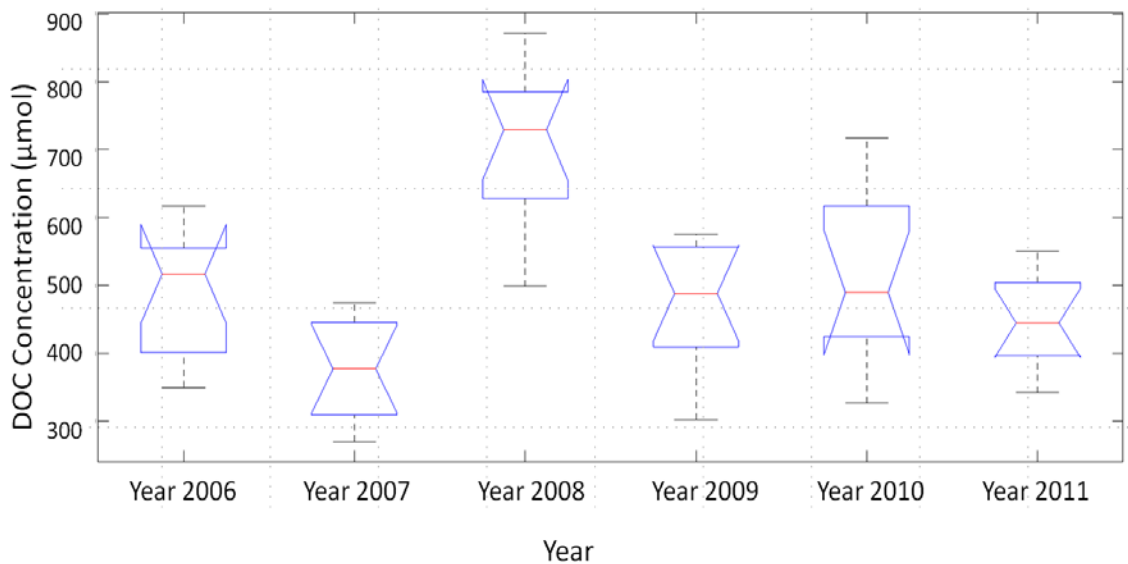
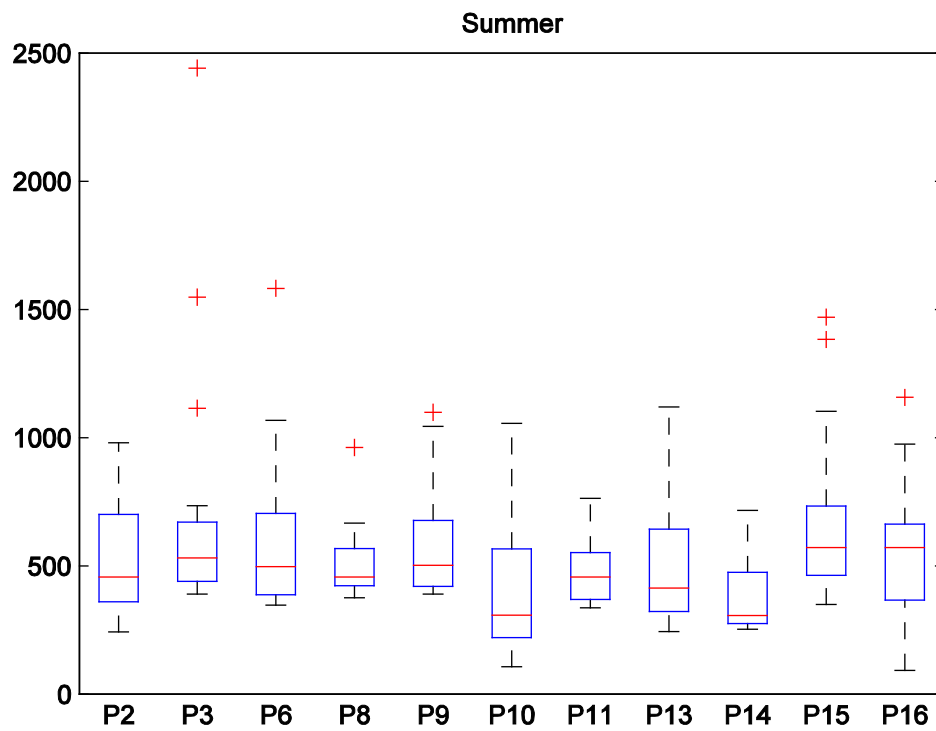
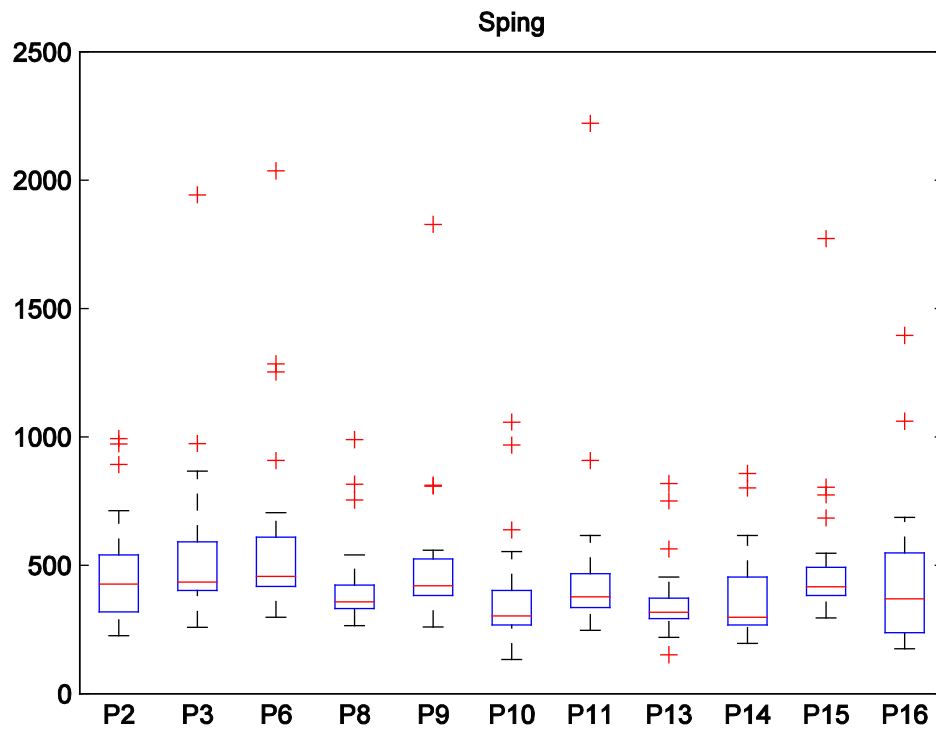


Figure 3.5. Boxplot of DOC concentrations from all sampling points in different years.



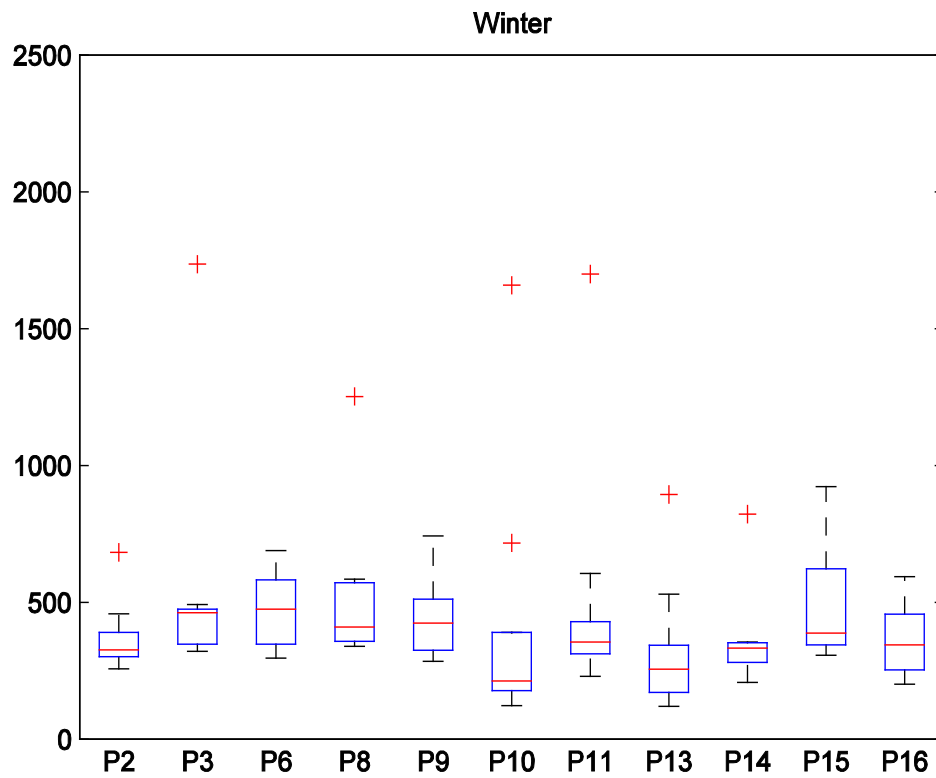
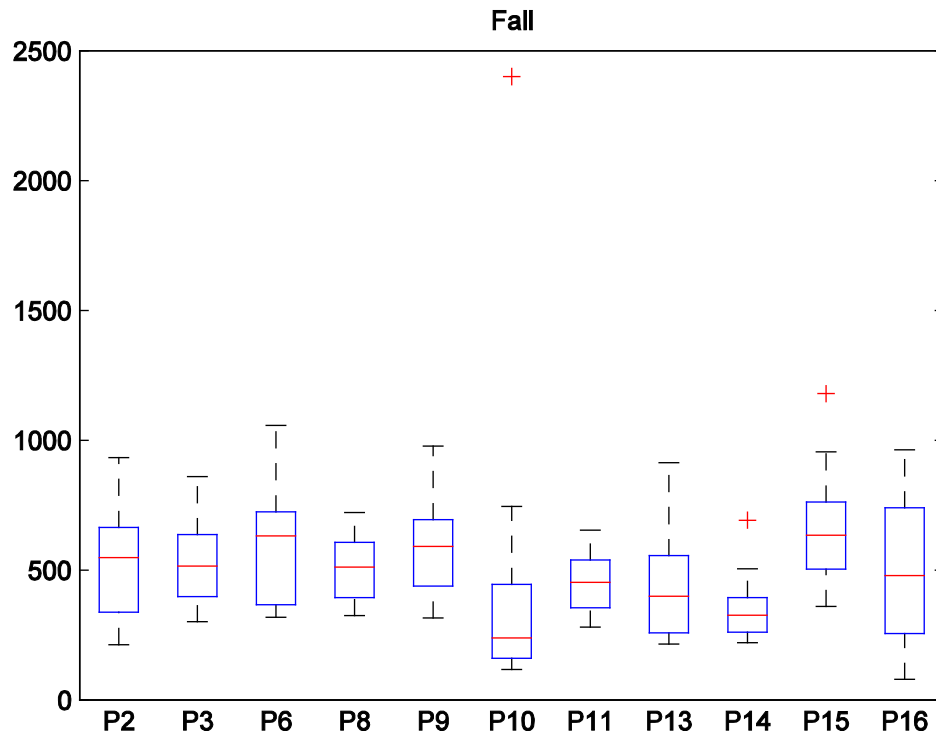


Figure 3.6. Boxplot of DOC concentration measurements in different seasons.

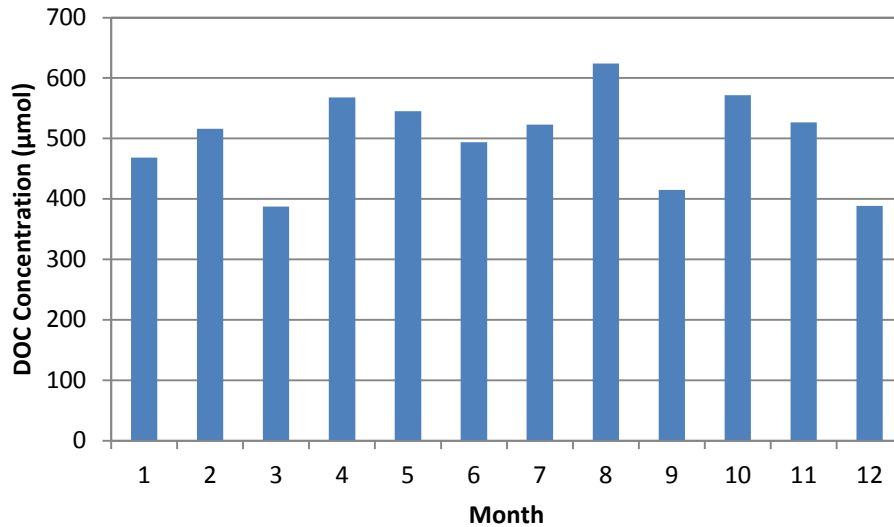


Figure 3.7. Comparison of DOC concentrations averaged from all sampling points among different months.

### 3.5.2 Watershed Characteristics and Their Correlation with Measured DOC Concentration

Watershed characteristics are grouped into topographic indices, land use type, soil type, and wetland type (Table 3.2). The 11 sub-basins and slope maps were created from the DEM downloaded from MassGIS. A 30 m spatial resolution land use map was obtained from the Massachusetts Forest Monitoring Program at Clark University. A soil type map, downloaded from MassGIS, was reclassified to eight soil types; and the major type of soil in all sub-basins is sandy loam. A wetland type map is a feature map obtained from the National Wetland Inventory. The five wetland type categories are lake, freshwater pond, riverine, freshwater forested/shrub wetland, and freshwater emergent wetland. The very small proportion of riverine wetland in all of the sub-basins is not considered in this

research. Slope, TMI, and basin area are the average value of each sub-basin. All the other parameters' values are estimated by the parameter's area and the associated sub-basin's area.

A few parameters have high standard deviations, which include the basin area in the topographic indices category, deciduous forest in the land use type category, rock area in the soil type category, low density residential area in the land use type category and loamy sand area in the soil type category. The coefficient of variation of salt marsh in the land use type category, basin area in the topographic indices category, lake wetland in the wetland type category, and silt loam in the soil type category are higher than 1.

Table 3.2. Sub-basins' watershed characteristics list.

Sampling Locations	Categories	Units	Mean	Standard Deviation	Coefficient of Variation	Minimum	Maximum	Number	
Slope	Topographic Indices	Degree	3.81	0.94	0.25	2.30	5.45	1	
TMI		*	2.57	0.19	0.07	2.25	2.86	2	
Basin Area		km <sup>2</sup>	39.65	60.18	1.52	3.83	207.58	3	
Orchard	Land Use Type	%	0.28	0.15	0.55	0.08	0.61	4	
Cranberry Bog		%	7.64	0.96	0.13	5.75	9.40	5	
Pasture/Row Crops		%	3.08	1.02	0.33	1.63	5.06	6	
Deciduous Forest		%	26.90	9.35	0.35	13.74	46.91	7	
Coniferous Forest		%	5.27	2.60	0.49	2.30	10.46	8	
Mixed Forest		%	12.30	3.44	0.28	9.69	19.49	9	
Golf Course		%	2.88	1.06	0.37	1.04	4.95	10	
Grassland		%	1.31	0.42	0.32	0.25	1.74	11	
Low Density Residential		%	22.25	6.75	0.30	11.23	31.29	12	
High Density Residential		%	3.49	1.25	0.36	1.31	5.05	13	
Commercial		%	3.69	2.92	0.79	0.26	10.50	14	
Impervious Area		%	15.10	3.98	0.26	9.47	21.82	15	
Wetland		%	4.35	1.71	0.39	2.58	7.50	16	
Salt Marsh		%	0.17	0.36	2.12	0.00	1.24	17	
Sand Quarry		%	0.74	0.68	0.92	0.06	2.37	18	
Bare Soil		%	2.21	1.05	0.47	0.82	4.42	19	
sandy loam		Soil Type	%	53.86	5.59	0.10	47.55	64.22	20
riparian			%	8.74	2.68	0.31	5.29	12.52	21
rock			%	11.52	8.62	0.75	3.06	30.83	22

urban		%	9.39	4.67	0.50	4.13	16.14	23
sand		%	2.20	1.71	0.77	0.11	5.54	24
loamy sand		%	6.91	6.17	0.89	0.08	19.79	25
loam		%	2.05	0.97	0.48	0.09	3.37	26
silt loam		%	1.23	1.50	1.22	0.00	4.09	27
lake	Wetland Type	%	2.77	3.58	1.29	0.00	10.19	28
pond		%	0.97	0.41	0.43	0.03	1.65	29
shrub wetland		%	7.42	1.61	0.22	3.87	9.59	30
emergent wetland		%	0.97	0.53	0.55	0.19	1.82	31

All these watershed characteristics work together to regulate DOC production and transportation, which makes it impossible to separate one from the others to explain its influence on DOC concentration in stream. Principal component analysis (PCA) is applied to analyze the interaction among all the parameters. The first three principal components explain 30.2%, 25.3% and 11.5% of variation in the whole set of watershed parameters (Figure 3.8).

Deciduous forest in the land use type category is the most important positive contributor to the first principal component. Rock area in the soil type category and slope in the topographic indices category are also important positive contributors. Sand in the soil type category, pond wetland in the wetland type category and commercial area, impervious area and sand quarry area in the land use type category are important negative contributors. For the second principal component, coniferous forest, mixed forest in the land use category and loamy sand in soil type category are the most significant positive contributors, Wetland in land use category and emergent wetland in wetland category are also positive contributors. Grassland and low density residential area in land use category

are the most significant negative contributors. Orchard in the land use category is the most significant positive contributor to the third principal component and also the sandy loam in soil type category (Figure 3.9). Urban, silt loam and rock in the soil type category, emergent wetland in the wetland category and slope in the topographic indices category are significant negative contributors to the third principal component. However, slope in the topographic indices category and urban and rock in the soil type category are also important contributors to the first principal component.

No significant correlations were found between the first two principal components and the average DOC concentrations at the sampling points. However, there is a significant negative correlation between the average DOC concentrations and the third principal component ( $R^2=0.43$ ). Based on the composition of the third principal component, higher DOC concentration over a long period tends to happen more in silt loam, more in emergent wetland, less in orchard, and less in sandy loam sub-basins within the Neponset River Watershed. Orchard occupies only a small proportion of any sub-basin and its contribution to DOC concentration is limited. Silt loam is mainly distributed along the main Neponset River channel, which has a good correlation with wetland area along the downstream channel. This is consistent with earlier research about the importance of wetland in DOC export (Huntington and Aiken 2012; Miller 2012).



### 3.5.3 Climate Data

Precipitation among 12 months is relatively evenly distributed based on 118 years of data. March, June, August, October, and December during 2006 to 2011 have greater average precipitation compared to the average precipitation from the 118 year record. A few extreme precipitation events were observed during 2006 to 2011 (e.g. May, June and November of 2006 etc., see Figure 3.10).

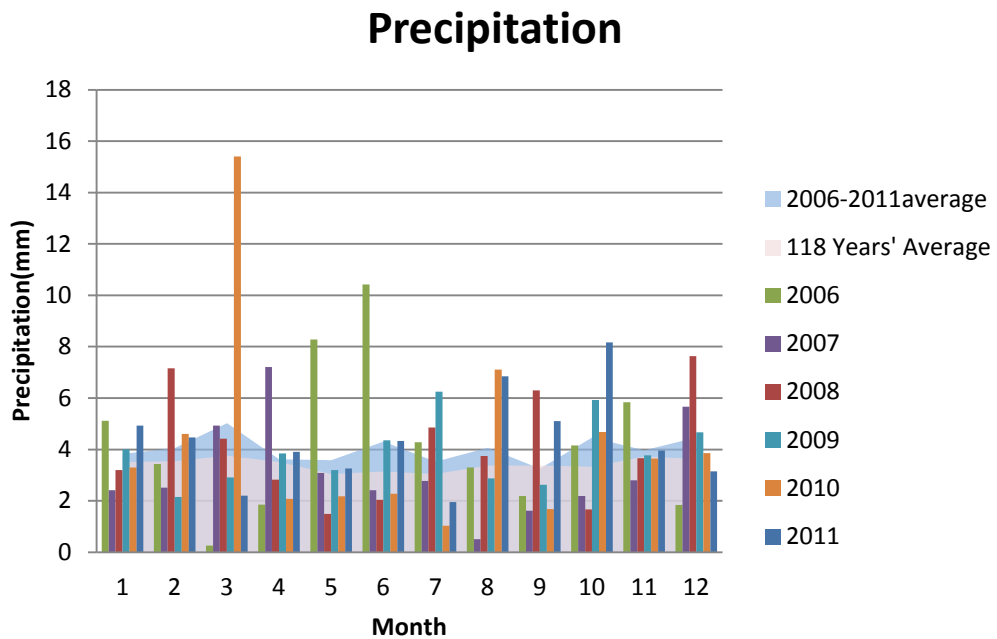


Figure 3.10. Comparison of the precipitation among 118 years' average and from year 2006 to year 2011.

## Maximum Temperature

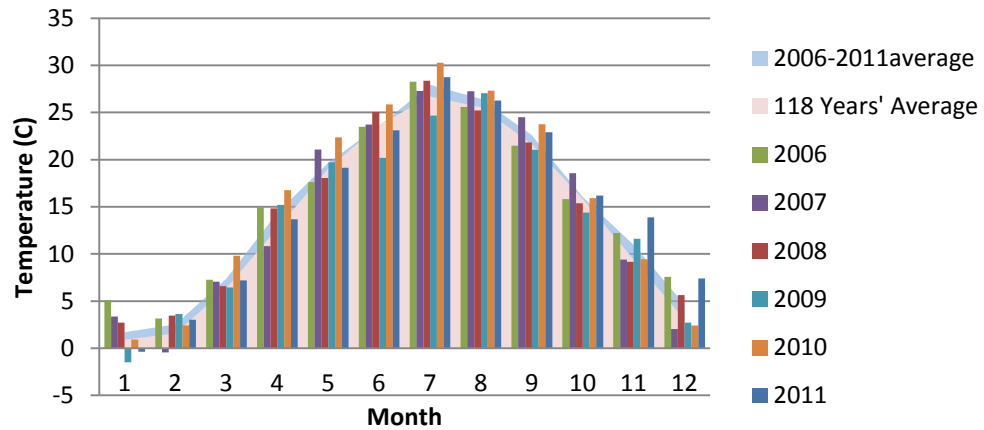


Figure 3.11. Comparison of the maximum temperature among 118 years' average and from year 2006 to year 2011.

## Minimum Temperature

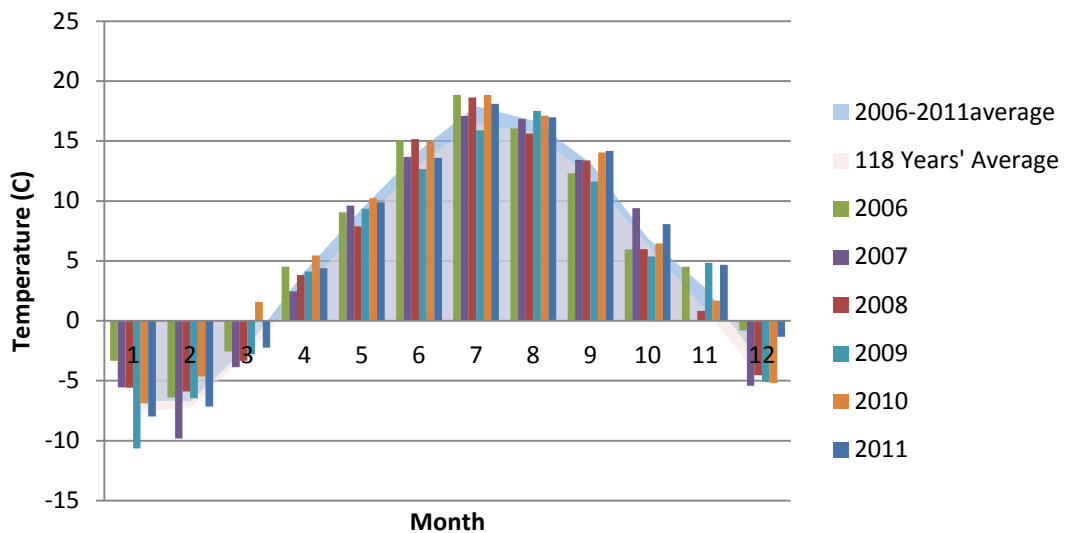


Figure 3.12. Comparison of the minimum temperature among 118 years' average and from year 2006 to year 2011.

The maximum and minimum average temperature during year 2006 to 2011 is higher than the average of 118 years. Year 2006, 2007 and 2008 had a warmer January and year 2010 had a warmer March compared with other years from 2006 to 2011 (Figure 3.11 and Figure 3.12).

### 3.5.3.1 Antecedent Precipitation Index (API)

In this study, API (Figure 3.13) was calculated as starting from January 12, 2006 with a value of 0 because almost no precipitation events happened from January 5 to January 11 of 2006. K was chosen as 0.85 based on the slope of the linear regression of plot of streamflow during a period without precipitation in a specific time interval. The time interval was 11 days in this study.

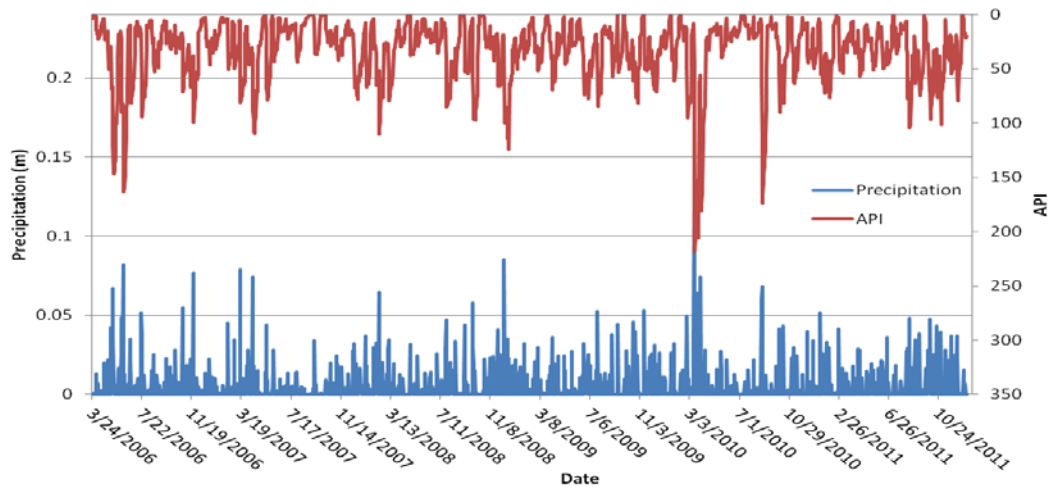


Figure 3.13. API estimated from precipitation data. The blue line shows precipitation data and the red line shows the API values.

DOC concentration is positively related to API. Pearson test's correlation coefficient  $R^2$  is 0.14 ( $p\text{-value} < 0.0001$ ) for all sampling days. The correlation between API and DOC concentration is high during the growing season ( $R^2 = 0.52$ ,  $p\text{-value} < 0.0001$ ) and low during leaf-off season ( $R^2 = 0.02$ ,  $p\text{-value} = 0.37$ ). The correlations between API and DOC concentration for both growing season and leaf-off season are even higher ( $R^2 = 0.59$ ,  $p\text{-value} < 0.0001$  and  $R^2 = 0.07$ ,  $p\text{-value} = 0.12$ ) if year 2008 is not considered. The low correlation between API and DOC concentration in winter and early spring is probably due to snow accumulation and snowmelt processes. The first snowmelt event leaches out a large amount of DOC and the DOC concentration decreases sharply after the first snowmelt (Hornberger et al. 1994). After the first snowmelt, even large precipitation does not bring high DOC concentration which may dampen the relationship between DOC concentration and precipitation.

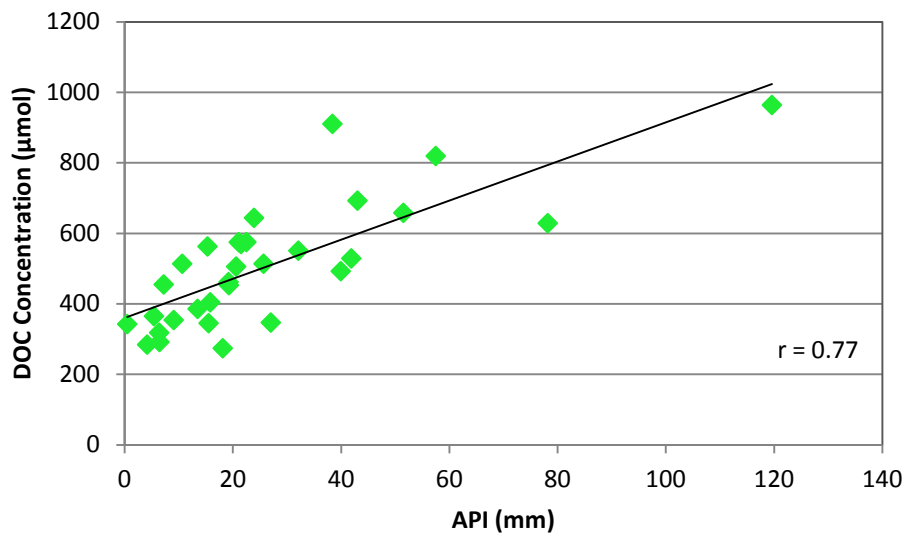


Figure 3.14 Plot of Average DOC concentrations and API values of samples from the growing season excluding year 2008.

### 3.5.3.2 The relationship between DOC concentration and temperature

The relationship between averaged DOC concentrations from all sampling points and the mean daily temperature on the sampling date is not significant. Monthly average temperature has a better correlation with DOC concentration, in that the logarithm of the corresponding DOC concentration has a good positive correlation with the logarithm of average temperature ( $R^2 = 0.09$ , p-value = 0.02) for all months in which the average temperature is larger than zero. The correlation is better ( $R^2 = 0.19$ , p-value = 0.01) if year 2008 is not included.

The correlation between DOC concentration and temperature is not significant during the winter and early spring. Snowmelt in this period may decrease the correlation between the temperature and DOC concentration. The high DOC concentration for the first snowmelt event does not relate to high temperature. Most studies show increasing DOC concentration during the early stages of snowmelt (Currie et al. 1996; Yavitt and Fahey 1985).

The strong correlation between temperature and DOC concentration can be mainly attributed to the period of late April and May (Figure 3.16). Since the precipitation from winter to early summer doesn't increase significantly, it is safe to conclude that temperature is an important seasonal factor regulating DOC concentration from winter to early summer.

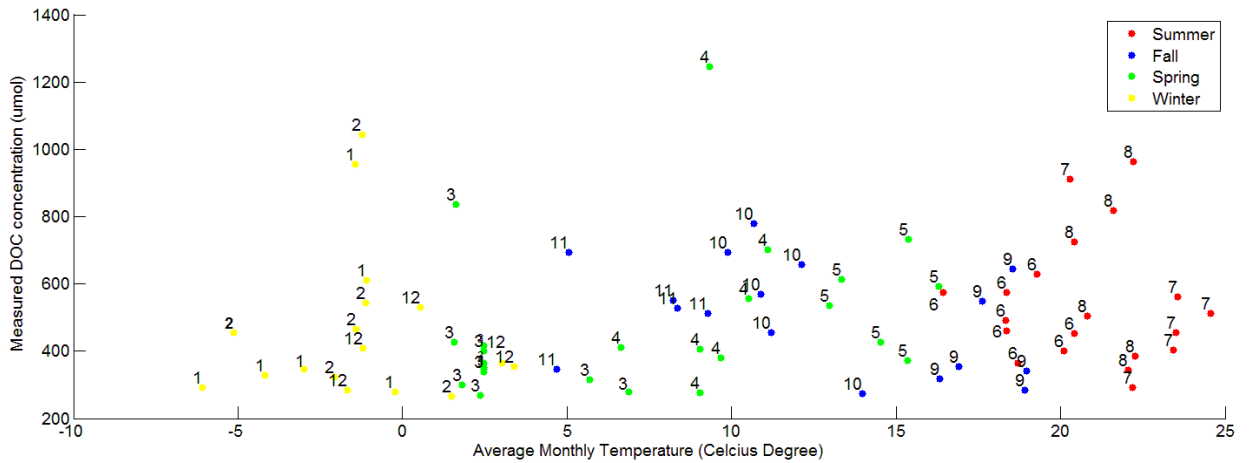


Figure 3.15. Plot of average monthly temperature and measured DOC concentration for all months. Points are numbered with the months in which they were sampled.

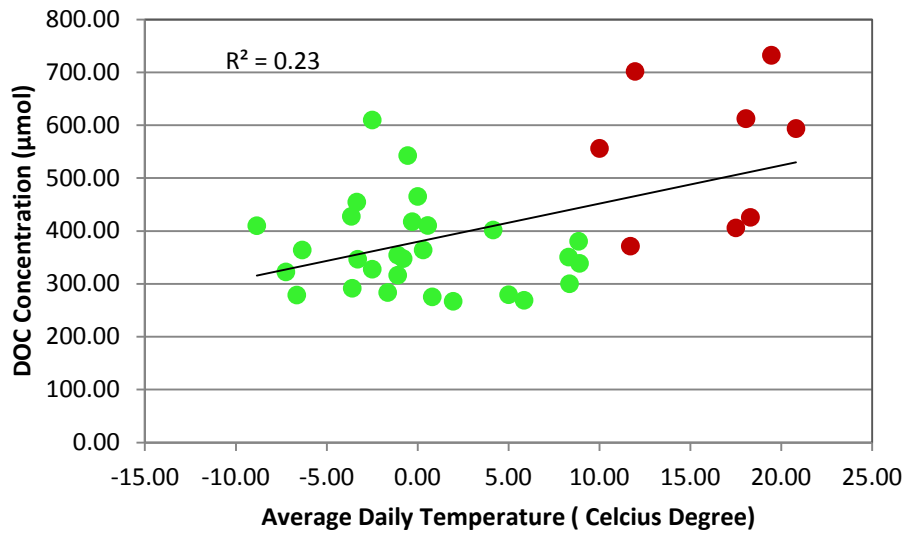


Figure 3.16. Plot of DOC concentrations averaged from all sampling sites for December and January to May and corresponding average daily temperature excluding year 2008. The red points represent samplings measured in late April and May. The green points represent samplings measured in December, January, February and March.

In conclusion, climate parameters function differently in growing season and leaf-off season. API, as a surrogate of precipitation, has a strong positive correlation with stream DOC concentration during the growing season. The logarithm of DOC concentration and logarithm of monthly average temperature has a positive linear relationship, and the correlation is higher if excluding year 2008. Temperature is also a key factor for the higher DOC concentration in late spring compared to winter and early spring.

#### 3.5.4 Stream Flow Data

The correlation between DOC concentration and stream flow is high during the growing season excluding year 2008 (Figure 3.17). The positive relationship between DOC concentration and streamflow corresponds with the relationship between DOC concentration and API as was reported by many studies (Ågren et al. 2010; Tian et al. 2013). The strong positive relationship between the two was also reported in the Penobscot watershed in Maine (Huntington and Aiken 2012).

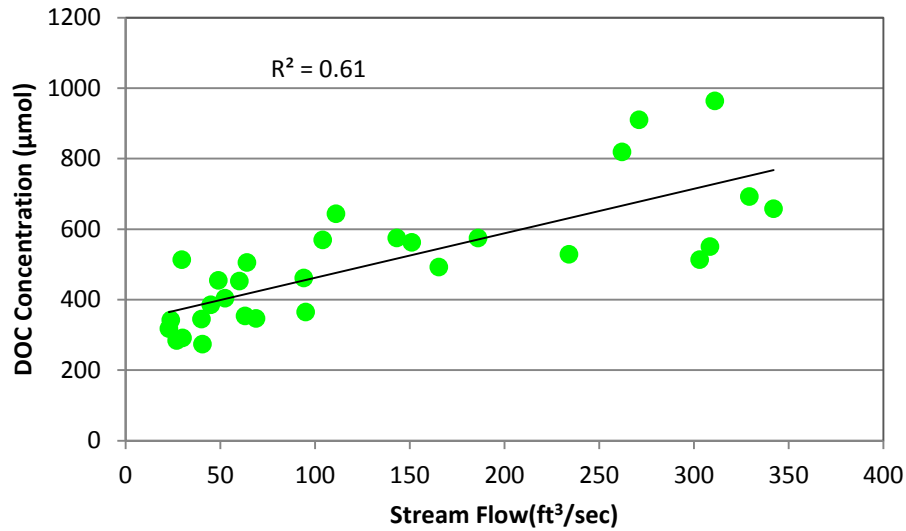


Figure 3.17. The correlation between measured DOC concentration and stream flow larger than 0.35 ft<sup>3</sup>/sec (0.098 m<sup>3</sup>/sec).

The DOC concentration decreases with stream flow as a logarithmic function when stream flow is less than 3.5 ft<sup>3</sup>/sec, which is 0.098 m<sup>3</sup>/sec. The decreased rate of DOC concentration is larger when the stream flow is lower. The DOC in the upper soil level might build up during periods of low flow (Boyer et al. 1996). However, since very low flow is normally hard to measure with high accuracy, noise from the USGS gauge station streamflow data may exist.

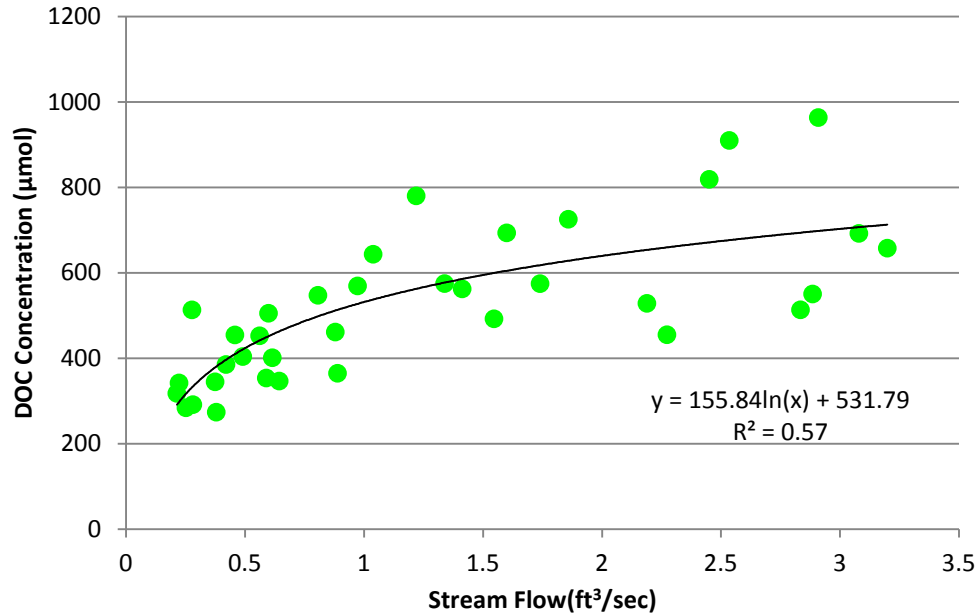


Figure 3.18. The correlation between DOC concentration and stream flow during the low flow.

### 3.5.5 Gross Primary Production (GPP)

The temporal relationship between the annual DOC concentrations and annual GPP data is not significant. Higher annual GPP does not necessarily combine with higher annual DOC concentration in the same year or in the following year. On the contrary, smaller GPP does not necessarily yield lower DOC concentrations during the following year. Year 2010 has the highest GPP while its DOC concentration is less than that in 2008. 8-day GPP values during the sampling dates are also not an indicator for higher average DOC concentration. The maximum 8-day GPP in 2011 is the highest while its DOC concentration is less than year 2006, 2008 and 2010.

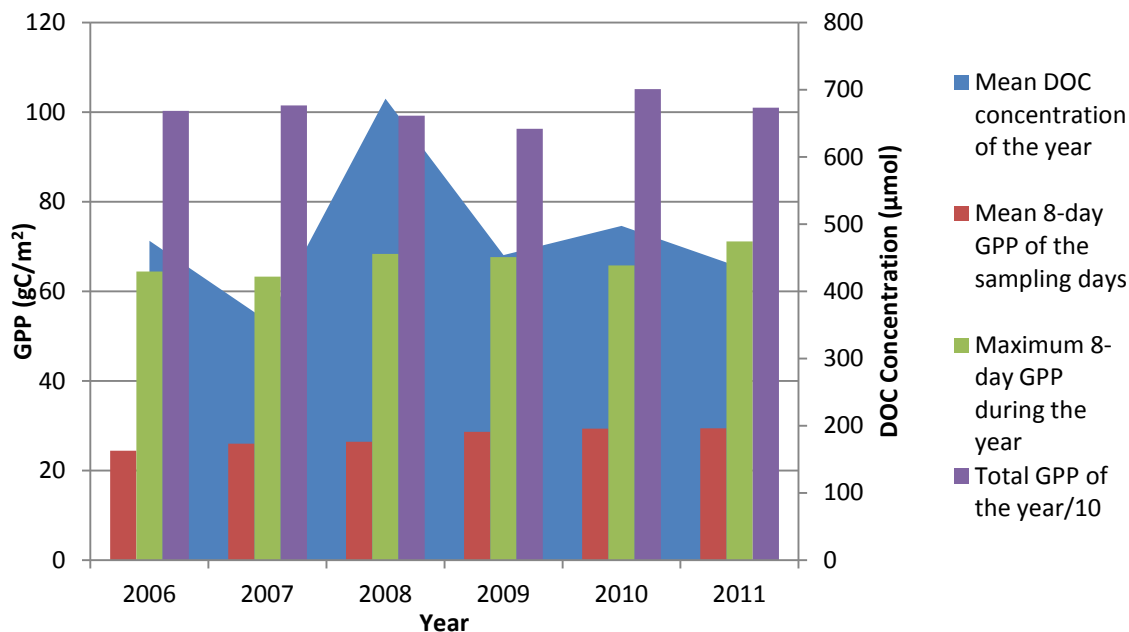


Figure 3.19. GPP and mean DOC concentration from year 2006 to year 2011.

Among the selected sampling locations, P13, P14 and P15 show no significant correlation between DOC concentrations and the corresponding GPP closest to sampling date, the GPP that is 8 days before the sampling date, or the GPP that is 16 days before the sampling date. The correlation between the GPP closest to the sampling date and DOC concentrations is good at P9. The DOC concentration at P16 is significantly correlated with the GPP closest to sampling date (Table 3.3).

The strong correlations between 8-day GPP and DOC concentrations at P9 and P16, which are not observed in other sub-basins, might be due to the large percentage of wetland area in these sub-basins. The correlation with the GPP closest to sampling date is higher than GPP that is 8 days or 16 days prior to the sampling dates, so the turnover rate of leaves and the decomposition rate of organic matter might be fast in wetland. The high

hydrological connectivity of wetland to the river channel can effectively leach the DOC from the land into the river channel. The low correlation over other sampling points suggests the source of stream DOC in these sub-basin may have a longer residence time. Another reason for the weak correlation is because GPP mainly reflects the source of DOC in soil, DOC export is also controlled by hydrological processes.

Table 3.3. The correlation between GPP and measured DOC concentration.

Sub-basins	Time	r	p
p9	8-day	0.46	0.02
	16-day	0.04	0.86
	32-day	0.06	0.77
p13	8-day	0.15	0.47
	16-day	-0.01	0.95
	32-day	-0.31	0.12
p14	8-day	-0.13	0.53
	16-day	0.00	0.99
	32-day	0.18	0.38
p15	8-day	-0.14	0.49
	16-day	0.07	0.75
	32-day	-0.23	0.26
p16	8-day	0.52	0.01
	16-day	0.37	0.12
	32-day	0.21	0.36

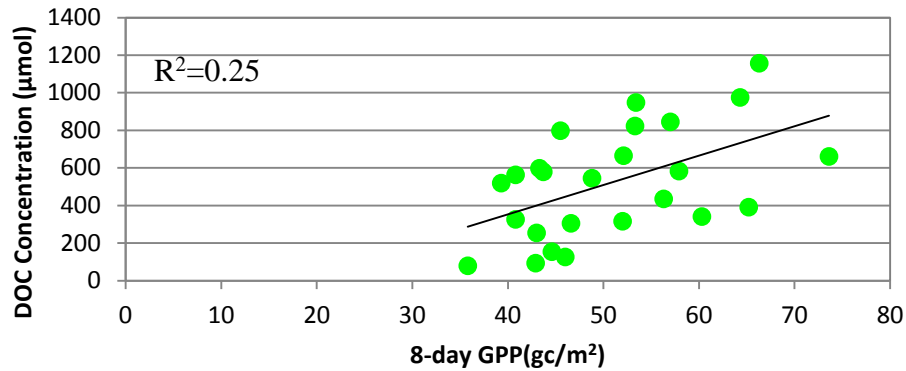


Figure 3.20. Plot of DOC concentration and 8-day GPP.

### 3.6. Conclusion

By analyzing remotely sensed data that describes sub-basins' watershed characteristics and observed climate and streamflow data, the temporal and spatial variation of DOC concentration during growing seasons can be partially explained.

- Using the watershed characteristics as input for the principal component analysis, the results show that higher DOC concentrations tend to exist in sub-basins that have larger area of silt loam and emergent wetland and less area of sandy loam. The occupancy of silt loam has high correlation with the wetland area in the main Neponset River channel, which suggests the importance of wetland area.
- Both precipitation and stream flow have strong positive correlation with the DOC concentration measured in stream channel during the growing season; the positive correlation is even higher if excluding year 2008 which was a strong La Nina year. The logarithm of average monthly temperature has good positive correlation

with the logarithm of DOC concentration, without considering year 2008, during all months that the average temperature is higher than zero.

- There is no direct correlation between annual GPP and annual DOC concentration in the same year or in the following year because other than the source of DOC in soil, DOC export is also regulated by hydrological processes. The DOC concentrations at P9 and P16 have strong positive correlation with the MODIS GPP data closest to the sampling date and do not show significant relationship with the GPP data 8 days and 16 days before the sampling dates during the growing season. The strong positive relationship in these two sub-basins (P9 and P16) may be due to the large area of wetlands in these locations and may indicate the rapid turnover rate and decomposition of organic matter in wetland.

## CHAPTER 4

### SENSITIVITY ANALYSIS AND SIMULATION OF DOC CONCENTRATION AND FLUX DURING INITIALIZATION OF THE RHESSYS MODEL

#### 4.1. Introduction

The flux of dissolved organic carbon (DOC) from the terrestrial system to the aquatic system is a fundamental part of the global carbon cycle. It tightly links together terrestrial, estuarine and marine carbon cycling (Richey et al. 2004b). DOC fluxes are largely controlled by microbial transformation and hydrological transport in the terrestrial system (Tranvik and Jansson 2002). Many studies have been conducted to investigate microbial transformation of DOC in soil (Hur et al. 2009; Lu et al. 2013) and controls on the proportion of DOC in hydrological transport such as mineral soil absorption of DOC in soil (Jardine et al. 1989; Lilienfein et al. 2004; Tipping et al. 1999). With the understanding of these basic mechanisms of DOC production and transportation, terrestrial hydro-ecological process-based models are capable of simulating DOC flux from the terrestrial to aquatic systems.

Despite the importance of the land-to-water DOC flux, there are still uncertainties about its origin, mechanisms and fate. Both litter and humus are commonly accepted as the most important sources of DOC in soil solution, though the proportion of individual contributions cannot be quantified (Kalbitz et al. 2000). Since humus needs longer time to decompose, litter primarily accounts for short-time variation of DOC production in soil solution. DOC export from land is also regulated by mineral soil absorption and the amount of water that passes through the soil (Olefeldt et al. 2012; Roulet and Moore 2006). DOC in stream channels comes from various sources that include groundwater DOC; DOC from the surface organic soil layers; DOC carried by water from the deep mineral soil layers; precipitated DOC; DOC from decomposition of in-channel litter; and in some urban watersheds, DOC in wastewater. The first three categories of DOC source are the major components but there are still uncertainties in how different mechanisms combine under different climate and land cover scenarios to give a particular DOC signature.

Many studies have been conducted to investigate parameters that influence DOC export. The phenomenon that a dry-wet cycle of hydrological conditions results in higher DOC concentrations has been reported in various study areas (Kalbitz and Knappe 1997; Lundquist et al. 1999; McDowell and Wood 1984; Tipping et al. 1999). Laboratory experiments concerning the influence of various climate parameters (e.g. temperature and nitrogen saturation) on DOC flux often contradict the field measurements due to the multiple interacting controls of land-to-water DOC flux. Warmer climates increase DOC production in watersheds, but the decomposition rate also increases, which at the same

time removes DOC (Kramer et al. 1990). McDowell et al. found no significant increase of DOC concentration over four years' nitrogen amendments, while DOC increased in laboratory experiments (McDowell et al. 1998).

Empirical models are applied by many studies to overcome the limitation of the spatial and temporal resolutions of field sampling of DOC flux and concentration (Dawson et al. 2011; Findlay et al. 2001; Huntington and Aiken 2012). However, they need a certain amount of measured DOC data to begin with, which is often unavailable, especially for small watersheds without gauges. When climate change and landuse change caused by human activities are included in research, empirical models are no longer suitable (Wu et al. 2013). Process-based models can not only provide useful predictions of future scenarios based on the understanding of key processes but also construct a frame to test new hypotheses. A few process-based models have been developed to simulate DOC flux from soil into rivers with emphases on either soil absorption (Neff and Asner 2001; Yurova et al. 2008), or hydrological rainfall-runoff processes (Xu et al. 2012), or DOC production from various sources (Currie and Aber 1997; Wu et al. 2013), or a combination of simple DOC production, soil absorption and leaching functions (Futter et al. 2009). While all these processes are important to DOC export, a model that integrates more detailed hydrological and ecological processes is needed to better understand DOC export. RHESSys is a hydro-ecological process-based based model that simulates carbon, water and energy flux at a daily time-step. The main objective of this research is to simulate DOC concentration and flux in the Neponset River Watershed using RHESSys and to compare the results with field measured data. It is the first time that RHESSys has been applied to a New England watershed and is used to simulate DOC flux from the

terrestrial to aquatic systems. Given the large population of the New England area and the important role of DOC in the aquatic system and the global carbon cycle, further study of DOC concentrations and flux in streams using process-based models can effectively link laboratory and field work with the fundamental biogeochemical processes and provide insights into the mechanisms of DOC flux from the terrestrial to the aquatic systems.

#### 4.2. Study Area and Data

The study area of this research is the Neponset River Watershed (Figure 4.1) with an area of around 300km<sup>2</sup>. Climate data, survey data and various remotely sensed data are used in this research.

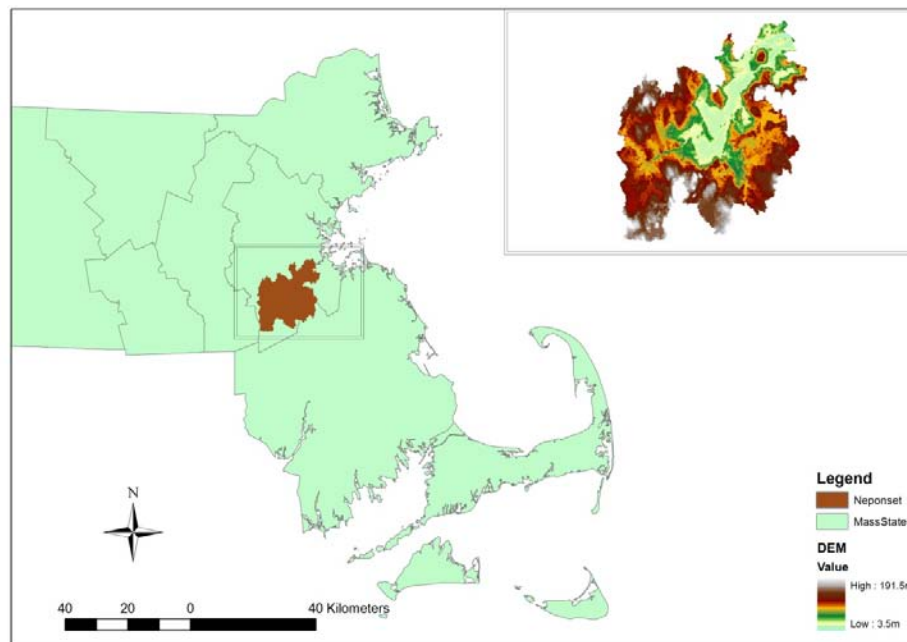


Figure 4.1 The Neponset River Watershed with Massachusetts State as the background. The upper right corner is the digital elevation map of the Neponset River watershed.

#### 4.2.1. Climate Data

Climate data for the Blue Hill Observatory which are available from 1893 were downloaded from the National Climatic Data Center (Figure 4.2). Daily Climate data include maximum temperature, minimum temperature and precipitation. The highest temperature occurs in July and the lowest temperature is in January. Precipitation is evenly distributed throughout the year with the lowest value in July.

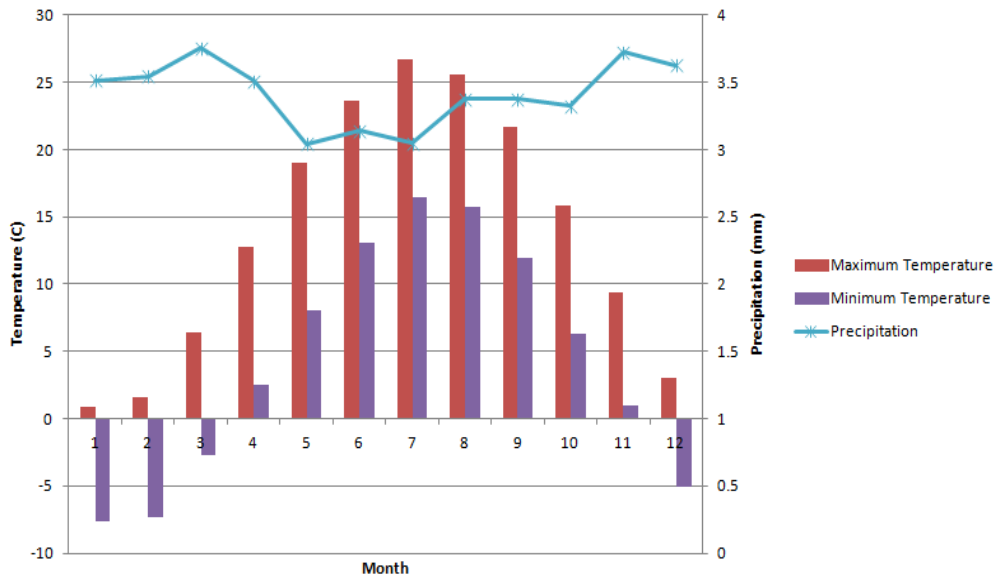


Figure 4.2. 100 years' climate data at the Blue Hill weather observation station.

#### 4.2.2. Digital Elevation Map

DEM data (Figure 4.3) for Massachusetts State are available from the MassGIS website (<http://www.mass.gov/mgis/>). The 1:500 scale DEM data were resampled to 30 m spatial resolution using a bilinear resampling method. The shape of the Neponset Watershed was defined using the USGS gauge station in Milton village as the watershed outlet.

#### 4.2.3. Land use

30 m resolution land use data was reclassified to three types (undeveloped, urban and agriculture) from an NLCD 2006 map downloaded from the USGS (Figure 4.4). Sixteen land cover types are included in the NLCD 2006 classification for the New England area. Urban includes all the developed areas, while agriculture area includes cultivated areas. Undeveloped area covers the remainder.

#### 4.2.4. Vegetation type

Vegetation type data (Figure 4.4) were reclassified from the Massachusetts Forest Monitoring Program map (30 m) provided by Clark University. Four vegetation types are used in RHESSys. These are Non-vegetation, deciduous forest, mixed forest and grass. The corresponding physiological parameters for each vegetation type are taken from RHESSys parameter libraries (<https://github.com/RHESSys/ParamDB>).

#### 4.2.5. Soil type

Soil type data from MassGIS were created based on the published soils surveys by the United States Department of Agriculture (USDA) Natural Resources Conservation Service (NRCS). The feature map was converted to a 5 m resolution raster map and resampled to 30 m. Six types of soils were classified: sandyloam, siltyloam, sandyclayloam, urban, riparian and rock (Figure 4.4).

#### 4.2.6. Impervious area

Orthoimagery acquired in April 2005 was downloaded from MassGIS and used to generate an impervious area map. The feature map was converted to 5 m spatial resolution impervious area data. Figure 4.5 is the patch map, the finest scale in RHESSys, created using the unique combinations of various vegetation, soil and hydrological characteristics.

#### 4.2.7. Phenology data

Vegetation phenology is an important factor in the biological effects of climate change. The daily MODerate resolution Imaging Spectroradiometer (MODIS) BRDF/albedo data were used to estimate phenology information (Zhang et al. 2003). The daily Nadir BRDF Adjusted Reflectance (NBAR) derived vegetation index which eliminate angular effects, are particularly well suited to capture rapidly changing surface conditions such as vegetation green-up in the spring.

#### 4.2.8. Hydrology data

Five USGS hydrological gauge stations (Figure 4.3) are distributed in the Neponset River Watershed and they are located at the Milton dam in Norwood, in Dedham, and in Canton. RHESSys was calibrated using stream flow data from the USGS gauge station at Milton Village. Mother Brook flow data were subtracted from the flow at Milton dam to eliminate the influence of stream flow from water imported from the Charles River

(connected by the Mother Brook canal). The original cubic feet per second unit was converted to millimeter per day per basin area to be comparable with the RHESSys output. Data from November 1996 to 2012 were used for RHESSys simulations.

## Gauge Stations in the Neponset Watershed



# Digital Elevation Map

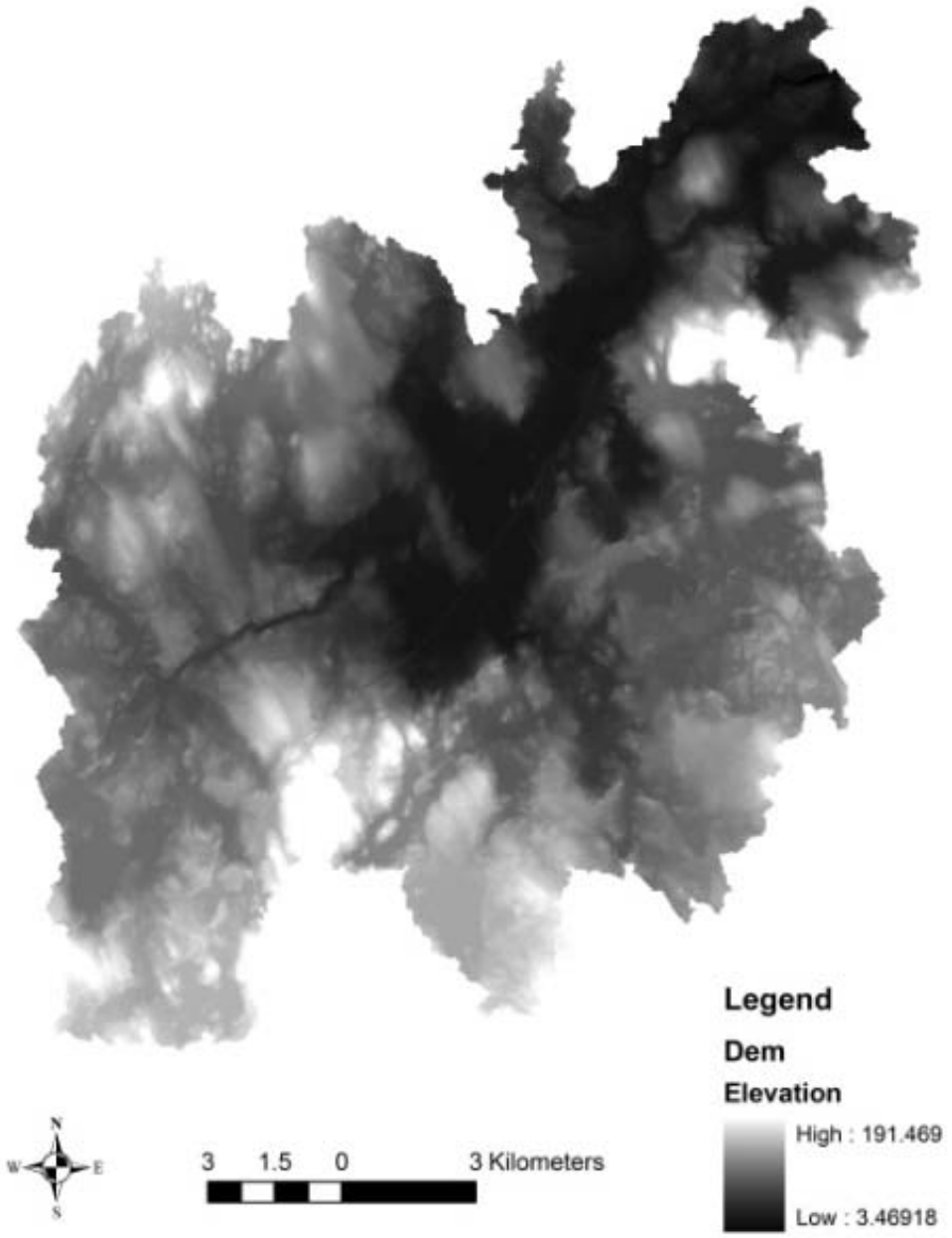


Figure 4.3. Location of USGS gauge stations in the Neponset River Watershed and DEM map of the Neponset River Watershed.

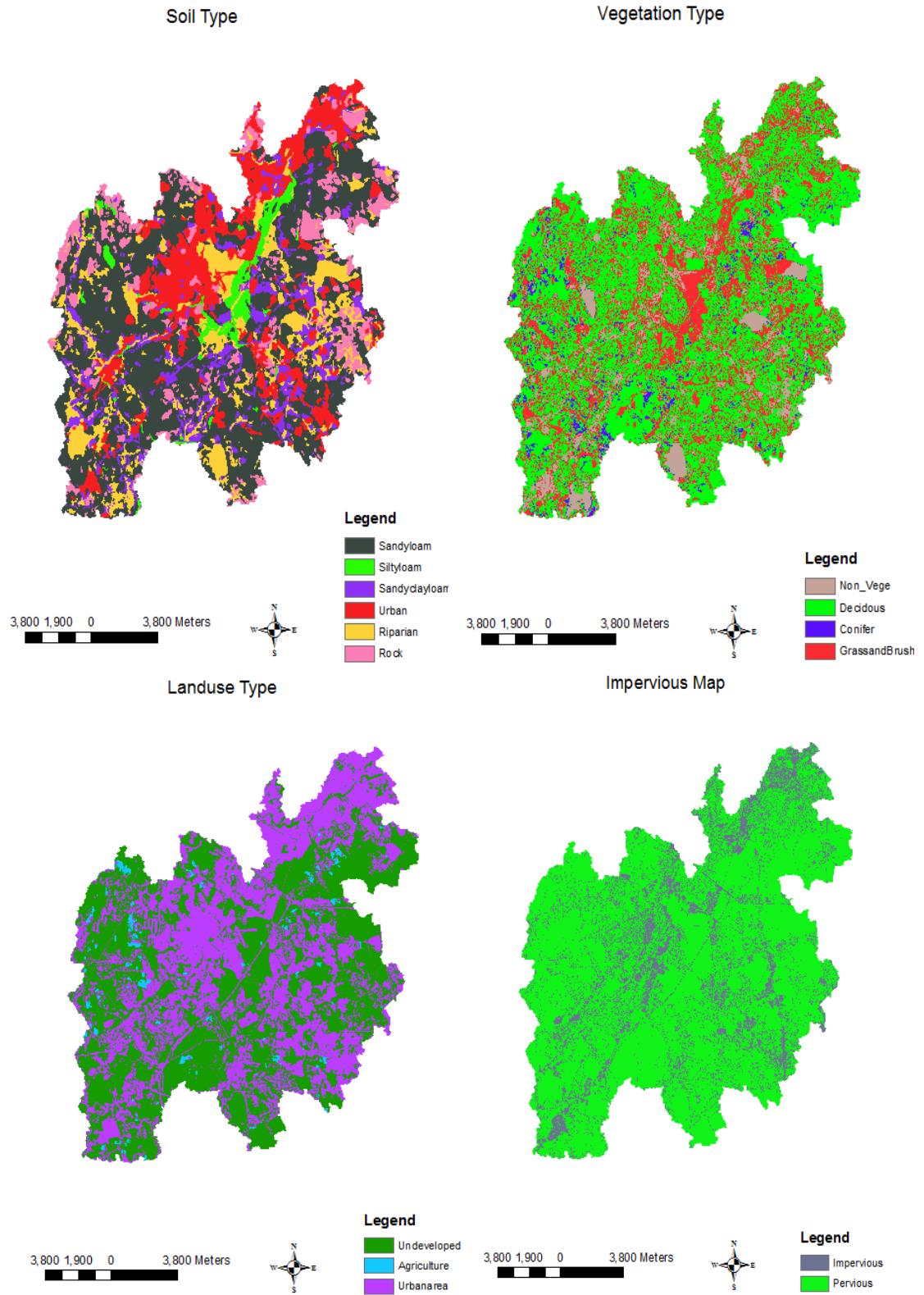


Figure 4.4. Input maps for RHESSys of the Neponset River Watershed.

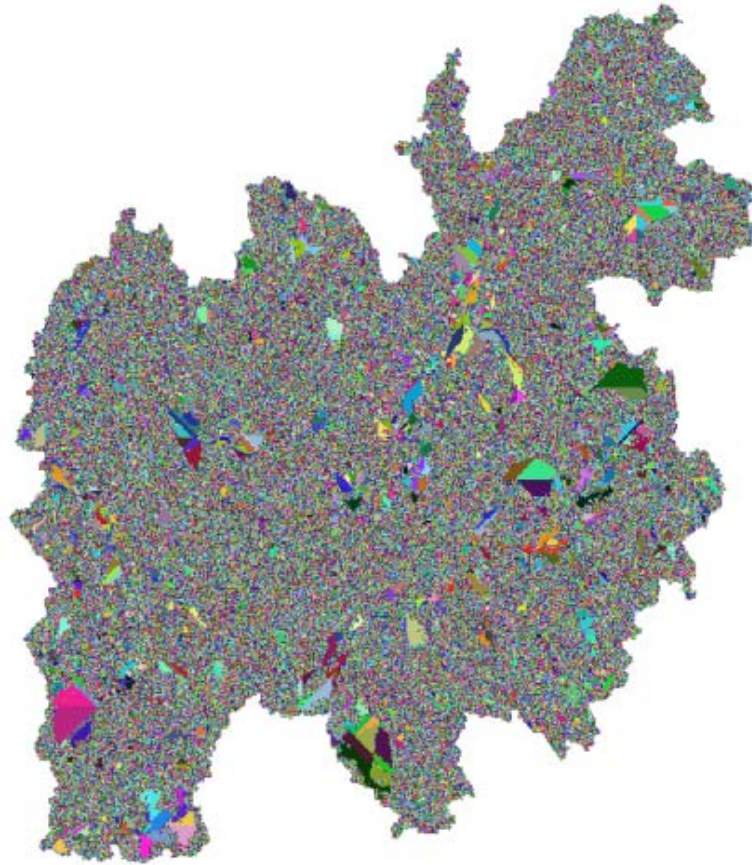


Figure. 4.5. Patches created from combining DEM, soil type, vegetation type, land use type in the Neponset River Watershed at 30 m resolution.

#### 4.2.9. Field measured DOC concentration and flux data

The DOC data were sampled from March 2006 to January 2012 on a monthly basis (Huang and Chen 2009). Samples for each month were collected and analyzed by Professor Robert Chen's research group at University of Massachusetts Boston. The discharge from USGS gauge station at Milton Dam was used to calculate DOC flux from the measured DOC concentration.

### 4.3. Methodology

#### 4.3.1. The Key Processes Relating to DOC Leaching in RHESSys

The Regional Hydro-Ecological Simulation Systems (RHESSys) is a spatially distributed daily time step model that simulates carbon, water, and energy fluxes within a watershed. It uses a hierarchical structure to present the landscape of study area and the structure includes basin, zone, hillslope and patch. RHESSys has been successfully applied in diverse watersheds under different climate conditions (Shields and Tague 2012; Tague et al. 2004), to study nitrogen export (Band et al. 2001), stream flow feedbacks to climate change (Band et al. 1996; Baron et al. 2000; Tague and Grant 2009; Tague et al. 2007), parameterize ungauged watersheds (Tague et al. 2012), study hydrologic vegetation gradient (Hwang et al. 2012), eco-hydrologic response to the combined impacts of projected climate change and altered fire frequencies (Tague et al. 2009b), and snow distribution (Christensen et al. 2008; Hartman et al. 1999; Tague and Grant 2009). RHESSys integrates process-based models for vegetation growth, hydrological process model and decomposition processes in soil. The combination of hydrological and ecological process models makes the study of DOC flux between land and water possible.

##### 4.3.1.1 Carbon Cycle Simulation in RHESSys

RHESSys is a semi-mechanistic carbon cycling model in which carbon is balance. Carbon and nitrogen in plant, litter and soil components are stoichiometrically linked.

Carbon is fixed from atmospheric CO<sub>2</sub> into the ecosystem by photosynthesis (Farquhar Equation) as a function of temperature, radiation, nutrient, and water supplement (Figure 4.6). The amount of carbon left after vegetation respiration is then allocated to various parts of plants. Vegetation components (e.g. leaves, stemwood, fine roots) turnover are partitioned into corresponding litter pools based on species specific turnover ratios. DOC in soil solution originates from the decomposition processes of four litter and four soil pools. Four soil carbon pools which are the fast soil carbon pool, the slow soil carbon pool, the shielded cellulosic soil carbon pool and the recalcitrant soil carbon pool correspond to four litter carbon pools: the labile litter carbon pool, the cellulosic litter carbon pool, the shielded cellulosic litter carbon pool and the lignin litter carbon pool. The decomposition rate is estimated by base decomposition rates for different litter and soil pools, and is then varied as a function of soil temperature, nutrient availability and soil water content. Nutrient availability is a key factor affecting both photosynthesis and decomposition processes.

#### 4.3.1.2. Hydrologic Processes in RHESSys

RHESSys simulates vertical and lateral soil moisture for each patch object. The DOC flux is associated with both the vertical and lateral flow at the patch level. Precipitation reaches the soil surface after being intercepted by vegetation. Infiltration into soil layers is estimated using Philip's infiltration equation (Philip 1957), and considers the throughfall (or precipitation when there is no canopy) intensity and duration and soil saturated hydraulic conductivity. The remaining throughfall turns to surface flow and is

discharged to adjacent lower elevation patches. Evaporation of intercepted canopy water, surface detention stores and litter and canopy transpiration is simulated by the Penman-Monteith equation (Monteith 1965). Canopy transpiration is controlled by stomata conductance which is computed separately for shaded and sunlit leaves. The simulation of stomata conductance is a function of vegetation specific maximum conductance and environmental controls, such as light, CO<sub>2</sub>, leaf water potential and vapor pressure deficit. For the part of throughfall that gets into soil, a simple three-layer model is used to model vertical water flux in RHESSys. The three layers are root zone, unsaturated zone and saturated zone. When the soil layers are saturated, lateral flow occurs and carries DOC out from soil. The amount of DOC in soil solution that is leached out into stream channels is related to soil porosity, the decay rate of soil porosity, root zone depth, soil depth, available DOC in soil solution, DOC distribution with depth (named as DOC decay rate in RHESSys) and DOC absorption rate (Figure 4.6). Available DOC is distributed in soil based on soil depth and DOC decay rate. With the dynamic changes of the water table, amount of potential leached DOC is regulated by the depth of saturated soil layer. Actual DOC flux is then computed by subtracting this potential DOC leached by the amount of DOC absorbed onto soil particles. The DOC absorption function, simulated by a soil specific DOC absorption rate and depth of saturated soil layer, is newly included in RHESSys to better simulate the seasonal variation of DOC flux.

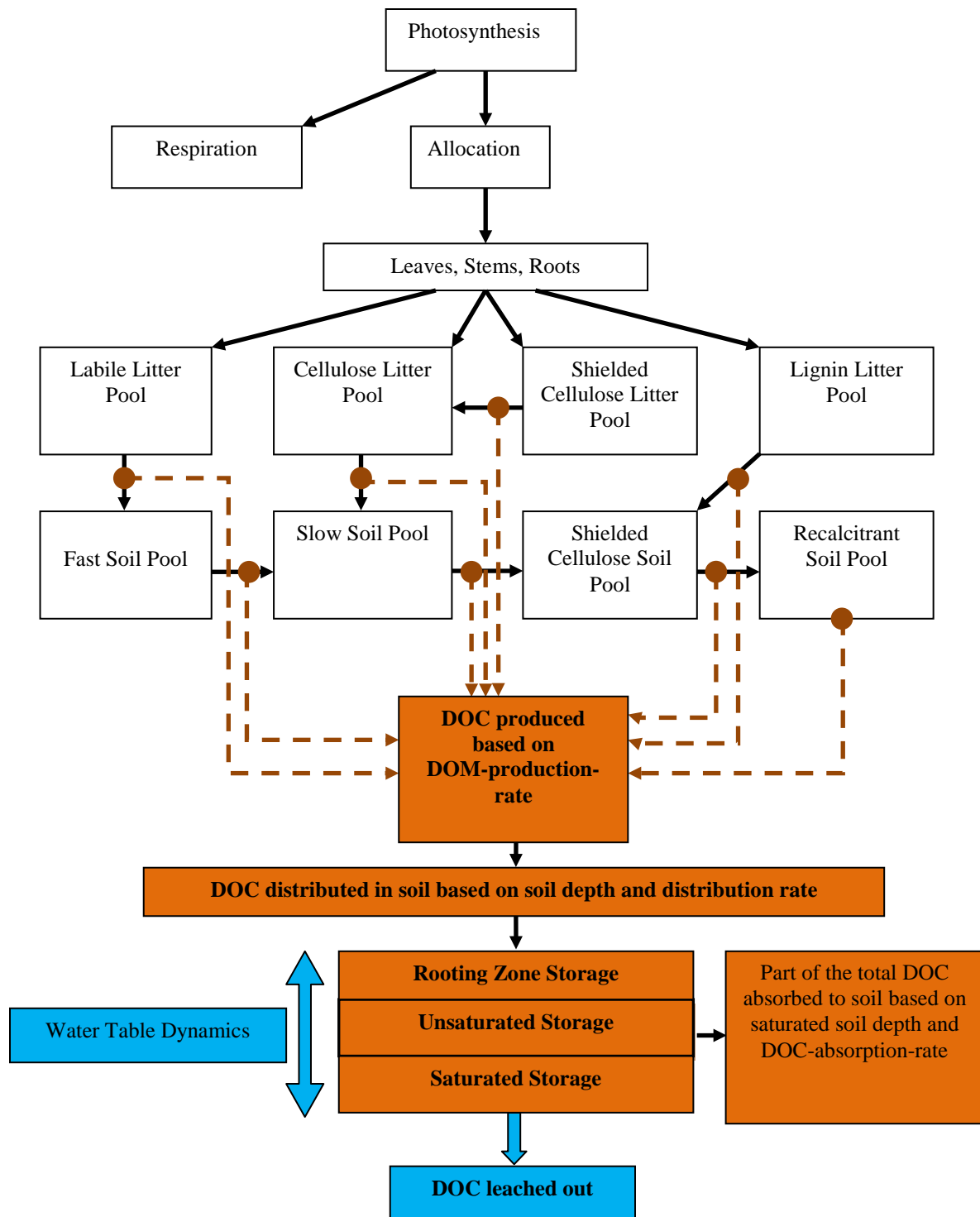


Figure 4.6. The simplified carbon cycle and the DOC production and transportation processes in RHESSys. DOM is dissolved organic matter which includes both dissolved organic carbon and dissolved organic nitrogen in RHESS.

## 4.3.2. The simulation of DOC Flux and Concentration in the Neponset River Watershed

### 4.3.2.1. Spin-up

Spin-up is necessary for process-based ecological models to get the simulated ecosystem to an initial state (values for all carbon, nitrogen and water pools) under a certain set of land cover and climate conditions. The initial state was evaluated through examination of soil carbon and soil nitrogen accumulation. The recalcitrant soil pool has a very long residence time which needs a long spin-up time to stabilize. Cold spin-up from zero carbon storage was used in this simulation. Background CO<sub>2</sub> concentration in the atmosphere and nitrogen deposition value (including both dry deposition and wet deposition) during the pre-industrial period were used for model spin up. All the vegetation was clear cut after spin-up and then simulated for another 80 years with increased CO<sub>2</sub> concentration and nitrogen deposition values representing the known land cover history of New England forests.

### 4.3.2.2. Calibration

The model was then calibrated using USGS gauge station data at Milton Village from November 1996 to November 2005, in order to bring the hydrological conditions in the model closer to reality. A number of drainage-related parameters that cannot be directly measured are typically needed for calibration in hydrological models (Beven and Freer 2001; Tague et al. 2013). The main parameters for calibration are the decay of hydraulic

conductivity with depth (m); saturated soil hydraulic conductivity at the surface (K); two groundwater parameters which control the proportion of infiltrated water that bypasses soil to a deeper groundwater table (gw1); and the rate of lateral flow from a hillslope-scale groundwater table to the stream channel (gw2). The calibration process used the Monte Carlo method with stream flow data. The goodness of fit between measured stream flow data and simulated results are estimated by both the Nash-Sutcliffe Index and the logarithm of it. The logarithm of the Nash-Sutcliffe Index can better capture recession and low flow behavior. Equifinality is a common problem during calibration, especially for complex hydro-ecological models (Beven and Freer 2001). To evaluate the uncertainty of simulated streamflow, generalized likelihood uncertainty estimation (GLUE) method was used. GLUE was introduced by *Beven* and *Binley* to quantify the equifinality of complex hydrological model predictions (Beven and Binley 1992). The parameter sets, that have a Nash-Sutcliffe Index larger than 0.65 and a logarithm of the Nash-Sutcliffe Index larger than 0.8, were chosen from hundreds of simulations.

## CHAPTER 5

### SENSITIVITY ANALYSIS AND SIMULATION OF DOC CONCENTRATIONS AND FLUX USING THE RHESSYS MODEL – THE RESULTS

With Chapter 4 focusing on the initialization of RHESSys model and methodology of hydro-ecological processes in RHESSys model, Chapter 5 is going to focus on the results of sensitivity analysis of DOC simulation using RHESSys and the simulated DOC concentration and DOC flux in the Neponset River Watershed.

#### 5.1. Sensitivity Analysis

Before running the fully parameterized RHESSys model for the Neponset Watershed, a sensitivity analysis for DOC transport was performed to fully explore the capabilities of the model. Physical hydro-ecological model simulation can improve our understanding of how various parameters affect stream flow DOC.

Three groups of parameters were tested using the RHESSys model for a single 30 m by 30 m patch with the average slope, elevation, and the majority land use, soil and vegetation types of the Neponset River Watershed. Thus, RHESSys was run as a lumped watershed model. Sensitivity analysis was done for three groups of parameters consisting of 1) model parameters which include DOM\_decay\_rate, DOC\_production\_rate and DOC\_absorption\_rate, 2) climate indices which included temperature and nitrogen deposition rates, and 3) soil and vegetation parameters which included soil depth, the ratio of infiltrated water bypass soil (via macropores and fractures) into a deeper groundwater table, and C:N ratio of leaf litter.

The sensitivity analyses results were evaluated by three indices: the feedback index, the annual average of daily stream DOC concentration and flux, and coefficient of variation of daily stream DOC concentration and flux. The feedback index (FI) estimates the extent of the changing parameters' influence on DOC flux and concentration.

$$FI = (\text{Stream\_DOC}_i - \text{stream\_DOC}_0) / (\beta_i - \beta_0)$$

where stream\_DOC<sub>i</sub> is the simulated annual average stream DOC flux/concentration using new values for the test parameter, stream\_DOC<sub>0</sub> is the simulated background stream DOC flux/concentration using original values for the test parameter,  $\beta_i$  is the new value of the test parameter, and  $\beta_0$  is the original value of the test parameter. A positive FI means larger values of the test parameter can increase DOC flux/concentration and a negative FI means larger values of the test parameter can decrease DOC flux/concentration.

The coefficient of variation calculated for the daily stream flow DOC flux/concentration output is also used to estimate whether changing parameters affect the distribution of the daily stream flow DOC flux/concentration output. Larger CV means higher peaks and/or lower low values of daily stream flow DOC flux, while lower CV means more evenly stable distribution of daily stream flow DOC flux.

### 5.1.2. Model Parameters

Hundreds of parameters are utilized in RHESSys and influence the stream DOC output, since stream DOC is so tightly linked to both ecological processes and hydrological processes. Most of these parameters, however, are not varied in a typical RHESSys simulation and are physiological parameters that set based on plant function type or soil parameters that are set based on soil classes. However, there are three key parameters (DOM\_decay\_rate, DOM\_production\_rate and DOC\_absorption\_rate) that directly affect stream DOC output. These physiological parameters are difficult to measure and there is much uncertainty in the values. A process-based model can not only test the influence of various values of these physiological parameters on DOC simulation but also improve our understanding of how the landscape characteristics (e.g. distribution of organic carbon in soil with depth) affect DOC export.

#### 5.1.2.1. DOM Decay Rate

DOM\_decay\_rate represents the distribution rate of dissolved organic matter (DOM) in soil with the change of soil depth. A higher DOM\_decay\_rate means more DOM located in deeper layers of soil and less DOM located in the surface soil. This parameter functions closely with soil depth, saturated hydraulic conductivity and the decay rate of saturated hydraulic conductivity to affect DOC export. 3 m and 10 m soil depths were simulated and analyzed to briefly show the impact of soil depth.

Figure 5.1 shows the changes of average daily stream DOC flux, the coefficient of variation of daily DOC flux and the feedback index calculated from 20 years' simulation with a 3 m soil depth. Average daily stream DOC flux decreases when DOM\_decay\_rate increases, since less available DOC is distributed more evenly with depth. The coefficient of variation (3.04 to 3.18) of simulated average daily stream DOC flux increases with increase of DOM\_decay\_rate, so the DOC flux is small most of the time, then a large proportion of DOC is leached out from the soil during a few large precipitation events. The feedback index of stream DOC flux shows a decreasing trend with the increase of DOM\_decay\_rate. Average daily stream DOC concentration decreases almost linearly from 236 to 226  $\mu\text{mol/l}$  when the DOM decay rate increases from 0 to 1 (Figure 5.2). Coefficient of variation of daily stream DOC concentration shows a similar, but ascending trend, but with less variation. The feedback index decreases linearly from -8.64 to -10.5  $\mu\text{mol/l}/\text{DOM\_decay\_rate}$ .

The daily DOC flux ranges from 0.018 to 0.035  $\text{gC}/\text{m}^2/\text{day}$  and daily DOC concentration changes from 580 to 1200  $\mu\text{mol/l}$  when the soil depth is increased to 10 m (Figure 5.3 and

Figure 5.4). The DOC flux and concentration slightly decrease when the DOM\_decay\_rate is smaller than 0.45 and increases rapidly when the DOM\_decay\_rate increases. The coefficient of variation of daily DOC flux keeps increasing with a DOM\_decay\_rate less than 0.7 and decreases when the DOM\_decay\_rate is between 0.7 and 0.8. The coefficient of variation slightly increases in the range of 0.8 to 1 of DOM\_decay\_rate. The coefficient of variation of DOC concentration and the feedback index show similar trends as the flux. The results indicate the ecosystem has a negative feedback of DOC export with increasing DOM\_decay\_rate then a positive feedback when DOM\_decay\_rate continues increasing.

DOC flux and concentration is larger with 10 m soil depth than with 3 m soil depth. The amount of DOC flux and concentration are directly affected by the amount of available DOC in soil and the amount of water passing through soil. The distribution of DOC in soil is an exponential function meaning more DOC at the surface than in deep soil. The amount of DOC in deep soil is larger if the DOM\_decay\_rate increases from a very small value. Therefore, less DOC would be leached out from the soil when the amount of water passing through the soil is the same. The change in the amount of DOC in deep soil becomes less if the DOM\_decay\_rate increases from a large value. The leached DOC is less for a shallow soil depth (e.g. 3 m) because of the limited involved water and soil depth. However, the small change of available DOC is traded off by the increasing amount of involved water and soil depth when soil is thick enough. Therefore, the DOC flux and concentration decrease first and then increase rapidly for 10 m soil depth.

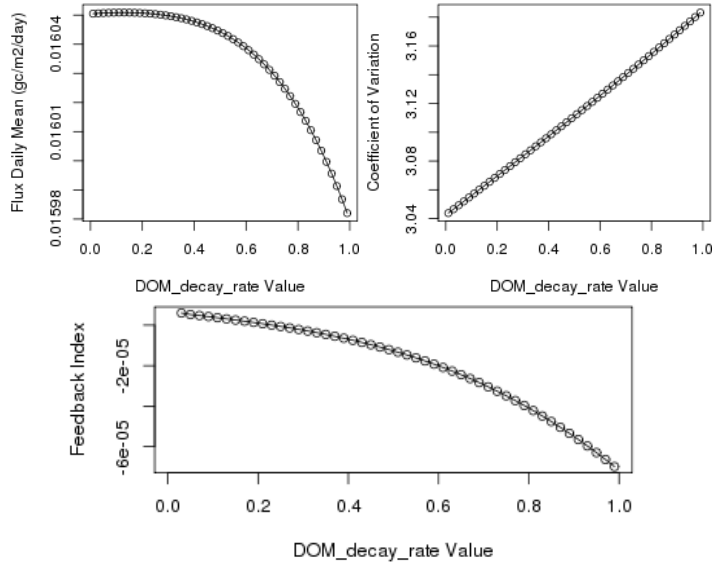


Figure 5.1. DOM\_decay\_rate changes for stream DOC flux when soil depth is 3 m.

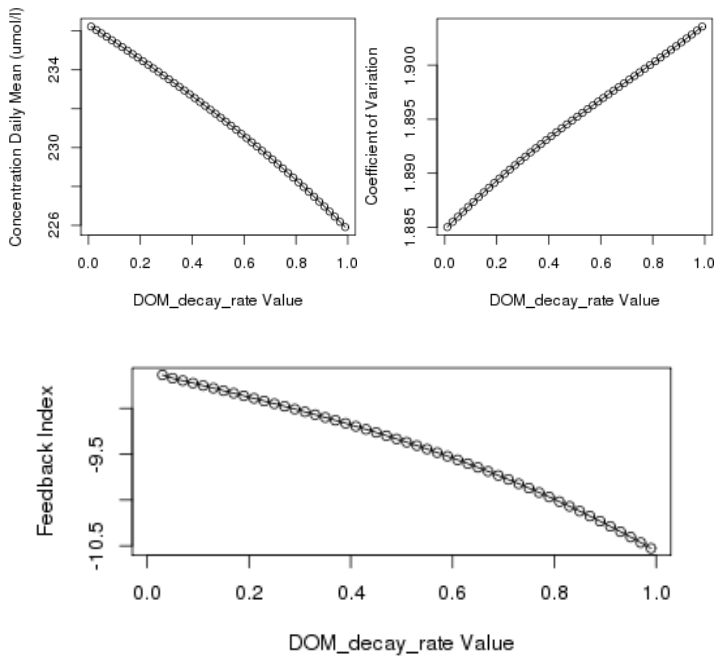


Figure 5.2. DOM\_decay\_rate changes for stream DOC concentration when soil depth is 3 m.

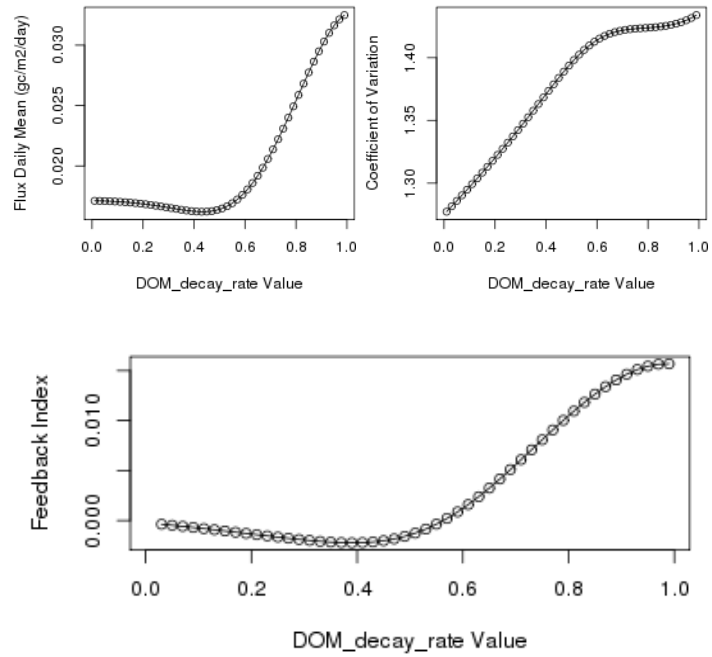


Figure 5.3. DOM\_decay\_rate changes for stream DOC flux when soil depth is 10 m.

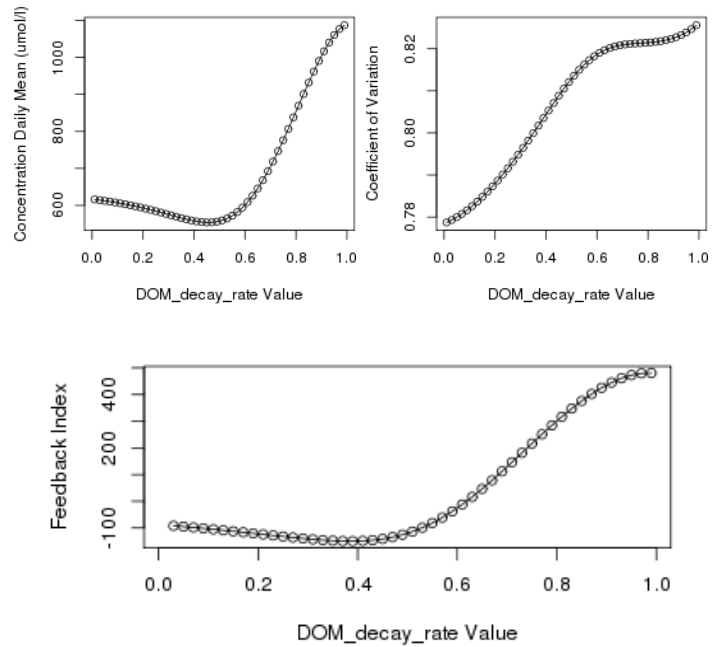


Figure 5.4. DOM\_decay\_rate changes for stream DOC concentration when soil depth is 10 m.

#### 5.1.2.2. DOM Production Rate

DOM\_production\_rate in RHESSys is a scalar from 0 to 1 based on different soil types. Normally the value of the DOM\_production\_rate is less than 0.05. The DyDOC model was applied to a deciduous forest in Tennessee and the transformation of soil organic matter to dissolved organic matter was set as 0.02 (Tipping et al. 2012). The variation of DOM\_production\_rate has influence on both the ecological and hydrological processes of DOC simulation. A higher DOM\_production\_rate means more litter carbon is converted to DOC, which is also the same for DON (dissolved organic nitrogen). A higher DOM\_production\_rate will ultimately increase the loss of nitrogen and then decrease Leaf Area Index (LAI), which decreases the amount of potential DOC that can be leached out. Although a higher DOM\_production\_rate produces more DOC, less water passing through may decrease the amount of DOC leached into stream.

The mean daily stream DOC flux increases very rapidly when the DOM\_production\_rate starts to increase from zero and then increases more slowly, ranging from 0.007 gC/m<sup>2</sup>/day to 0.031 gC/m<sup>2</sup>/day when DOM\_production\_rate changes from 0.08 to 1 (Figure 5.5). The coefficient of variation (1.5 to 0.7) of the average daily stream DOC flux decreases with increasing DOM\_production\_rate. As DOM\_production\_rate increases, the feedback index (0.47 to 0.02 gC/m<sup>2</sup>/day/DOM\_production\_rate) drops dramatically and then the change stabilizes close to zero. The change of DOM\_production\_rate at lower levels of DOM\_production\_rate causes greater increases of daily stream DOC flux. The three indices of daily stream DOC concentration show similar trends to the change in DOC flux (Figure 5.6). Feedback index has a very

substantial change with per unit change of DOM\_production\_rate, ranging from 17500 to 0  $\mu\text{mol/l}/\text{DOM\_production\_rate}$ . DOC export undergoes positive feedback with the increase of DOM\_production\_rate. However the influence of the DOM\_production\_rate on DOC export tends to be smaller with higher DOM\_production\_rate.

Total plant carbon decreases with an increase of the DOM\_production\_rate from zero, because more DON is produced during decomposition, thus nitrogen is less available for vegetation growth (Figure 5.7). Less litter is supplied at this situation, which eventually decreases the production of DOC in the system. The results indicate vegetation plays an important role in the DOC flux process by controlling the litter production, which is the source of DOC in soil. The results also illustrates a tight coupling between vegetation and nitrogen availability and DOM production.

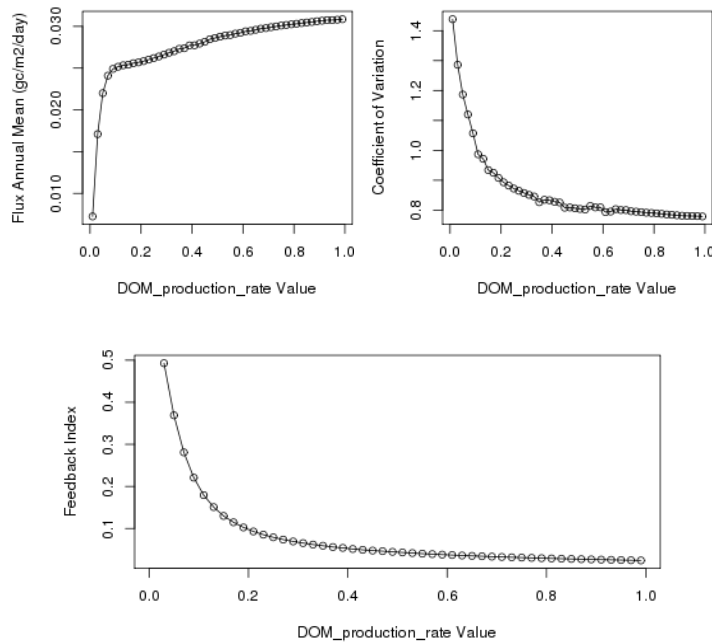


Figure 5.5. Stream DOC flux changes with DOM\_production\_rate.

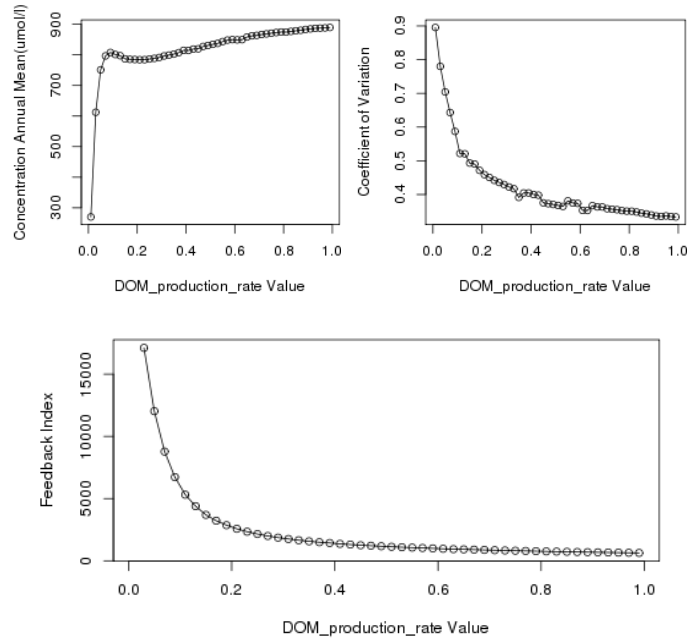


Figure 5.6. Stream DOC concentration changes with DOM\_production\_rate.

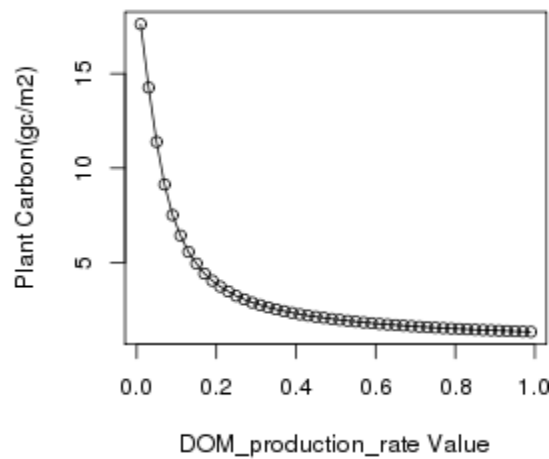


Figure 5.7. Plant carbon amount changes with DOM\_production\_rate.

### 5.1.2.3. DOC Absorption Rate

DOC\_absorption\_rate is a soil specific parameter that is used to estimate the amount of DOC absorbed in soil. Its unit is mgC/Kg soil. An earlier study, using 17 soil profiles,

found the amount of DOC absorbed in the soil surfaces was  $23 \pm 73$  mgC/Kg soil (Kothawala et al. 2008). DOM\_decay\_rate controls the amount of DOM in soil available to be flushed out of the terrestrial system. The daily stream DOC flux has a good linear relationship with DOC\_absorption\_rate (Figure 5.8). However, the difference between the maximum and minimum DOC flux is very small (0.01713 to 0.017 gC/m<sup>2</sup>/day) due to the shallow soil depth (3 m) used. More DOC is accumulated in the soil during normal precipitation events with a higher DOC\_absorption\_rate. However, this accumulated DOC gets leached out once larger precipitation occurs. This phenomena is consistent with field observations (Inamdar and Mitchell 2006) that storms carry most of the DOC out of the terrestrial system. The coefficient of variation ranging from 1.27 to 1.33 also has a positive linear relationship with DOC\_absorption\_rate. The feedback index of average daily stream DOC flux is also small, with a range of 0.0046 to 0.0035 gC/m<sup>2</sup>/day/DOC\_absorption\_rate.

The average daily stream DOC concentration has a negative relationship with DOC\_absorption\_rate (Figure 5.9). The coefficient of variation increases from 0.77 to 0.79 when the DOC\_absorption\_rate increases from zero to 0.000245 kgC/kg soil. The feedback index changes from -44970 to -44860 umol/l/DOC\_absorption\_rate. DOC\_absorption\_rate is directly related to soil weight. Soil depth is a key parameter controlling the amount of DOC available to be leached out. The average daily DOC concentration changes very little for shallow soil depth when the DOC\_absorption\_rate is within the normal range. The DOC\_absorption\_rate mainly affects the timing of DOC leaching.

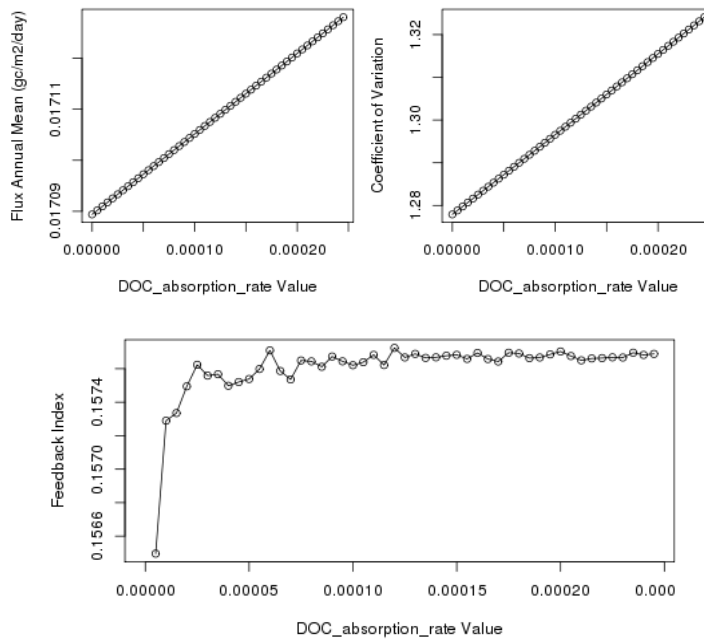


Figure 5.8. Stream DOC flux changes with the DOC\_absorption\_rate.

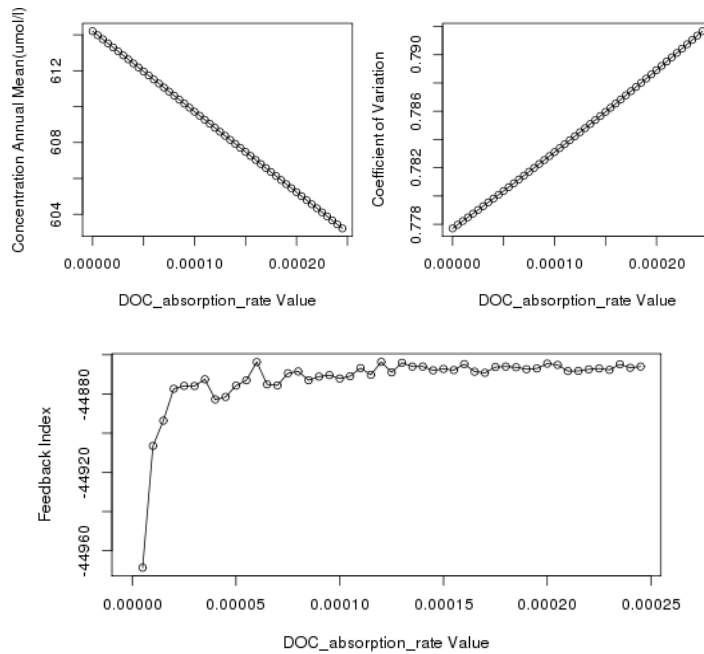


Figure 5.9. Stream DOC concentration changes with the DOC\_absorption\_rate.

For the three above parameters, DOM\_decay\_rate works closely with soil depth, hydraulic conductivity and the decay rate of hydraulic conductivity. The variation of DOC export with changing DOM\_decay\_rate for a constant soil depth is less than the variation of DOC export with differing soil depth. DOM\_production\_rate is the most sensitive among these three model parameters. However, since DOM\_production\_rate affects vegetation growth, there is a threshold existing for its influence on DOC simulation. When DOM\_production\_rate is less than the threshold, DOC export increases quickly with the increase of DOM\_production\_rate. When DOM\_production\_rate is larger than the threshold, DOC export increases very slowly with the increase of the DOM\_production\_rate. The threshold may change based on various patch characteristics, such as vegetation type, soil type and climate type. There is only a small alteration in model response with variation in the DOC\_absorption\_rate. It has large influence on the seasonal patterns of DOC export with the dynamics of water table, which cannot be shown from the 20 years' average daily DOC export.

### 5.1.3. Climate Indices

Climate changes significantly affect ecosystems. However, few studies estimate the influence of changing climate on stream DOC flux and concentration. Two climate indices (nitrogen deposition and temperature) were analyzed using the RHESSys model.

#### 5.1.3.1. Nitrogen Deposition

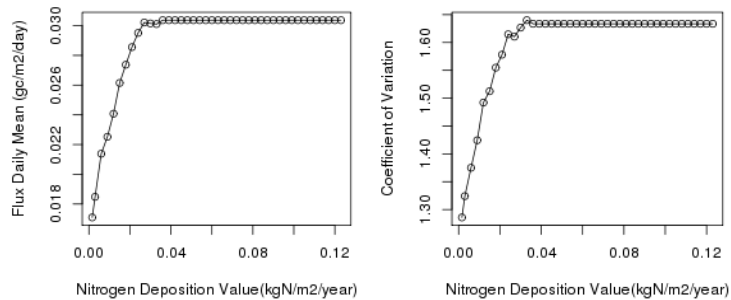
Nitrogen is one of the most limiting factors for vegetation growth in the study area (Aber et al. 1993). Increasing nitrogen deposition provides more nitrogen to vegetation and raises the photosynthetic rate and the amount of carbon fixed in the ecosystem. In the meantime, the increased leaf area may consume more water and reduce the amount of water that transfers DOC out of the soil, decreasing the DOC flux and concentration. DOC in the forest floor leachate is expected to decline under N saturation status because of the increased energy demand associated with immobilization of nitrogen (Aber, 1992). However, field experiments with N amendments did not support this hypothesis and no significant DOC concentration change was observed (Guggenberger and Zech 1994; Gundersen et al. 1998; McDowell et al. 1998; Rustad et al. 1996). In this study, sensitivity analysis of DOC simulation to nitrogen deposition was performed over a longer period with more varied nitrogen deposition levels. Plant carbon increases significantly with more average daily stream DOC flux and concentration when nitrogen deposition is larger than  $0.016 \text{ KgN/m}^2/\text{year}$  (Figure 5.10, Figure 5.11 and Figure 5.12). Nitrogen is no longer a limiting factor for vegetation growth when nitrogen deposition reaches around  $0.035 \text{ KgN/m}^2/\text{year}$ . This threshold is larger than chronic nitrogen addition conducted by Aber in Harvard forest, which is around  $0.014 \text{ KgN/m}^2/\text{year}$  (Aber et al. 1993). Plant carbon stops growing and becomes stable. However they did not find nitrogen was saturated in the hardwood site at this value. The coefficient of variation of DOC flux (1.2 to 1.7) has a similar trend as the coefficient of variation of DOC concentration (0.75 to 1.1). Per unit change of nitrogen deposition causes about  $1.0 \text{ gC/m}^2/\text{day}$  change of average daily stream DOC flux, while the effect decreases as the

nitrogen deposition gets higher. The feedback index of DOC concentration shows a similar trend as the feedback index of DOC flux.

### 5.1.3.2. Temperature Increase

Temperature affects the photosynthesis rate, respiration rate, decomposition rate, evaporation rate and transpiration rate. Higher temperature increases the primary vegetation production by accelerating photosynthesis, and also enhances vegetation respiration and organic matter decay rates.

Increasing temperature raises the stream DOC flux (0.0161 to 0.031 gC/m<sup>2</sup>/day) and concentration (600 to 1200 umol/l). The DOC flux and concentration start to decrease when the temperature reaches a limit of vegetation growth. (Figure 5.13 and Figure 5.14). Slightly higher temperature can stimulate the growth of vegetation and also increase decomposition rate (Davidson et al. 1998), while the growth of vegetation can be limited under very high temperatures which exceed the tolerance of vegetation growth (Bassow et al. 1994; Wayne et al. 1998).



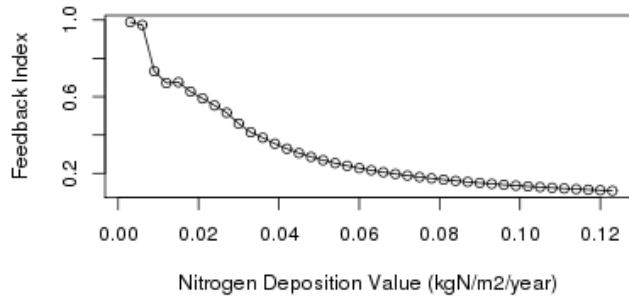


Figure 5.10. Stream DOC flux changes with nitrogen deposition.

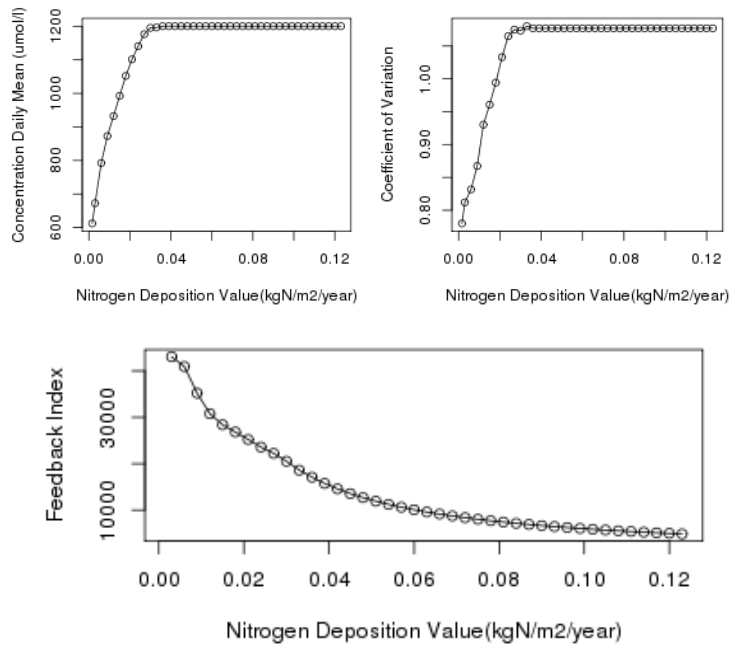


Figure 5.11. Stream DOC concentration changes with nitrogen deposition.

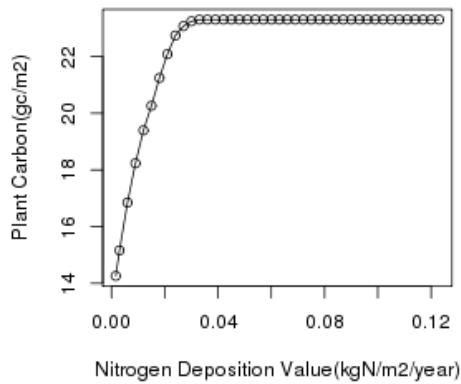


Figure 5.12. Plant carbon storage changes with nitrogen deposition changes.

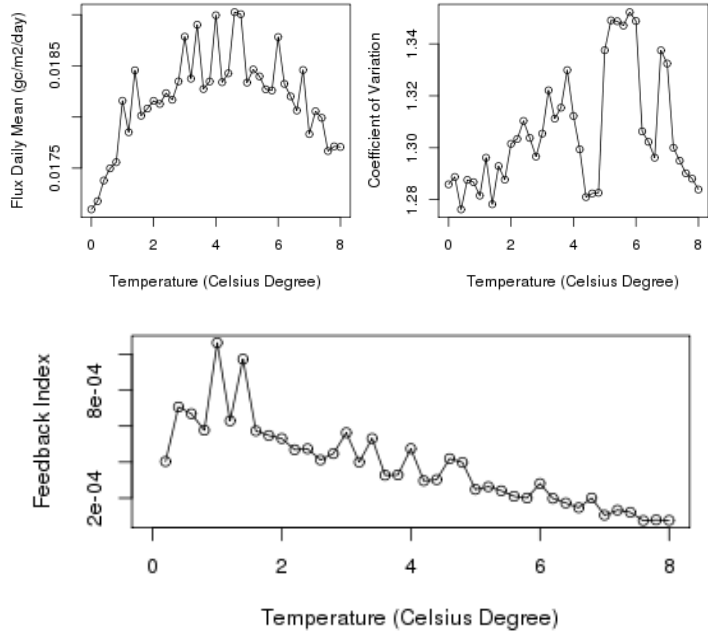


Figure 5.13. Stream DOC flux changes with change in temperature.

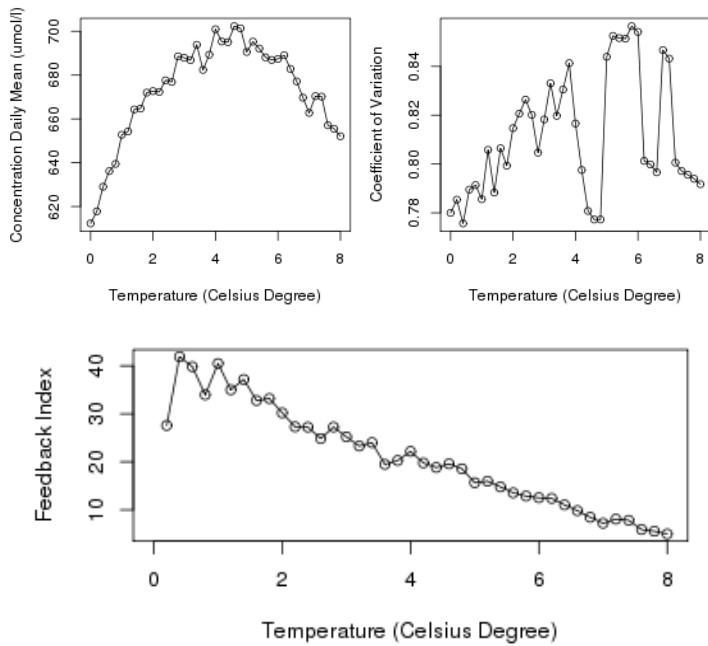


Figure 5.14. Stream DOC concentration changes with change in temperature.

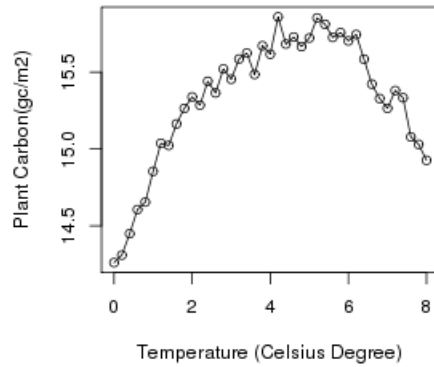


Figure 5.15. Plant carbon storage changes with change in temperature.

Nitrogen deposition has a more significant influence than temperature given expected ranges for nitrogen deposition and temperature in the Neponset River Watershed. The feedback index gets close to zero when a threshold is reached for both of these climate parameters. Sensitivity analysis of climate indices has some limitations. The feedback index is calculated from the average value of twenty year's daily stream DOC flux and concentration, which ignores the nonlinear relationship between DOC export and changing testing parameters. With the temperature and nitrogen deposition change, changes of plant organisms (such as leaf structure) are not considered in this analysis.

#### 5.1.4. Soil and vegetation parameters

The sensitivity of soil depth, the proportion of surface water that becomes groundwater, and litter composition (which is one of the vegetation parameters) are analyzed in this section.

### 5.1.4.1. Soil Depth

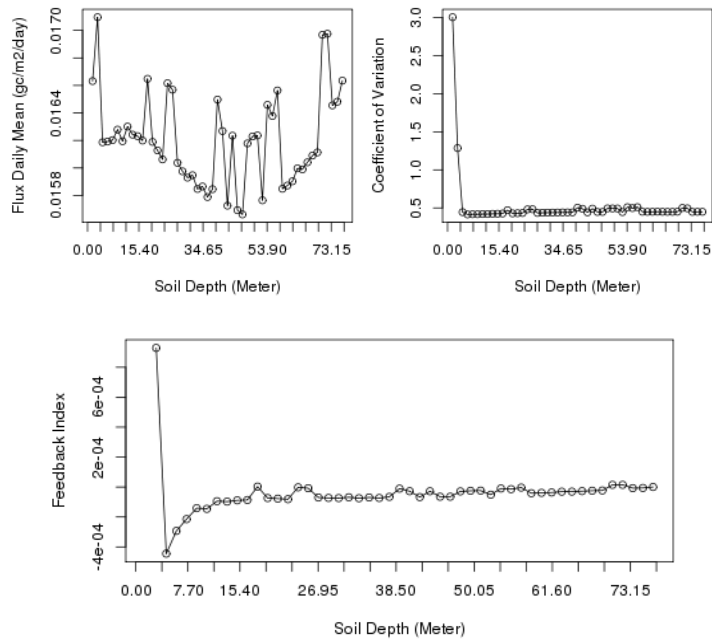


Figure 5.16. Stream DOC flux changes with soil depth.

Soil depth is a key parameter that controls the production of lateral flow, soil moisture, and vegetation growth. Soil depth is shallow with an average of 3 m for the Neponset River Watershed. Soil depth influences stream DOC concentration more than stream DOC flux (Figure 5.16 and Figure 5.17). Therefore, soil depth has a stronger effect on hydrological processes than on ecological processes. DOC flux and concentration significantly increase and their coefficient of variation and the feedback index of DOC flux decrease while the feedback index of DOC concentration increases, as soil depth increases from 3 m to 15 m. Less change was found for DOC flux and concentration, coefficient of variation, feedback index of DOC flux and concentration, and plant carbon storage, when soil depth is larger than 15 m. The turning point of soil depth may vary based on different soil texture, surface saturated hydraulic conductivity (K) and the decay

rate of K (m). For study areas with shallow soil depth, accurate assessment of soil depth is a key factor that affects accurate simulation of DOC export.

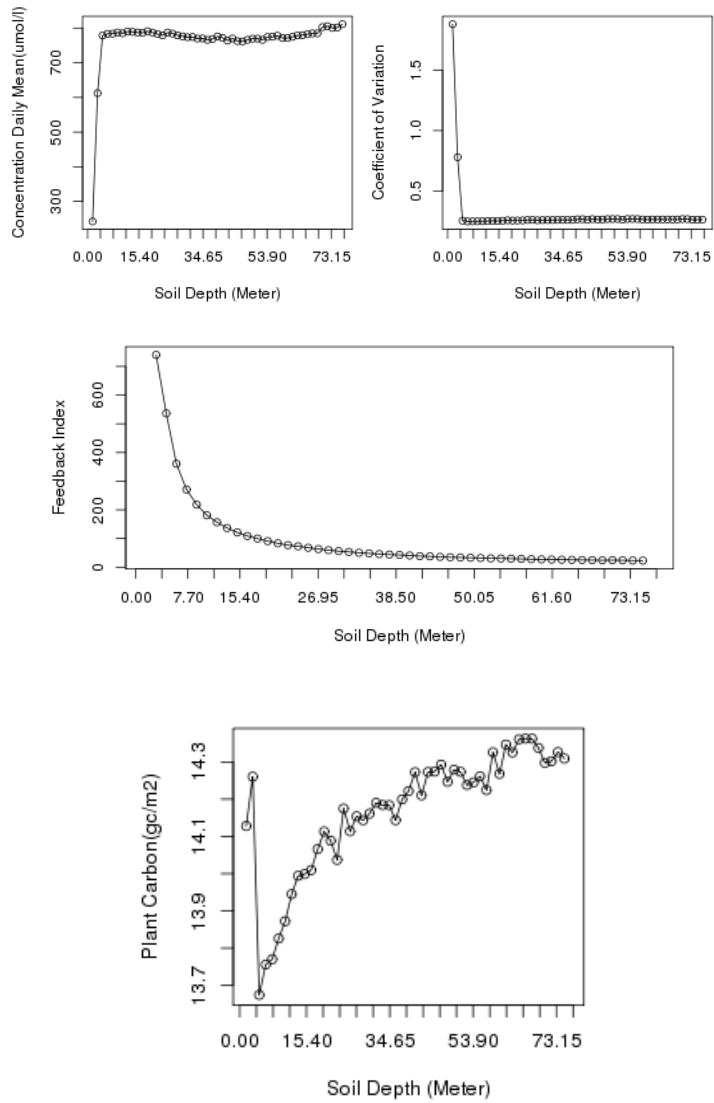


Figure 5.17. Stream DOC concentration changes with soil depth and plant carbon storage changes with soil depth.

#### 5.1.4.2 The proportion of surface water that becomes groundwater

The proportion of surface water that bypasses soil layers and goes directly into ground water is unavailable for vegetation growth and DOC leaching. The proportion of surface water that becomes groundwater has a high correlation with daily DOC flux (Figure 5.18) because of the limiting effect of this parameter on vegetation growth.

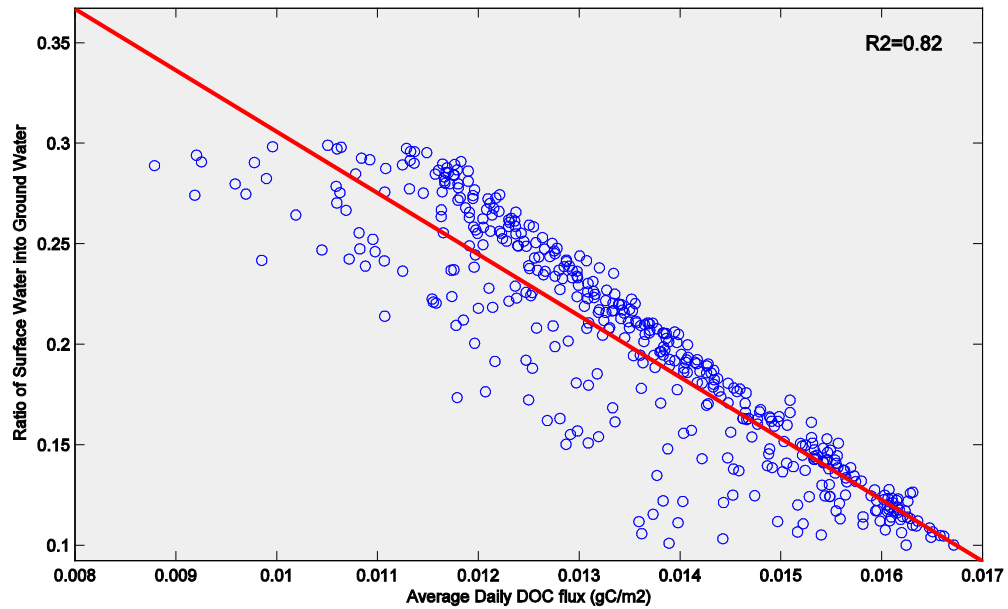


Figure 5.18. The correlation between average daily DOC flux and the proportion of surface water that becomes groundwater.

#### 5.1.4.3 C:N Ratio of Leaf Litter

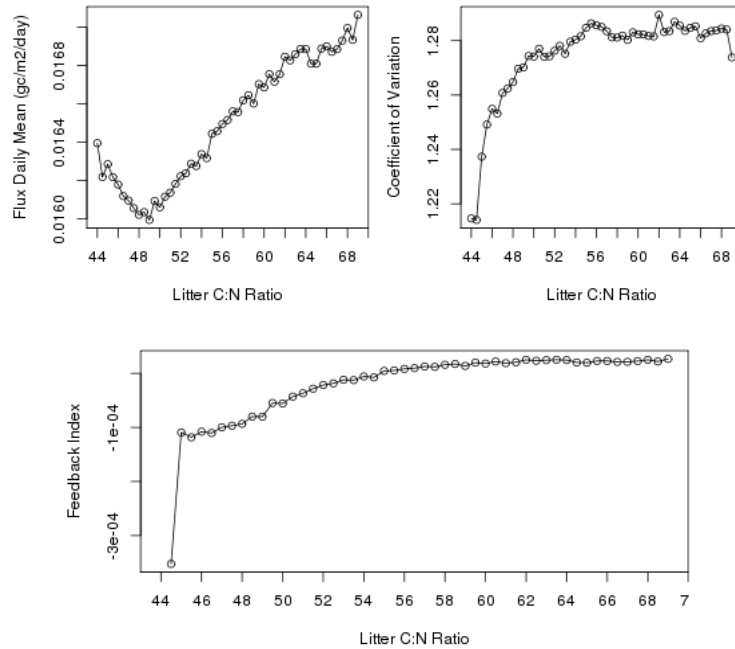


Figure 5.19. Stream DOC flux changes with the litter composition.

Carbon fixed through photosynthesis is allocated into different parts of the plant.

Nitrogen is correspondingly allocated in the plant by the carbon to nitrogen ratio (C:N) in leaf, root and stem. Leaf litter is a source of DOC and DON, so the C:N value is

important for DOC export. The reasonable range of leaf litter C:N is from 42 to 70 based on literature reviews (White et al. 2000). The daily stream DOC flux changes from 0.016 to 0.017 gC/m<sup>2</sup>/day while the smallest DOC flux occurs when leaf litter C:N is 48 (Figure 5.19). A similar trend also appears in DOC concentration.(Figure 5.20). The coefficient

of variation of DOC flux (1.21 to 1.29) and concentration (0.69 to 0.78) increases when litter C:N is less than 48, and then maintains a relatively slow and stable increase. Plant carbon storage increases (14.0 to 14.3 gC/m<sup>2</sup>) with the litter C:N ratio (Figure 5.21).

DOC export has a negative feedback with increasing leaf litter C:N. However, with the increase of leaf litter C:N, the negative feedback becomes smaller and is close to zero

when leaf litter C:N is larger than 68. Therefore, for vegetation that has less leaf litter C:N ratio (especially around 48), DOC export simulation is sensitive to leaf litter C:N ratio.

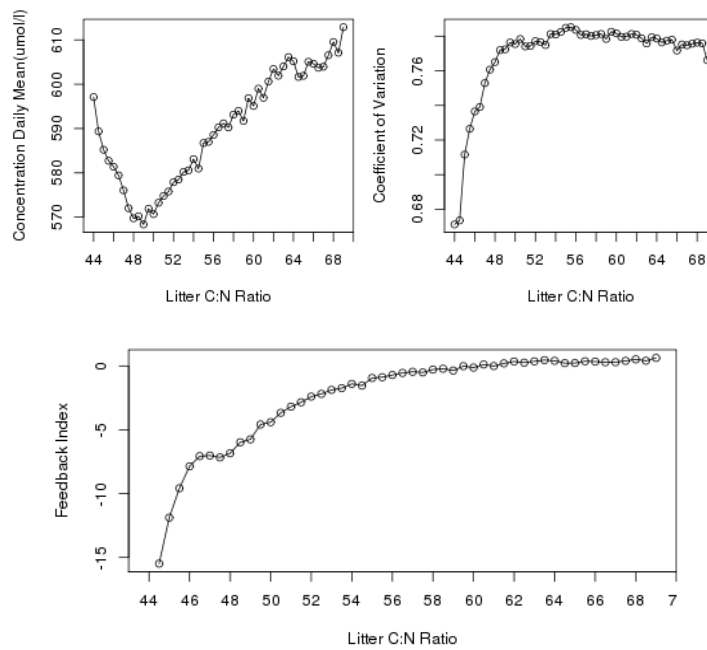


Figure 5.20. Stream DOC concentration changes with the litter composition.

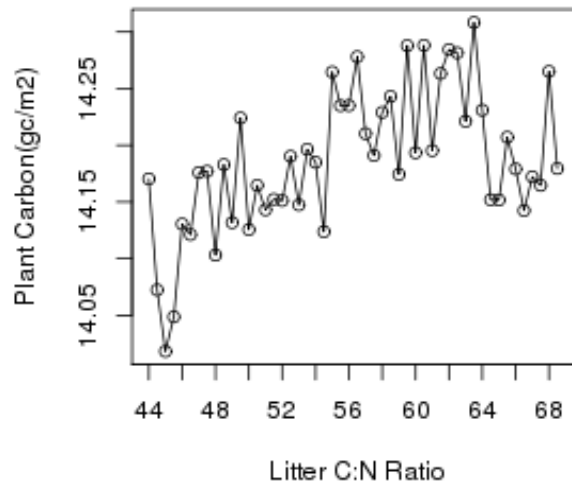


Figure 5.21. Plant carbon storage changes with the litter composition.

## 5.2. Neponset Results

### 5.2.1. Calibration using the Generalized Likelihood Uncertainty Estimation (GLUE) method

GLUE was introduced by Beven and Binley (1992) to quantify the uncertainty of model predictions (Beven and Binley 1992). For complex hydro-ecological models like RHESSys, it is unavoidable to have several sets of parameters that function equally well when compared with the observed data; this is called equifinality. Combined with Monte Carlo analysis, GLUE can represent the uncertainty of a model simulation in relation to equifinality. Parameters that were calibrated are surface hydraulic conductivity (K), decay rate of surface hydraulic conductivity with depth (m), the amount of water from precipitation that goes directly to groundwater (gw1), and the amount of water that leaves the groundwater pool to streamflow (gw2). The Nash-Sutcliffe index, calculated from the simulated stream flow and logarithms of simulated stream flow, was used to measure the likelihood of model performance. The model was run to simulate streamflow for the period from 11/01/1996 to 10/31/2005 with 432 different sets of calibration parameters. The criterion for acceptance of parameter sets was based on the criterion that the Nash-Sutcliffe index of simulated stream flow was larger than 0.65 and the index based on the logarithm of simulated stream flow was larger than 0.80. 277 out of 432 simulations were selected.

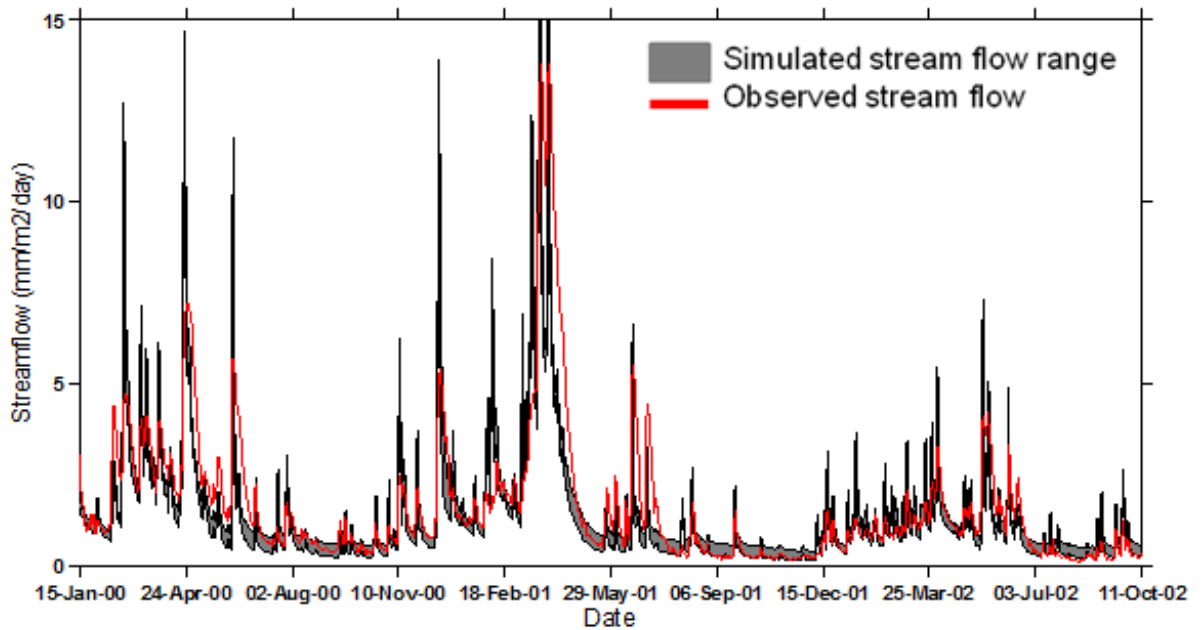


Figure 5.22. Uncertainty assessment of the stream flow simulation. The grey area was defined by using the 5% and 95% confidence levels of the acceptable simulated stream flow. The red line was the observed stream flow at the outlet of the Neponset River Watershed.

All the acceptable simulations tend to have high peaks, while there is more uncertainty during low flow conditions (Figure 5.22 and Figure 5.23). The simulated high peaks are higher than observed for high precipitation events and the simulated stream flow is lower than observed during the recession periods. For example, a large precipitation event was observed in late March of 2001 (March 22<sup>nd</sup> to April 5<sup>th</sup>) with the highest daily precipitation of 14mm/m<sup>2</sup> making this March the wettest from 1891 to present. Stream flow following extreme precipitation events is hard to simulate. One reason that needs to be noted is the uncertainty of the precipitation input. Many studies report that spatial rainfall measurement is important for streamflow simulation and its uncertainty has more influence on small watershed modeling (Arnaud et al. 2011; Berne et al. 2004; Emmanuel

et al. 2012; Vaze et al. 2011). Another factor that affects streamflow simulation is the duration of precipitation events. Including an accurate measurement of the duration of each precipitation events can significantly improve the accuracy of simulated streamflow. However, such data are unavailable for the Neponset River Watershed.

According to the storm water management policies issued by the Massachusetts Department of Environmental Protection, all new development projects need to match pre-development and post-development peak runoff rates. A variety of techniques have been developed and implemented to control peak runoff after development (e.g. dry extended detention ponds, porous pavement, grassed filter strips and wet ponds) but this kind of information is difficult to collect and was not provided in the input data.

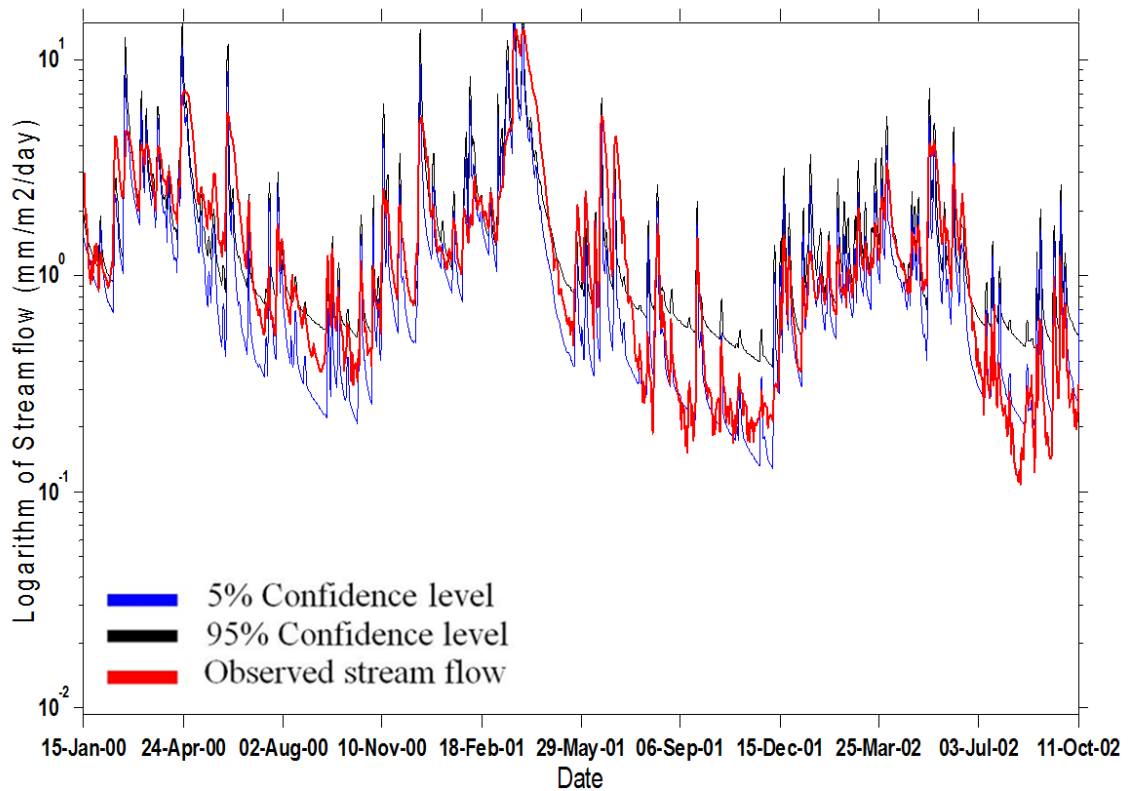


Figure 5.23. Uncertainty assessment of logarithms of stream flow simulation.

### 5.2.2. Simulated Root Zone Soil Moisture

Root zone soil moisture was calculated from simulated root zone water storage and root zone depth based on daily climate data and water availability. Measured soil moisture was collected from two sub-basins (Sharon and Milton) in the Neponset River Watershed in 2011 on a weekly basis. Sampling points in Sharon were located in dense forested and undeveloped areas, while all sampling points in Milton are in residential areas (back yards or public grassland). The  $R^2$  between the simulated and observed root zone soil moisture is 0.68 in Sharon and 0.35 in Milton (Figure 5.24). The simulated root zone soil moisture volume is comparably lower than the average of measured Sharon and Milton soil moistures. Most of the sampling points in Sharon are in forest while the simulated soil moisture for the whole sub-basin includes different land types. In Milton, all the sampling points are in developed grass land and experience irrigation during dry periods, which affects the correlation between simulated and observed soil moisture (as irrigation volume cannot be effectively estimated).

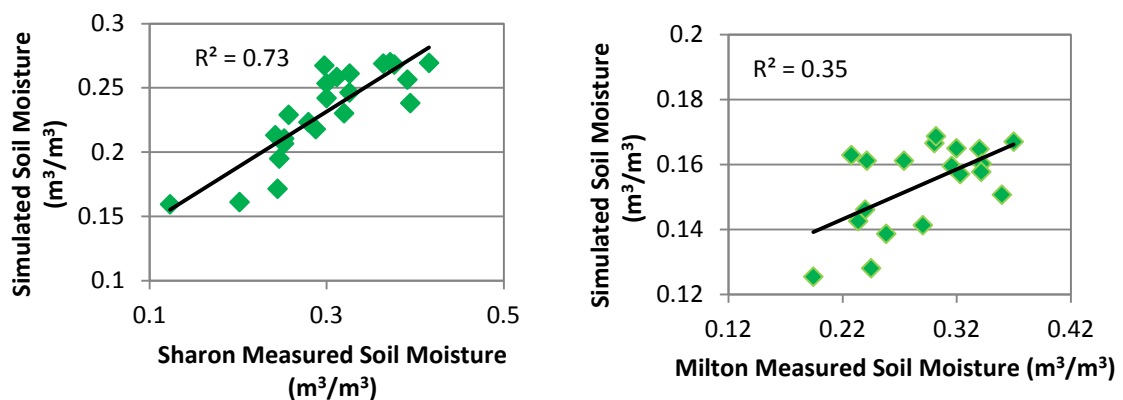


Figure 5.24. Simulated root zone soil moisture of the whole Neponset River Watershed comparing with average measured soil moisture in Sharon and Milton sub-basins.

The simulated root zone soil moisture of the two sub-basins in the Neponset River Watershed has a good correlation with field measured soil moisture. When field measured soil moisture data are not available, EVI2 estimated TVDI at both MODIS and Landsat scales, and especially MODIS scale, can be used to evaluate RHESSys simulated soil moisture.

### 5.2.3. Simulated Daily Stream DOC Concentration and Flux

The simulated DOC concentration generally agrees with observed values, though the model tends to overestimate DOC concentration over large precipitation events, and the simulated DOC misses the very high peaks in April, May and August of 2008 (Figure 5.25). The measured high peak of DOC concentration at the beginning of 2008 is caused by the accumulation of soil carbon during the second half of year 2007, and higher precipitation at the beginning of 2008. RHESSys simulation successfully caught the low DOC concentration during the second half of year 2007 and also produced relatively high DOC concentration in January and February of 2008. This is consistent with other studies about the memory of eco-systems, which means the store of DOC concentration in a year can impact DOC export in the following year (Yurova et al. 2008). However, RHESSys simulation did not capture the very high DOC concentration in April and May of 2008. It is possible that RHESSys did not capture this pattern because of the use of a constant soil specific DOC\_absorption\_rate rather than a dynamic DOC absorption function that varies with soil depth. This is also found in TRIPLEX-DOC model simulations (Wu et al. 2013). DOC is absorbed in soil surfaces based on the DOC\_absorption\_rate, which is a constant for all soil layers. However, in reality, the top layer of soil is normally an organic layer

which accumulates a large amount of DOC and has less mineral soil (and therefore less DOC absorption). Deep soil layers are mainly mineral soil which strongly absorbs DOC. Therefore, when water passes only through the top soil layer, the model may overestimate absorbed DOC and eventually underestimate DOC concentration in streamflow.

Comparing to the measured DOC concentration in July of 2008, 2009, 2010 and 2011, the simulated DOC concentrations are underestimated. High measured DOC concentrations during low flows were noticed by *Raymond* and *Saiers* and they suggested the possible reason might be autotrophic in-stream production (Raymond and Saiers 2010). The underestimation of DOC concentration in summer was reported by DOC simulation using INCA-C in four Swedish watersheds (Futter et al. 2011).

The correlation between the simulated and observed DOC flux matches better than DOC concentration (Figure 5.26). The overall correlation using all five years' data is 0.53. The correlation increases to 0.66 if the very low flows of July and August are removed. Overestimation of DOC flux during extreme precipitation events also occurs. The reason is consistent with the high peak streamflow simulation. The stream DOC simulation is largely influenced by the hydrological cycle. Extreme precipitation events result in large amounts of DOC being leached into streams. Small precipitation events leach relatively less DOC into streams even though there is a large store of DOC in the soil. Additional research concerning soil absorption and desorption would likely improve the simulation of stream DOC during peak and low flow periods.

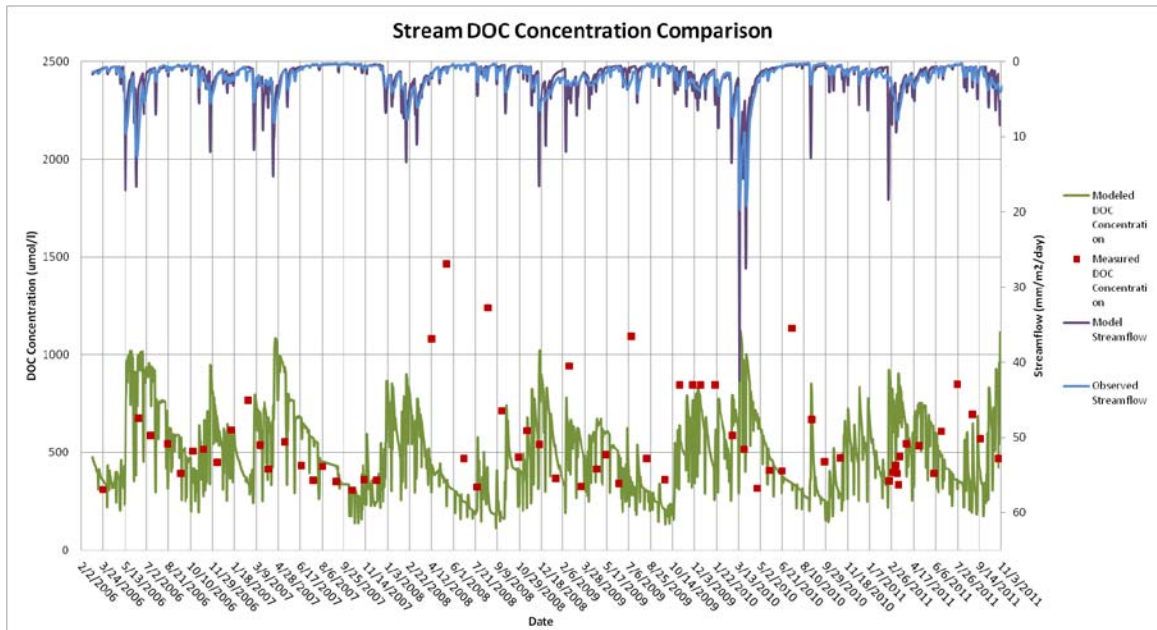


Figure 5.25. Simulated daily DOC concentration compared with observed DOC concentration and simulated daily stream flow compared with observed stream flow.

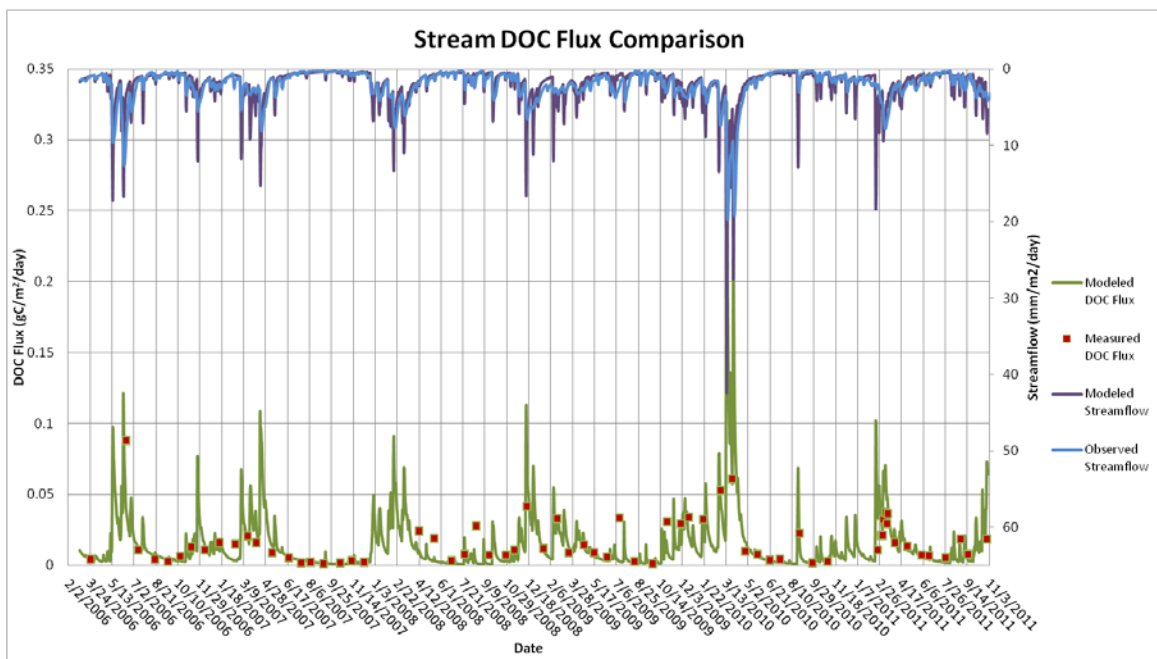


Figure 5.26. Simulated daily DOC flux compared with observed DOC flux and simulated daily stream flow compared with observed stream flow.

### 5.3. Conclusion

Physical process-based hydro-ecological models can not only be used to model ecosystems and predict future conditions but also offer a frame work for analyzing and unveiling mechanisms underlying various phenomena. This research used the RHESSys model to conduct a comprehensive stream DOC simulation sensitivity analysis of an urban coastal watershed using typical soil types and climate conditions for the northeast United States. In particular, the stream DOC flux and concentration were simulated over the Neponset River Watershed, one of the major rivers draining into Boston Harbor. The uncertainty of the simulated stream flow was analyzed using the GLUE method. The simulated DOC flux and concentration values matched well with observed data. Low flow situations tended to have more variation than peak flow periods indicating that RHESSys can simulate the DOC flux and concentrations very well during normal and wet seasons. However, RHESSys tended to overestimate stream flow volume, which decreased DOC concentration during the dry season. RHESSys simulation of DOC concentration and flux during the end of year 2007 and the beginning of year 2008 shows the memory of ecosystem. A better understanding of soil absorption and desorption will further improve the stream DOC simulations. The major conclusions are as follows:

- Slightly higher DOM\_production\_rate, nitrogen deposition, temperature, and deeper soil depth, can increase the stream DOC flux and concentration. The increase of DOC flux and concentration is not obvious when the soil depth increases over a certain threshold. This threshold is determined by soil characteristics, surface saturated hydraulic conductivity and the decay of the hydraulic conductivity. For study areas that have shallow soil layers, soil depth is

a key input for accurate estimation of DOC export. If sufficient inorganic nitrogen is available for vegetation growth when the DOM\_production\_rate is too high, this will eventually decrease the stream DOC flux and concentration. The influence of nitrogen deposition vanishes if the nitrogen deposition is large enough that nitrogen is no longer the limiting factor for vegetation growth. Increasing temperature will eventually become a limitation for vegetation growth. The increasing temperature will increase respiration rate and decreases stream DOC flux and concentration.

- Nitrogen deposition and DOM\_production\_rate are the most sensitive parameters based on the sensitivity analysis of DOC simulation using RHESSys. However, the increase of DOC export is only found under a certain threshold of these two parameters.
- The proportion of surface water that bypasses soil and becomes groundwater is an important but easily been overlooked model parameter that influences vegetation growth and stream DOC flux and concentration.
- The DOC absorption function can influence the timing of DOC leaching. This function does not significantly change the annual amount of stream DOC flux and concentration, but affect the pattern of DOC leaching based on the depth of the dynamic water table. A dynamic DOC absorption function that varies with soil depth will further improve the accuracy of DOC simulation.

## CHAPTER 6

### SUMMARY

The main goal of this research was to study the DOC flux from a terrestrial urbanized watershed to an estuarine system using a process-based regional hydro-ecological model and remotely sensed data. A special emphasis was placed on the effects of soil moisture on the system and the utility of various remotely sensed indices of soil moisture. Given a majority of the Earth's population now live in coastal cities, the ability to understand and accurately model the hydrologic and carbon cycling of the coastal urban ecosystem has become crucial. The RHESSys model, initialized and evaluated with remotely sensed data, represents an ideal platform to explore these complex systems.

During the course of this research, a number of important tasks were accomplished. This project represented the first time that the RHESSys model was applied to a watershed in the northeast United States and in particular to an urbanized coastal watershed in the

region. A comprehensive sensitivity analysis of the DOC simulation using RHESSys was undertaken to help separate and evaluate the influence of hydrological and ecological processes on DOC leaching from terrestrial to aquatic systems. A new soil absorption function was integrated into the baseline RHESSys code to improve its ability to simulate DOC transport.

This study also explored the use of various remotely sensed measures of the DEM, GPP, land use, soil and vegetation types, phenology and, in particular, soil moisture. These included a simple topographic moisture index (TMI) estimated using slope and water accumulation area, and a temperature vegetation dryness index (TVDI) estimated using various vegetation indices and land surface temperature. In general the coefficient of variation with field measured soil moisture decreases in wet conditions. Field soil moisture measures taken in the forest covered Sharon sub-basin of the Neponset River (further southwest of Boston) were found to exhibit a relatively stable correlation with TMI, while those measured in the urbanized Milton sub-basin nearer to Boston exhibited a larger variation of correlation with TMI. Thus the average correlation between measured soil moisture and TMI in this study region was weak and could not capture the temporal variation of the soil moisture. Compared with TMI, the TVDI was able to represent the temporal change of land surface soil moisture condition with better accuracy. The TVDI calculated from MODIS data displayed a strong correlation with measured soil moisture in the Greater Boston Area. The TVDI calculated from Landsat data had a weaker correlation with the measured soil moisture from the two sub-basins in the Neponset River Watershed, especially in the forest covered Sharon sub-basin. It

would appear that relatively wet land surface conditions, only one thermal band of Landsat data, and the variability of land covers at this higher spatial resolution all contributed to a decrease in the strength of this correlation. For TVDI<sub>s</sub> estimated from both MODIS and Landsat, the two-band EVI derived TVDI performed similarly to the SAVI derived TVDI, and both were slightly better than NDVI derived TVDI. The traditional NDVI derived TVDI tended to overestimate the dryness condition in dry areas under all conditions, and showed less sensitivity to changes in land surface soil moisture condition during high LAI periods. Therefore, this research suggests that the two-band EVI derived TVDI is best to be used as surrogate measure of field surface moisture at both MODIS and Landsat scales, especially at the MODIS scale.

In the Neponset River Watershed, the location of silt loam soils, strongly associated with the presence of the main channel wetland, and emergent wetland land use were found (via principal component analysis) to be highly correlated with the measured DOC concentrations among the different sampling points. Land cover and topographic characteristics controlled the long-term DOC concentration variation among various sub-basins. Short-term DOC concentrations depended primarily on climate conditions (e.g. temperature and precipitation). DOC concentration appears to be regulated by different factors in the growing and leaf-off seasons. Monthly average temperature, stream flow and API (antecedent precipitation index) all displayed a good correlation with the measured average DOC concentration at all sampling points during the growing season. However annual terrestrial GPP did not show a significant relationship with the annual DOC concentration. The eight-day GPP only displayed a good correlation with the DOC

concentration measured within the sub-basins in the vicinity of abundant wetland, which supports higher decomposition rates in the wetland. However, it is hard to identify the factors affecting the DOC concentration in the leaf-off season. Both the timing of snow melt and previous DOC leaching status can significantly affect the DOC concentrations during the leaf-off season, but it is hard to fully quantify their influence due to a lack of detailed measurements during the snow melt period.

By embracing various land surface information and daily climate data, physical process-based models such as RHESSys are shown effectively to simulate DOC concentrations, DOC flux and soil moisture. The simulated DOC flux has less extreme variations than the simulated DOC concentrations due to large variations in hydrological processes associated with high precipitation events. Factors that regulate the hydrological processes appear to have had a larger influence on DOC concentration than the factors affecting vegetation growth. However, factors affecting vegetation growth have had more influence on DOC flux by limiting the source of DOC. Nitrogen deposition is another key factor that influenced DOC concentration and flux through vegetation growth. Soil depth influenced DOC concentration through a regulation of the depth of water table. Thus RHESSys was found to reasonably estimate the DOC concentrations and the DOC flux in the Neponset River Watershed. The complexity of this urban system's hydrological processes and wetlands added difficulty to the model simulation. Lack of the information in the model about anthropogenic strategies to control peak flow by the Department of Environmental Protection appears to be one of the main reasons for an overestimation of the peak flow in the DOC simulation.

The physical based process model RHESSY furthered our understanding of DOC leaching mechanisms by quantitatively simulating DOC concentration and DOC flux in the Neponset Watershed. The RHESSys simulated land surface soil moisture successfully captured the surface moisture conditions, even in a highly heterogeneous urban area such as Boston. The hierarchical structure of RHESSys was able to represent the complex urban spatial components and consider the effects of impervious areas, roads, and the sewage system. The successful application of RHESSys for DOC and soil moisture simulation provides a framework to test various hypotheses to improve our understanding and management of the urban system in the future.

However, this research also uncovered some topics which will need further study. A comparison among simulations using different vegetation phenology estimation methods (a constant phenology value, the MODIS phenology and a dynamic phenology model) should be conducted. Long term soil moisture monitoring, corresponding with the increased availability of high quality remotely sensed data will improve our understanding and use of TVDI. Estimating TDVI from remotely sensed data with resolutions finer than Landsat will further improve our understanding of the effect of spatial resolution and scale, especially for such highly heterogeneous urban areas. More field studies need to be conducted during the leaf-off season to explore the factors that affect DOC concentrations in the stream channels. More frequent DOC sampling during snow melt periods would also be very helpful. Although hydrological processes are the main factors influencing the short term variation of DOC concentrations in the streams in this study, the DOC absorption in mineral soil needs further study to more quantitatively

understand the DOC export. The integration of a more detailed DOC absorption function would also improve the model simulation of DOC in the stream during low flow seasons. The urbanized study area used in this study increases the difficulty of the simulation. Thus more detailed information about the management strategies employed on these watersheds to adjust peak flow would improve the ability of the model to accurately simulate peak flow.

Despite the limitations of this work and the lines of future inquiry laid out above, this present study enhanced our understanding of the carbon cycle of an urbanized coastal watershed through the use of remotely sensed data and a regional hydro-ecological process based model. This study also demonstrated the utility in modeling the DOC flux of specific complex watersheds (and especially for unmonitored watersheds) to quantitatively estimate DOC flux at regional scales.

## REFERENCE

- Aber, J.D., Magill, A., Boone, R., Melillo, J.M., & Steudler, P. (1993). Plant and soil responses to chronic nitrogen additions at the Harvard Forest, Massachusetts. *Ecological Applications*, 3, 156-166
- Ågren, A., Buffam, I., Bishop, K., & Laudon, H. (2010). Modeling stream dissolved organic carbon concentrations during spring flood in the boreal forest: A simple empirical approach for regional predictions. *Journal of Geophysical Research*, 115
- Ågren, A., Buffam, I., Cooper, D., Tiwari, T., Evans, C., & Laudon, H. (2013). Can the heterogeneity in stream dissolved organic carbon be explained by contributing landscape elements? *Biogeosciences Discussions*, 10, 15913-15949
- Aitkenhead, J.A., & McDowell, W.H. (2000). Soil C:N ratio as a predictor of annual riverine DOC flux at local and global scales. *Global Biogeochemical Cycles*, 14, 127-138
- Albergel, C., de Rosnay, P., Gruhier, C., Muñoz-Sabater, J., Hasenauer, S., Isaksen, L., Kerr, Y., & Wagner, W. (2012). Evaluation of remotely sensed and modelled soil moisture products using global ground-based in situ observations. *Remote Sensing of Environment*, 118, 215-226
- Arnaud, P., Lavabre, J., Fouchier, C., Diss, S., & Javelle, P. (2011). Sensitivity of hydrological models to uncertainty in rainfall input. *Hydrological Sciences Journal—Journal des Sciences Hydrologiques*, 56, 397-410
- Band, L.E., Mackay, D.S., Creed, I.F., Semkin, R., & Jeffries, D. (1996). Ecosystem processes at the watershed scale: Sensitivity to potential climate change. *Limnology and Oceanography*, 41, 928-938
- Band, L.E., Patterson, P., Nemani, R., & Running, S.W. (1993). Forest ecosystem processes at the watershed scale: incorporating hillslope hydrology. *Agricultural and Forest Meteorology*, 63, 93-126
- Band, L.E., Tague, C.L., Groffman, P., & Belt, K. (2001). Forest ecosystem processes at the watershed scale: hydrological and ecological controls of nitrogen export. *Hydrological Processes*, 15, 2013-2028
- Baron, J.S., Hartman, M.D., Band, L.E., & Lammers, R.B. (2000). Sensitivity of a high-elevation Rocky Mountain watershed to altered climate and CO<sub>2</sub>. *Water Resources Research*, 36, 89-99

- Bassow, S., McConnaughay, K., & Bazzaz, F. (1994). The Response of Temperate Tree Seedlings Grown in Elevated CO<sub>2</sub> to Extreme Temperature Events. *Ecological Applications*, 593-603
- Beljaars, A.C., Viterbo, P., Miller, M.J., & Betts, A.K. (1996). The anomalous rainfall over the United States during July 1993: Sensitivity to land surface parameterization and soil moisture anomalies. *Monthly Weather Review*, 124, 362-383
- Berne, A., Delrieu, G., Creutin, J.-D., & Obled, C. (2004). Temporal and spatial resolution of rainfall measurements required for urban hydrology. *Journal of Hydrology*, 299, 166-179
- Beven, K., & Binley, A. (1992). The future of distributed models: model calibration and uncertainty prediction. *Hydrological Processes*, 6, 279-298
- Beven, K., & Freer, J. (2001). Equifinality, data assimilation, and uncertainty estimation in mechanistic modelling of complex environmental systems using the GLUE methodology. *Journal of Hydrology*, 249, 11-29
- Beven, K., & Kirkby, M.J. (1979). A physically based, variable contributing area model of basin hydrology. *Hydrological Sciences*, 24, 43-69
- Bianchi, T.S., DiMarco, S.F., Smith, R.W., & Schreiner, K.M. (2009). A gradient of dissolved organic carbon and lignin from Terrebonne–Timbalier Bay estuary to the Louisiana shelf (USA). *Marine Chemistry*, 117, 32-41
- Bissett, W.P., Schofield, O., Mobley, C.D., Crowley, M.F., & Moline, M.A. (2001). Optical remote sensing techniques in biological oceanography. *Methods in Microbiology*, Vol 30, 30, 519-538
- Boeing, W.J., Leech, D.M., Williamson, C.E., Cooke, S., & Torres, L. (2004). Damaging UV radiation and invertebrate predation: conflicting selective pressures for zooplankton vertical distribution in the water column of low DOC lakes. *Oecologia*, 138, 603-612
- Boissier, J.M., & Fontvielle, D. (1993). Biodegradable Dissolved Organic-Carbon in Seepage Waters from 2 Forest Soils. *Soil Biology & Biochemistry*, 25, 1257-1261
- Borken, W., Ahrens, B., Schulz, C., & Zimmermann, L. (2011). Site-to-site variability and temporal trends of DOC concentrations and fluxes in temperate forest soils. *Global Change Biology*, 17, 2428-2443
- Bourbonniere, R.A. (1989). Distribution patterns of dissolved organic matter functions in natural waters from eastern Canada. *Organic Geochemistry*, 14, 97-107
- Boyer, E.W., Hornberger, G.M., Bencala, K.E., & McKnight, D. (1996). Overview of a simple model describing variation of dissolved organic carbon in an upland catchment. *Ecological Modelling*, 86, 183-188

- Bricaud, A., Morel, A., & Prieur, L. (1981). Absorption by dissolved organic matter of the sea (yellow substance) in the UV and visible domains. *Limnology and Oceanography*, 26, 43-53
- Brocca, L., Melone, F., Moramarco, T., & Morbidelli, R. (2010). Spatial-temporal variability of soil moisture and its estimation across scales. *Water Resources Research*, 46, W02516
- Brocca, L., Morbidelli, R., Melone, F., & Moramarco, T. (2007). Soil moisture spatial variability in experimental areas of central Italy. *Journal of Hydrology*, 333, 356-373
- Carlson, T. (2007). An overview of the "triangle method" for estimating surface evapotranspiration and soil moisture from satellite imagery. *Sensors*, 7, 1612-1629
- Chen, J., Wang, C., Jiang, H., Mao, L., & Yu, Z. (2011). Estimating soil moisture using Temperature–Vegetation Dryness Index (TVDI) in the Huang-huai-hai (HHH) plain. *International Journal of Remote Sensing*, 32, 1165-1177
- Chen, R.F. (1999). In situ fluorescence measurements in coastal waters. *Organic Geochemistry*, 30, 397-409
- Chen, R.F., Zhang, Y., Vlahos, P., & Rudnick, S.M. (2002). The fluorescence of dissolved organic matter in the Mid-Atlantic Bight. *Deep-Sea Research Part II-Topical Studies in Oceanography*, 49, 4439-4459
- Chittleborough, D.J., Smettem, K.R.J., Cotsaris, E., & Leaney, F.W. (1992). Seasonal-Changes in Pathways of Dissolved Organic-Carbon through a Hillslope Soil (Xeralf) with Contrasting Texture. *Australian Journal of Soil Research*, 30, 465-476
- Choi, M., & Hur, Y. (2012). A microwave-optical/infrared disaggregation for improving spatial representation of soil moisture using AMSR-E and MODIS products. *Remote Sensing of Environment*, 124, 259-269
- Chow, A.T., Tanji, K.K., Gao, S., & Dahlgren, R.A. (2006). Temperature, water content and wet–dry cycle effects on DOC production and carbon mineralization in agricultural peat soils. *Soil Biology and Biochemistry*, 38, 477-488
- Christensen, L., Tague, C.L., & Baron, J.S. (2008). Spatial patterns of simulated transpiration response to climate variability in a snow dominated mountain ecosystem. *Hydrological Processes*, 22, 3576-3588
- Clutterbuck, B., & Yallop, A. (2010). Land management as a factor controlling dissolved organic carbon release from upland peat soils 2: changes in DOC productivity over four decades. *Science of the total environment*, 408, 6179-6191
- Currie, W.S., & Aber, J.D. (1997). Modeling Leaching as a Decomposition Process in Humid Mountain Forests. *Ecology*, 78, 1844-1860

- Currie, W.S., Aber, J.D., McDowell, W.H., B., R.D., & H.M., A. (1996). Vertical transport of dissolved organic C and N under long-term N amendments in pine and hardwood forests. *Biogeochemistry*, 35, 471-505
- Davidson, E., Belk, E., & Boone, R.D. (1998). Soil water content and temperature as independent or confounded factors controlling soil respiration in a temperate mixed hardwood forest. *Global Change Biology*, 4, 217-227
- Dawson, J.J., Tetzlaff, D., Speed, M., Hrachowitz, M., & Soulsby, C. (2011). Seasonal controls on DOC dynamics in nested upland catchments in NE Scotland. *Hydrological Processes*, 25, 1647-1658
- Delpla, I., Jung, A.-V., Baures, E., Clement, M., & Thomas, O. (2009). Impacts of climate change on surface water quality in relation to drinking water production. *Environment International*, 35, 1225-1233
- Dosskey, M.G., & Bertsch, P.M. (1997). Transport of dissolved organic matter through a sandy forest soil. *Soil Science Society of America Journal*, 61, 920-927
- Draper, C.S., Walker, J.P., Steinle, P.J., de Jeu, R.A., & Holmes, T.R. (2009). An evaluation of AMSR-E derived soil moisture over Australia. *Remote Sensing of Environment*, 113, 703-710
- Dyson, K.E., Billett, M.F., Dinsmore, K.J., Harvey, F., Thomson, A.M., Piirainen, S., & Kortelainen, P. (2011). Release of aquatic carbon from two peatland catchments in E. Finland during the spring snowmelt period. *Biogeochemistry*, 103, 125-142
- Emmanuel, I., Andrieu, H., Leblois, E., & Flahaut, B. (2012). Temporal and spatial variability of rainfall at the urban hydrological scale. *Journal of Hydrology*, 430, 162-172
- Engman, E.T. (1991). Applications of microwave remote sensing of soil moisture for water resources and agriculture. *Remote Sensing of Environment*, 35, 213-226
- Engman, E.T., & Chauhan, N. (1995). Status of Microwave Soil-Moisture Measurements with Remote-Sensing. *Remote Sensing of Environment*, 51, 189-198
- Entekhabi, D., Njoku, E.G., O'Neill, P.E., Kellogg, K.H., Crow, W.T., Edelstein, W.N., Entin, J.K., Goodman, S.D., Jackson, T.J., & Johnson, J. (2010). The soil moisture active passive (SMAP) mission. *Proceedings of the IEEE*, 98, 704-716
- Evans, C.D., Chapman, P.J., Clark, J.M., Monteith, D.T., & Cresser, M.S. (2006). Alternative explanations for rising dissolved organic carbon export from organic soils. *Global Change Biology*, 12, 2044-2053
- Evans, C.D., Monteith, D.T., & Cooper, D.M. (2005). Long-term increases in surface water dissolved organic carbon: observations, possible causes and environmental impacts. *Environ Pollut*, 137, 55-71

- Famiglietti, J.S., Ryu, D., Berg, A.A., Rodell, M., & Jackson, T.J. (2008). Field observations of soil moisture variability across scales. *Water Resources Research*, *44*, W01423
- Fedora, M.A., & Beschta, R.L. (1989). Storm Runoff Simulation Using an Antecedent Precipitation Index (Api) Model. *Journal of Hydrology*, *112*, 121-133
- Findlay, S., Quinn, J.M., Hickey, C.W., Burrell, G., & Downes, M. (2001). Effects of land use and riparian flowpath on delivery of dissolved organic carbon to streams. *Limnology and Oceanography*, *46*, 345-355
- Forsius, M., Saloranta, T., Arvola, L., Salo, S., Verta, M., Ala-Opas, P., Rask, M., & Vuorenmaa, J. (2010). Physical and chemical consequences of artificially deepened thermocline in a small humic lake – a paired whole-lake climate change experiment. *Hydrology and Earth System Sciences Discussions*, *7*, 2915-2947
- Futter, M., Forsius, M., Holmberg, M., & Starr, M. (2009). A long-term simulation of the effects of acidic deposition and climate change on surface water dissolved organic carbon concentrations in a boreal catchment
- Futter, M.N., Lofgren, S., Kohler, S.J., Lundin, L., Moldan, F., & Bringmark, L. (2011). Simulating dissolved organic carbon dynamics at the swedish integrated monitoring sites with the integrated catchments model for carbon, INCA-C. *Ambio*, *40*, 906-919
- Gao, J., Christensen, P., & Li, W. (2012). Application of the WEAP model in strategic environmental assessment: Experiences from a regional plan in an arid semi-arid area of China. *Journal of Environmental Management*
- García, M., Sandholt, I., Ceccato, P., Ridler, M., Mougin, E., Kergoat, L., Morillas, L., Timouk, F., Fensholt, R., & Domingo, F. (2013). Actual evapotranspiration in drylands derived from in-situ and satellite data: Assessing biophysical constraints. *Remote Sensing of Environment*, *131*, 103-118
- Giesler, R., Hogberg, M., & Hogberg, P. (1998). Soil chemistry and plants in Fennoscandian boreal forest as exemplified by a local gradient. *Ecology*, *79*, 119-137
- Green, S.A., & Blough, N.V. (1994). Optical-Absorption and Fluorescence Properties of Chromophoric Dissolved Organic-Matter in Natural-Waters. *Limnology and Oceanography*, *39*, 1903-1916
- Groffman, P.M., & Turner, C.L. (1995). Plant Productivity and Nitrogen Gas Fluxes in a Tallgrass Prairie Landscape. *Landscape Ecology*, *10*, 255-266
- Guggenberger, G., & Zech, W. (1994). Dissolved Organic-Carbon in Forest Floor Leachates - Simple Degradation Products or Humic Substances. *Science of the total environment*, *152*, 37-47

- Gundersen, J.S., Gardner, W.D., Richardson, M.J., & Walsh, I.D. (1998). Effects of monsoons on the seasonal and spatial distributions of POC and chlorophyll in the Arabian Sea. *Deep-Sea Research Part II-Topical Studies in Oceanography*, 45, 2103-2132
- Haaland, S., & Mulder, J. (2009). Dissolved organic carbon concentrations in runoff from shallow heathland catchments: effects of frequent excessive leaching in summer and autumn. *Biogeochemistry*, 97, 45-53
- Hartman, M.D., Baron, J.S., Lammers, R.B., Cline, D.W., Band, L.E., Liston, G.E., & Tague, C. (1999). Simulations of snow distribution and hydrology in a mountain basin. *Water Resources Research*, 35, 1587-1603
- Haynes, R.J., & Swift, R.S. (1991). Concentrations of extractable Cu, Zn, Fe and Mn in a group of soils as influenced by air-and oven-drying and rewetting. *Geoderma*, 49, 319-333
- Hedges, J.I., Keil, R.G., & Benner, R. (1997). What happens to terrestrial organic matter in the ocean? *Organic Geochemistry*, 27, 195-212
- Hornberger, G., Bencala, K., & McKnight, D. (1994). Hydrological controls on dissolved organic carbon during snowmelt in the Snake River near Montezuma, Colorado. *Biogeochemistry*, 25, 147-165
- Houser, P.R., Shuttleworth, W.J., Famiglietti, J.S., Gupta, H.V., Syed, K.H., & Goodrich, D.C. (1998). Integration of soil moisture remote sensing and hydrologic modeling using data assimilation. *Water Resources Research*, 34, 3405-3420
- Huang, W., & Chen, R.F. (2009). Sources and transformations of chromophoric dissolved organic matter in the Neponset River Watershed. *Journal of Geophysical Research*, 114
- Huete, A., Justice, C., & Liu, H. (1994). Development of Vegetation and Soil Indexes for Modis-Eos. *Remote Sensing of Environment*, 49, 224-234
- Huete, A.R. (1988). A Soil-Adjusted Vegetation Index (Savi). *Remote Sensing of Environment*, 25, 295-309
- Huete, A.R., Liu, H.Q., Batchily, K., & vanLeeuwen, W. (1997). A comparison of vegetation indices global set of TM images for EOS-MODIS. *Remote Sensing of Environment*, 59, 440-451
- Huntington, T., & Aiken, G.R. (2012). Export of dissolved organic carbon from the Penobscot River basin in north-central Maine
- Hur, J., Park, M.-H., & Schlautman, M.A. (2009). Microbial transformation of dissolved leaf litter organic matter and its effects on selected organic matter operational descriptors. *Environmental Science & Technology*, 43, 2315-2321

- Hwang, T., Band, L.E., Vose, J.M., & Tague, C. (2012). Ecosystem processes at the watershed scale: Hydrologic vegetation gradient as an indicator for lateral hydrologic connectivity of headwater catchments. *Water Resources Research*, 48
- Hwang, T., Song, C., Vose, J.M., & Band, L.E. (2011). Topography-mediated controls on local vegetation phenology estimated from MODIS vegetation index. *Landscape Ecology*, 26, 541-556
- Inamdar, S.P., & Mitchell, M.J. (2006). Hydrologic and topographic controls on storm-event exports of dissolved organic carbon (DOC) and nitrate across catchment scales. *Water Resources Research*, 42
- Jardine, P., McCarthy, J., & Weber, N. (1989). Mechanisms of dissolved organic carbon adsorption on soil. *Soil Science Society of America Journal*, 53, 1378-1385
- Jiang, Z., Huete, A., Didan, K., & Miura, T. (2008). Development of a two-band enhanced vegetation index without a blue band. *Remote Sensing of Environment*, 112, 3833-3845
- Julien, Y., Sobrino, J.A., & Jiménez-Muñoz, J.-C. (2011). Land use classification from multitemporal Landsat imagery using the Yearly Land Cover Dynamics (YLCD) method. *International Journal of Applied Earth Observation and Geoinformation*, 13, 711-720
- Kalbitz, K., & Knappe, S. (1997). Influence of soil properties on the release of dissolved organic matter (DOM) from the topsoil. *Zeitschrift Fur Pflanzenernahrung Und Bodenkunde*, 160, 475-483
- Kalbitz, K., Solinger, S., Park, J.H., Michalzik, B., & Mather, T.N. (2000). Controls on the dynamics of Dissolved Organic Matter in soils: a review. *Soil Science*, 165, 277-304
- Kicklighter, D.W., Hayes, D.J., McClelland, J.W., Peterson, B.J., McGuire, A.D., & Melillo, J.M. (2013). Insights and issues with simulating terrestrial DOC loading of arctic river networks. *Ecological Society of America*
- Kohler, M.A., & Linsley, R.K. (1951). Predicting the runoff from storm rainfall. *US Department of Commerce, Weather Bureau*
- Kothawala, D., Moore, T., & Hendershot, W. (2008). Adsorption of dissolved organic carbon to mineral soils: A comparison of four isotherm approaches. *Geoderma*, 148, 43-50
- Kramer, J.R., Brassard, P., Collins, P., Clair, T.A., & Takats, P. (1990). Variability of organic acids in watersheds. *Organic acids in aquatic ecosystems*, 127-139
- Leopold, L.B., & Dunne, J. (1978). Water in environmental planning. *New York*, 818p

- Liechty, H.O., Kuuseoks, E., & Mroz, G.D. (1995). Dissolved organic carbon in northern hardwood stands with differing acidic inputs and temperature regimes. *Journal of Environmental Quality*, 24, 927-933
- Lilienfein, J., Qualls, R.G., Uselman, S.M., & Bridgham, S.D. (2004). Adsorption of Dissolved Organic Carbon and Nitrogen in Soils of a Weathering Chronosequence. *Soil Science Society of America*, 68, 292-305
- Lu, Y., Bauer, J.E., Canuel, E.A., Yamashita, Y., Chambers, R., & Jaffé, R. (2013). Photochemical and microbial alteration of dissolved organic matter in temperate headwater streams associated with different land use. *Journal of Geophysical Research: Biogeosciences*
- Lundquist, E.J., Jackson, L.E., & Scow, K.M. (1999). Wet-dry cycles affect dissolved organic carbon in two California agricultural soils. *Soil Biology & Biochemistry*, 31, 1031-1038
- Luo, C., Xu, G., Wang, Y., Wang, S., Lin, X., Hu, Y., Zhang, Z., Chang, X., Duan, J., & Su, A. (2009). Effects of grazing and experimental warming on DOC concentrations in the soil solution on the Qinghai-Tibet plateau. *Soil Biology and Biochemistry*, 41, 2493-2500
- MacDonald, N.W., Randlett, D.L., & Zak, D.R. (1999). Soil warming and carbon loss from a lake states spodosol. *Soil Science Society of America Journal*, 63, 211-218
- Martell, A.E., Motekaitisand, R.J., & Smith, R.M. (1988). Structure-stability relationships of metal complexes and metal speciation in environmental aqueous solutions. *Environmental Toxicology and Chemistry*, 7, 417-434
- Masek, J.G., Vermote, E.F., Saleous, N.E., Wolfe, R., Hall, F.G., Huemmrich, K.F., Gao, F., Kutler, J., & Lim, T.K. (2006). A landsat surface reflectance dataset for North America, 1990-2000. *Geoscience and Remote Sensing Letters, IEEE*, 3, 68-72
- Mayer, L.M. (1994). Relationships between mineral surfaces and organic carbon concentrations in soils and sediments. *Chemical Geology*, 114, 347-363
- McDowell, W.H., Currie, W.S., Aber, J.D., & Yano, Y. (1998). Effects of Chronic Nitrogen Amendments on Production of Dissolved Organic Carbon and Nitrogen in Forest Soils. *Water, Air, and Soil Pollution*, 105, 175-182
- McDowell, W.H., & Wood, T. (1984). Podzolization: soil processes control dissolved organic carbon concentrations in stream water. *Soil Science*, 137, 23-32
- Michalzik, B., & Matzner, E. (1999). Dynamics of dissolved organic nitrogen and carbon in a Central European Norway spruce ecosystem. *European Journal of Soil Science*, 50, 579-590

- Miller, M.P. (2012). The influence of reservoirs, climate, land use and hydrologic conditions on loads and chemical quality of dissolved organic carbon in the Colorado River. *Water Resources Research*, 48, n/a-n/a
- Monteith, J. (1965). Evaporation and environment. In, *Symp. Soc. Exp. Biol* (p. 4)
- Moore, I.D., Gessler, P.E., Nielsen, G.A., & Peterson, G.A. (1993). Soil Attribute Prediction Using Terrain Analysis. *Soil Science Society of America Journal*, 57, 443-452
- Neff, J.C., & Asner, G.P. (2001). Dissolved Organic Carbon in Terrestrial Ecosystems: Synthesis and a Model. *Ecosystems*, 4, 29-48
- Nelson, P.N., Dector, M.C., & Soulas, G. (1994). Availability of organic carbon in soluble and particle-size fractions from a soil profile. *Soil Biology & Biochemistry*, 26, 1549-1555
- Nemani, R., Hashimoto, H., Votava, P., Melton, F., Wang, W., Michaelis, A., Mutch, L., Milesi, C., Hiatt, S., & White, M. (2009). Monitoring and forecasting ecosystem dynamics using the Terrestrial Observation and Prediction System (TOPS). *Remote Sensing of Environment*, 113, 1497-1509
- Nemani, R., Pierce, L., Running, S., & Goward, S.N. (1993). Developing Satellite-derived Estimates of Surface Moisture Status. *Journal of Applied Meteorology*, 32, 548-557
- Nemani, R., & Running, S. (1988). Estimation of Regional Surface Resistance to Evapotranspiration from NDVI and Thermal-IR AVHRR Data. *Journal of Applied Meteorology*, 28, 276-284
- Njoku, E.G., & Entekhabi, D. (1996). Passive microwave remote sensing of soil moisture. *Journal of Hydrology*, 184, 101-129
- Nowak, D.J. (2000). The effects of urban trees on air quality. *USDA Forest Service*, 4
- Nowak, D.J., & Crane, D.E. (2002). Carbon storage and sequestration by urban trees in the USA. *Environmental Pollution*, 16, 381-389
- Olefeldt, D., Roulet, N., Giesler, R., & Persson, A. (2012). Total waterborne carbon export and DOC composition from ten nested subarctic peatland catchments—importance of peatland cover, groundwater influence, and inter-annual variability of precipitation patterns. *Hydrological Processes*
- Parton, W.J., Mosier, A.R., Ojima, D.S., Valentine, D.W., Schimel, D.S., Weier, K., & Kulmala, A.E. (1996). Generalized model for N<sub>2</sub> and N<sub>2</sub>O production from nitrification and denitrification. *Global Biogeochemical Cycles*, 10, 401-412

- Patel, N.R., Anapashsha, R., Kumar, S., Saha, S.K., & Dadhwal, V.K. (2009). Assessing potential of MODIS derived temperature/vegetation condition index (TVDI) to infer soil moisture status. *International Journal of Remote Sensing*, 30, 23-39
- Pearson, R.L., & Miller, L.D. (1972). Remote mapping of standing crop biomass for estimation of the productivity of the shortgrass prairie. *Remote Sensing of Environment*, 1, 1355-1972
- Penna, D., Borga, M., Norbiato, D., & Dalla Fontana, G. (2009). Hillslope scale soil moisture variability in a steep alpine terrain. *Journal of Hydrology*, 364, 311-327
- Perdue, E.M., Beck, K.C., & Reuter, H.J. (1976). Organic complexes of iron and aluminium in natural waters, 418-420
- Petropoulos, G., Carlson, T.N., Wooster, M.J., & Islam, S. (2009). A review of T-s/VI remote sensing based methods for the retrieval of land surface energy fluxes and soil surface moisture. *Progress in Physical Geography*, 33, 224-250
- Philip, J.R. (1957). The theory of infiltration. *Soil Science*, 84, 257-264
- Pouyat, R., Groffman, P., Yesilonis, I., & Hernandez, L. (2002). Soil carbon pools and fluxes in urban ecosystems. *Environ Pollut*, 116, 107-118
- Preston, M.D., Eimers, M.C., & Watmough, S.A. (2011). Effect of moisture and temperature variation on DOC release from a peatland: conflicting results from laboratory, field and historical data analysis. *Sci Total Environ*, 409, 1235-1242
- Rao, P., Hutyra, L.R., Raciti, S.M., & Finzi, A.C. (2013). Field and remotely sensed measures of soil and vegetation carbon and nitrogen across an urbanization gradient in the Boston metropolitan area. *Urban Ecosystems*, 1-24
- Raymond, P.A., & Saiers, J.E. (2010). Event controlled DOC export from forested watersheds. *Biogeochemistry*, 100, 197-209
- Richey, J.E., Field, C., & Raupach, M. (2004a). Pathways of atmospheric CO<sub>2</sub> through fluvial systems. *The Global Carbon Cycle: integrating humans, climate and the natural world*, 329-340
- Richey, J.E., Field, C.B., & Raupach, M.R. (2004b). Pathways of atmospheric CO<sub>2</sub> through fluvial systems. *The Global Carbon Cycle: integrating humans, climate and the natural world*, 329-340
- Rodhe, A., & Seibert, J. (1999). Wetland occurrence in relation to topography: a test of topographic indices as moisture indicators. *Agricultural and Forest Meteorology*, 98-9, 325-340

- Roulet, N., & Moore, T.R. (2006). Environmental chemistry: Browning the waters. *Nature*, 444, 283-284
- Runkel, R.L., Crawford, C.G., & Cohn, T.A. (2004). Load estimator (LOADEST): A FORTRAN program for estimating constituent loads in streams and rivers. *US Department of the Interior, US Geological Survey*
- Running, S.W., Nemani, R.R., Heinsch, F.A., Zhao, M.S., Reeves, M., & Hashimoto, H. (2004). A continuous satellite-derived measure of global terrestrial primary production. *bioscience*, 54, 547-560
- Rustad, L.E., Fernandez, I.J., David, M.B., Mitchell, M.J., Nadelhoffer, K.J., & Fuller, R.B. (1996). Experimental soil acidification and recovery at the Bear Brook Watershed in Maine. *Soil Science Society of America Journal*, 60, 1933-1943
- Ryan, M.G. (1991). A simple method for estimating gross carbon budgets for vegetation in forest ecosystems. *Tree Physiology*, 9, 255-266
- Sandholt, I., Rasmussen, L., & Andersen, J. (2002). A simple interpretation of TS\_NDVI space for assessment of surface moisture status. *Remote Sensing of Environment*, 79, 213-224
- Schaaf, C.B., Gao, F., Strahler, A.H., Lucht, W., Li, X.W., Tsang, T., Strugnell, N.C., Zhang, X.Y., Jin, Y.F., Muller, J.P., Lewis, P., Barnsley, M., Hobson, P., Disney, M., Roberts, G., Dunderdale, M., Doll, C., d'Entremont, R.P., Hu, B.X., Liang, S.L., Privette, J.L., & Roy, D. (2002). First operational BRDF, albedo nadir reflectance products from MODIS. *Remote Sensing of Environment*, 83, 135-148
- Schaaf, C.B., Liu, J., Gao, F., & Strahler, A.H. (2011). Aqua and Terra MODIS albedo and reflectance anisotropy products. *Land Remote Sensing and Global Environmental Change* (pp. 549-561): Springer
- Schwarz, G.E., Hoos, A.B., Alexander, R.B., & SMITH, r.a. (2006). The SPARROW surface water-quality model: Theory, application and user documentation. *US Department of the Interior, US Geological Survey*
- Shields, C.A., & Tague, C.L. (2012). Assessing the Role of Parameter and Input Uncertainty in Ecohydrologic Modeling: Implications for a Semi-arid and Urbanizing Coastal California Catchment. *Ecosystems*, 15, 775-791
- Siddiqui, M.S., Amy, G.L., & Murphy, B.D. (1997). Ozone enhanced removal of natural organic matter from drinking water sources. *Water Research*, 31, 3098-3106
- Sims, D., Rahman, A., Cordova, V., Elmasri, B., Baldocchi, D., Bolstad, P., Flanagan, L., Goldstein, A., Hollinger, D., & Misson, L. (2008). A new model of gross primary productivity for North American ecosystems based solely on the enhanced vegetation

index and land surface temperature from MODIS. *Remote Sensing of Environment*, 112, 1633-1646

Smith, S., & Mackenzie, F. (1987). The ocean as a net heterotrophic system: implications from the carbon biogeochemical cycle. *Global BioGeochemical Cycles*, 1, 187-198

Sobrino, J., & Raissouni, N. (2000). Toward remote sensing methods for land cover dynamic monitoring: application to Morocco. *International Journal of Remote Sensing*, 21, 353-366

Strohmeier, S., Knorr, K.H., Reichert, M., Frei, S., Fleckenstein, J.H., Peiffer, S., & Matzner, E. (2013). Concentrations and fluxes of dissolved organic carbon in runoff from a forested catchment: insights from high frequency measurements. *Biogeosciences*, 10, 905-916

Sun, Z.G., Wang, Q.X., Matsushita, B., Fukushima, T., Ouyang, Z., Watanabe, M., & Gebremichael, M. (2011). Evaluation of the VI-T-s method for estimating the land surface moisture index and air temperature using ASTER and MODIS data in the North China Plain. *International Journal of Remote Sensing*, 32, 7257-7278

Tague, C., Band, L., Kenworthy, S., & Tenebaum, D. (2010). Plot- and watershed-scale soil moisture variability in a humid Piedmont watershed. *Water Resources Research*, 46

Tague, C., Choate, J., & Grant, G. (2013). Parameterizing sub-surface drainage with geology to improve modeling streamflow responses to climate in data limited environments. *Hydrology and Earth System Sciences*, 17, 341-354

Tague, C., & Grant, G. (2009). Groundwater dynamics mediate low-flow response to global warming in snow-dominated alpine regions. *Water Resources Research*, 45

Tague, C., Grant, G., Farrell, M., Choate, J., & Jefferson, A. (2007). Deep groundwater mediates streamflow response to climate warming in the Oregon Cascades. *Climatic Change*, 86, 189-210

Tague, C., Heyn, K., & Christensen, L. (2009a). Topographic controls on spatial patterns of conifer transpiration and net primary productivity under climate warming in mountain ecosystems. *Ecohydrology*, 2, 541-554

Tague, C., McMichael, C., Hope, A., Choate, J., & Clark, R. (2004). Application of the RHESSys model to a California semi-arid shrubland watershed. *Journal of the American Water Resources Association*, 40, 575-589

Tague, C., Seaby, L., & Hope, A. (2009b). Modeling the eco-hydrologic response of a Mediterranean type ecosystem to the combined impacts of projected climate change and altered fire frequencies. *Climatic Change*, 93, 137-155

- Tague, C.L., & Band, L.E. (2004). RHESSys: Regional Hydro-Ecologic Simulation System-An Object-Oriented Approach to Spatially Distributed Modeling of Carbon, Water, and Nutrient Cycling. *Earth Interactions*, 8
- Tague, C.L., Choate, J.S., & Grant, G. (2012). Parameterizing sub-surface drainage with geology to improve modeling streamflow responses to climate in data limited environments. *Hydrology and Earth System Sciences Discussions*, 9, 8665-8700
- Tenenbaum, D.E., Band, L.E., Kenworthy, S.T., & Tague, C.L. (2006). Analysis of soil moisture patterns in forested and suburban catchments in Baltimore, Maryland, using high-resolution photogrammetric and LIDAR digital elevation datasets. *Hydrological Processes*, 20, 219-240
- Tian, Y.Q., Yu, Q., Feig, A.D., Ye, C., & Blunden, A. (2013). Effects of climate and land-surface processes on terrestrial dissolved organic carbon export to major U.S. coastal rivers. *Ecological Engineering*, 54, 192-201
- Tipping, E., Chamberlain, P.M., Fröberg, M., Hanson, P.J., & Jardine, P.M. (2012). Simulation of carbon cycling, including dissolved organic carbon transport, in forest soil locally enriched with <sup>14</sup>C. *Biogeochemistry*, 108, 91-107
- Tipping, E., Marker, A.F.H., Butterwick, G.D., Collett, P.A., Cranwell, J.K.G., & Ingram, D.V. (1997). Organic carbon in the Humber rivers. *Science of the total environment*, 194, 345-355
- Tipping, E., Woof, C., Rigg, E., Harrison, A.F., Ineson, P., Taylor, K., Benham, D., Poskitt, J., Rowland, A.P., Bol, R., & Harkness, D.D. (1999). Climatic influences on the leaching of dissolved organic matter from upland UK Moorland soils, investigated by a field manipulation experiment. *Environment International*, 25, 83-95
- Tranvik, L.J., & Jansson, M. (2002). Climate change - Terrestrial export of organic carbon. *Nature*, 415, 861-862
- Trumbore, S.E. (1993). Comparison of Carbon Dynamics in Tropical and Temperate Soils Using Radiocarbon Measurements. *Global Biogeochemical Cycles*, 7, 275-290
- Valor, E., & Caselles, V. (1996). Mapping Land Surface Emissivity from NDVI: Application to European, African, and South American Areas. *Remote Sensing of Environment*, 57, 167-184
- Vaze, J., Post, D., Chiew, F., Perraud, J.-M., Teng, J., & Viney, N. (2011). Conceptual rainfall-runoff model performance with different spatial rainfall inputs. *Journal of Hydrometeorology*, 12, 1100-1112
- Verstraeten, W.W., Veroustraete, F., Wagner, W., Roey, T., Heyns, W., Verbeiren, S., & Feyen, J. (2010). Remotely sensed soil moisture integration in an ecosystem carbon flux model. The spatial implication. *Climatic Change*, 103, 117-136

- Wan, Z., Wang, P., & Li, X. (2004). Using MODIS land surface temperature and normalized difference vegetation index products for monitoring drought in the southern Great Plains, USA. *International Journal of Remote Sensing*, 25, 61-72
- Wan, Z.M., Zhang, Y.L., Zhang, Q.C., & Li, Z.L. (2002). Validation of the land-surface temperature products retrieved from Terra Moderate Resolution Imaging Spectroradiometer data. *Remote Sensing of Environment*, 83, 163-180
- Wang, C., Qi, S., Niu, Z., & Wang, J. (2004). Evaluating soil moisture status in China using the temperature-vegetation dryness index (TVDI). *Canadian Journal of Remote Sensing*, 30, 671-679
- Wang, H., Li, X., Long, H., Xu, X., & Bao, Y. (2010). Monitoring the effects of land use and cover type changes on soil moisture using remote-sensing data: A case study in China's Yongding River basin. *Catena*, 82, 135-145
- Wayne, P., Reekie, E., & Bazzaz, F. (1998). Elevated CO<sub>2</sub> ameliorates birch response to high temperature and frost stress: implications for modeling climate-induced geographic range shifts. *Oecologia*, 114, 335-342
- Weng, L., Temminghoff, E.J., Lofts, S., Tipping, E., & Van Riemsdijk, W.H. (2002). Complexation with dissolved organic matter and solubility control of heavy metals in a sandy soil. *Environmental Science & Technology*, 36, 4804-4810
- Western, A.W., & Blöschl, G. (1999). On the spatial scaling of soil moisture. *Journal of Hydrology*, 217, 203-224
- Western, A.W., Grayson, R.B., Blöschl, G., Willgoose, G.R., & McMahon, T.A. (1999). Observed spatial organization of soil moisture and its relation to terrain indices. *Water Resources Research*, 35, 797-810
- Western, A.W., Zhou, S.-L., Grayson, R.B., McMahon, T.A., Blöschl, G., & Wilson, D.J. (2004). Spatial correlation of soil moisture in small catchments and its relationship to dominant spatial hydrological processes. *Journal of Hydrology*, 286, 113-134
- Whelan, M., & Gandolfi, C. (2002). Modelling of spatial controls on denitrification at the landscape scale. *Hydrological Processes*, 16, 1437-1450
- White, M.A., Thornton, P.E., Running, S.W., & Nemani, R.R. (2000). Parameterization and sensitivity analysis of the BIOME-BGC terrestrial ecosystem model: net primary production controls. *Earth Interactions*, 4, 1-85
- Wigmosta, M.S., Vail, L.W., & Lettenmaier, D.P. (1994). A Distributed Hydrology-Vegetation Model for Complex Terrain. *Water Resources Research*, 30, 1665-1679

- Williamson, C.E., Dodds, W., Kratz, T.K., & Palmer, M.A. (2008). Lakes and streams as sentinels of environmental change in terrestrial and atmospheric processes. *Frontiers in Ecology and the Environment*, 6, 247-254
- Williamson, C.E., & Zagarese, H. (1994). Impact of UV-B radiation on pelagic freshwater ecosystems. *E. Schweizerbart'sche Verlagsbuchhandlung*
- Wu, H., Peng, C., Moore, T., Hua, D., Li, C., Zhu, Q., Peichl, M., Arain, M., & Guo, Z. (2013). Modeling dissolved organic carbon in temperate forest soils: TRIPLEX-DOC model development and validation. *Geoscientific Model Development Discussions*, 6, 3473-3508
- Xenopoulos, M.A., Lodge, D.M., Frentress, J., Kreps, T.A., Bridgham, S.D., Grossman, E., & Jackson, C.J. (2003). Regional comparisons of watershed determinants of dissolved organic carbon in temperate lakes from the Upper Great Lakes region and selected regions globally. *Limnology and Oceanography*, 48, 2321-2334
- Xin, J., Tian, G., Liu, Q., & Chen, L. (2006). Combining vegetation index and remotely sensed temperature for estimation of soil moisture in China. *International Journal of Remote Sensing*, 27, 2071-2075
- Xu, N., Saiers, J.E., Wilson, H.F., & Raymond, P.A. (2012). Simulating streamflow and dissolved organic matter export from a forested watershed. *Water Resources Research*, 48
- Yano, Y., McDowell, W.H., & kinner, N.E. (1998). Quantification of biodegradable dissolved organic carbon in soil solution with flow-through bioreactors. *Soil Science Society of America*, 62, 1556-1564
- Yavitt, J.B., & Fahey, T.J. (1985). Chemical composition of interstitial water in decaying lodgepole pine bole wood. *Canadian Journal of Forest Research*, 15, 1149-1153
- Yurova, A., Sirin, A., Buffam, I., Bishop, K., & Laudon, H. (2008). Modeling the dissolved organic carbon output from a boreal mire using the convection-dispersion equation: Importance of representing sorption. *Water Resources Research*, 44, n/a-n/a
- Zabowski, D., & Ugolini, F.C. (1990). Lysimeter and centrifuge soil solutions: seasonal differences between methods. *Soil Science Society of America*, 54, 1130-1135
- Zhang, X., Friedl, M.A., Schaaf, C.B., Strahler, A.H., Hodges, J.C., Gao, F., Reed, B.C., & Huete, A. (2003). Monitoring vegetation phenology using MODIS. *Remote Sensing of Environment*, 84, 471-475
- Zierl, B., Bugmann, H., & Tague, C.L. (2007). Water and carbon fluxes of European ecosystems: An evaluation of the ecohydrological model RHESSys. *Hydrological Processes*, 21, 3328-3339

Zinko, U., Seibert, J., Dynesius, M., & Nilsson, C. (2005). Plant species numbers predicted by a topography-based groundwater flow index. *Ecosystems*, 8, 430-441

Zsolnay, A., Baigar, E., Jimenez, M., Steinweg, B., & Saccomandi, F. (1999). Differentiating with fluorescence spectroscopy the sources of dissolved organic matter in soils subjected to drying. *Chemosphere*, 38, 45-50